NICKEL (II)-CATALYZED AND ACID-CATALYZED HYDROXAMIC ACID FORMATION FROM CARBOXYLIC ACIDS AND SOME OF THEIR DERIVATIVES

by

JAMES WILLIAM MUNSON

A thesis submitted in partial fulfillment of the requirements for the degree of

DOCTOR OF PHILOSOPHY

(Pharmacy)

at the

UNIVERSITY OF WISCONSIN

1971

ACKNOWLEDGEMENTS

I wish to express my sincere gratitude to Professor Kenneth A. Connors for his guidance and suggestions during the course of this investigation. I also appreciate his interest in the development of my scientific career.

I would also like to thank Dr. Robert E. Notari for his role in developing my early interests in science.

Financial support was provided by the National Institute of Dental Research Training Program (DE-171) and the University of Wisconsin Research Committee. For this, I am extremely grateful.

TO

Bev and Kevin

TABLE OF CONTENTS

TABLE OF CONTENTS - Cont.

I. INTRODUCTION

Hydroxamic acids, I, first synthesized by Lossen in 1869 (1), are readily formed by the reaction of hydroxylamine and a carboxylic acid derivative (Eq. 1).

$$R\text{-}\overset{\overset{O}{\|}}{C}\text{-}X + NH_2OH \longrightarrow R\text{-}\overset{\overset{O}{\|}}{C}\text{-}NHOH + HX \qquad (1)$$

I

The reaction is base catalyzed but the mechanism of this catalysis is unknown. Substrates that are known to form hydroxamic acids include carboxylic acid esters, amides, imides, acid halides, anhydrides, lactones, lactams, thiol esters, and isocyanates.*

Hydroxamic acids occur in a wide variety of fungi, yeasts, bacteria, and plants. They are not found in higher animals (2). Naturally occurring hydroxamic acids have been found to act, variously, as antitumor agents, antibiotics, fungistatic agents, cell division factors, growth factors, and antibiotic antagonists (2). An iron-free trihydroxamate preparation (Desferal^R, Ciba Pharmaceutical Company) has been used in children for treating accidental iron poisoning (2).

---

*See reference (20). The reaction sequence is:

$$R\text{-}N{=}C{=}O + NH_2OH \longrightarrow R\text{-}NH\text{-}\overset{\overset{OH}{|}}{C}{=}NOH \rightleftharpoons R\text{-}NH\text{-}\overset{\overset{O}{\|}}{C}\text{-}NHOH$$

An important occurrence of hydroxamic acids has been in the determination of carboxylic acid derivatives and of transition metal ions. Substituted hydroxylamines such as N-benzoyl-N-phenylhydroxylamine (II) have been used extensively for the determination of transition metal ions.

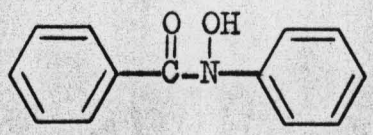

II

NBPHA

NBPHA forms insoluble complexes with transition metals. These metals are determined gravimetrically via these insoluble complexes. Certain transition metals can also be extracted into organic solvents by complexation with NBPHA.*

Hydroxamic acids form colored complexes with ferric iron (Eq. 2).

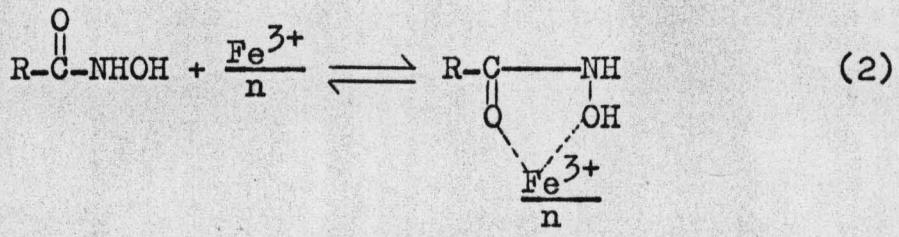

(2)

*These methods will not be discussed in greater detail here. Further information can be found in references (3)-(5).

The 1:1 complex is formed in acidic solutions with higher order complexes being formed as the pH is increased (7). Ferrous ions do not give a color with hydroxamic acids. Carboxylic acid derivatives can be determined colorimetrically as their hydroxamic acids by carrying out Eq. (1) and then forming the ferric-hydroxamate complex.

A. Nature of the Reaction

The reaction of hydroxylamine with carboxylic acid derivatives* takes place in both neutral and basic solutions. Labile substrates such as acid chlorides, phenyl esters, acid anhydrides, and lactones react readily at neutral pH. Less reactive substrates such as alkyl esters, amides,** and imides react slowly at neutral pH and generally require basic catalysis for facile reaction. Carboxylic acids generally do not react at significant rates in neutral or alkaline conditions. Acylation of the nitrogen atom of hydroxylamine is the usual overall reaction, but acylation of the oxygen is known (7,8,12).

Jencks has found that aromatic esters of acetic acid, such as phenyl acetate, react with hydroxylamine to form

---

*This reaction is also referred to as the hydroxylaminolysis of an acyl function.

**Reactions of amides at neutral pH will be discussed later.

initially an O-acylhydroxylamine (Eq. 3), which reacts with an additional molecule of hydroxylamine to form the hydroxamic acid (7,8) (Eq. 4).

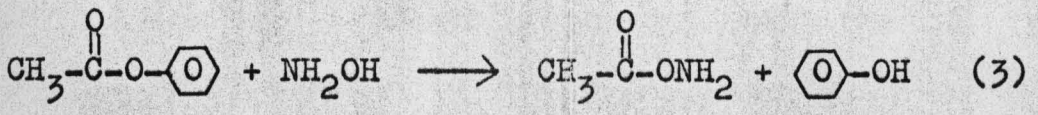

(3)

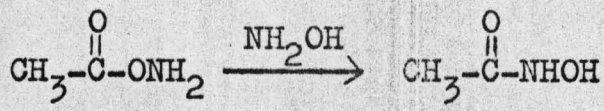

(4)

It appears that the oxygen atom of hydroxylamine is a better nucleophilic site toward the acetyl group of aromatic esters of acetic acid than is the nitrogen atom, despite the greater basicity of the nitrogen atom. This unusual reactivity suggests that it is not the free hydroxyl group, but rather the oxygen anion of the dipolar form of hydroxylamine (III) that is the reactive nucleophilic species (10).

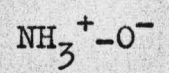

III

A possible mechanism for this is given in Equation (5).

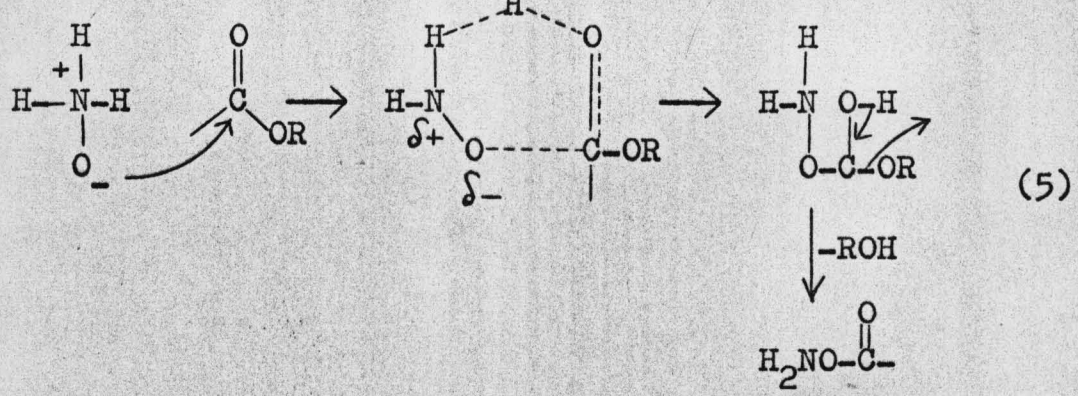

(5)

However, infrared spectroscopic data indicate that hydroxylamine is predominantly in the uncharged form in solution (11). If the observed reaction is due to a small fraction of III present, then the reactivity of the oxygen anion must be very much higher than that for the uncharged molecule in order to account for the observed reaction. No evidence for O-acylhydroxylamine formation could be obtained with ethyl acetate, which reacted with hydroxylamine at a slower rate than did O-acetylhydroxylamine, or with acetyl chloride, which reacted with solvent more rapidly than with hydroxylamine (8).

The rate equation for the formation of aceto-hydroxamic acid from phenyl acetate is given by Equation (6) (11).

$$v = 0.7\,(\text{ester})(NH_2OH) + 6.0\,(\text{ester})(NH_2OH)^2 + 1.7\,(\text{ester})(NH_2OH)(NH_3{}^+OH) \qquad (6)$$

This rate equation implicates general base catalysis by hydroxylamine and general acid catalysis by hydroxyl-ammonium ion.

A kinetic scheme (Eq. 7) has been proposed by Notari involving an O-acetylhydroxylamine intermediate in the hydroxylaminolysis of ethyl acetate in basic solution (12).

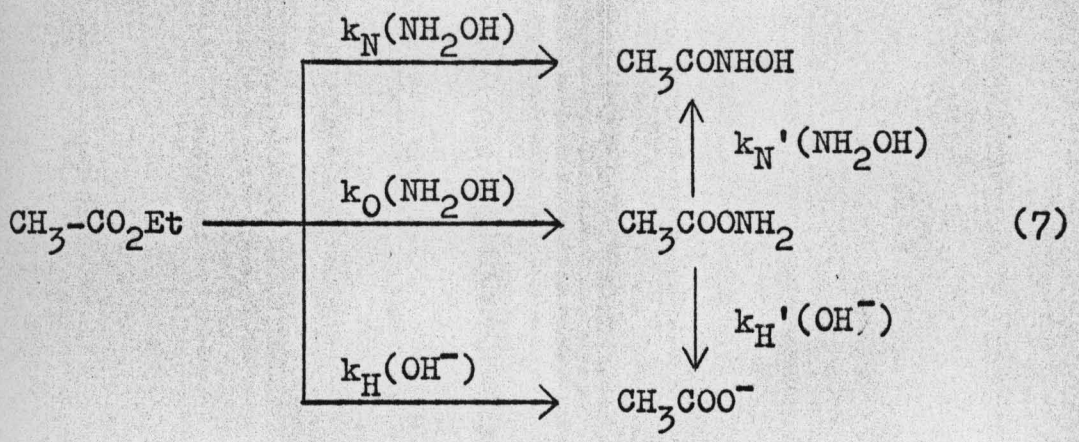

The intermediacy of O-acetylhydroxylamine was postulated because of higher observed yields of acetic acid than would be expected from only the hydrolysis of ethyl acetates.

The hydroxylaminolysis of γ-butyro- and δ-valerolactones give third and fourth order rate terms (14) (Eq. 8).

$$V = k_4(NH_2OH)^2(OH^-)(\text{lactone}) + k_3(NH_2OH)^2(\text{lactone}) \quad (8)$$

When the reaction takes place in the presence of imidazole, an additional term, $k_{IM}(NH_2OH)(\text{imidazole})(\text{lactone})$, appears. These rate terms suggest that two mechanisms are involved, one involving general base catalysis and one involving both specific base and general base catalysis.

Succinimide reacts with hydroxylamine to form a monohydroxamic acid, which rapidly cyclizes to N-hydroxysuccinimide in basic solutions, perhaps as shown in Equation (9) (14).

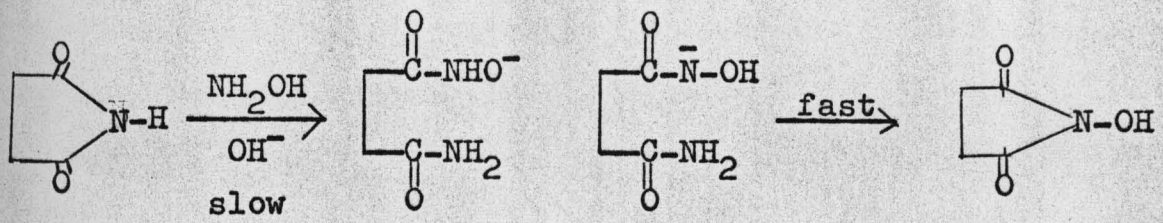

(9)

Although carboxylic acids do not react with hydroxylamine in neutral or alkaline solutions, hydroxamic acids are readily formed from carboxylic acids in acidic solution (15). The observed rate of reaction is reasonably large ($t_{1/2}$ = 350 min at 25° in 1.0 N HCl), but the position of equilibrium is shifted far to the left of Equation (10).

$$CH_3COOH + NH_2OH \rightleftharpoons CH_3CONHOH + H_2O \qquad (10)$$

Metal ion catalysis of hydroxamic acid formation from acetic acid in neutral solutions has recently been reported by Lawlor (16). Nickel (II) ions catalyze this reaction as do beryllium (II) and cobalt (II) ions.

Hydroxamic acids can be formed by the reaction of a carboxylic acid, hydroxylamine, and a carbodiimide, IV (17). The carbodiimide acts as a condensing agent (Eq. 11).

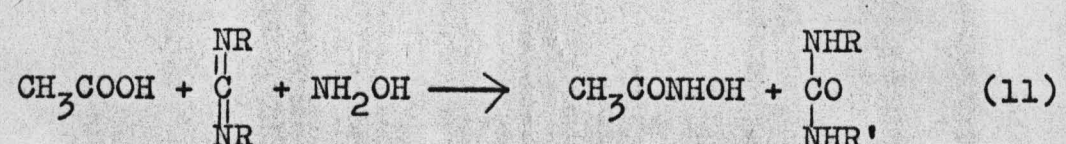

(11)

IV

A severe limitation of this reaction is that the hydroxamic acid also reacts with the carbodiimide to form the corresponding amine (Eqs. 12-14).

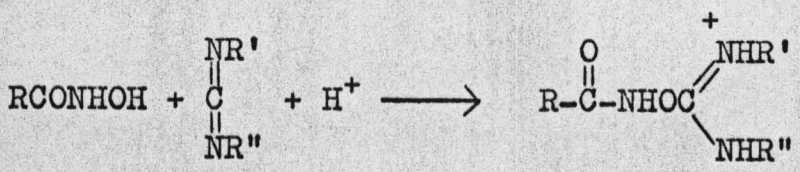

(12)

V

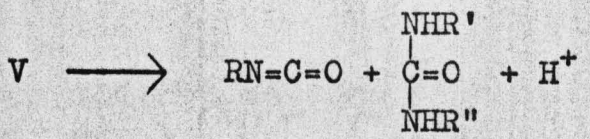

(13)

(14)

Simple amides react relatively fast with hydroxylamine at neutral pH. Jencks and Gilchrist (18) obtained a bell-shaped pH-rate profile for the hydroxylaminolysis of formamide, with the maximum being at pH 6.2-6.5. Evidence was obtained to indicate that the hydroxylammonium ion catalyzed the reaction and that a transition occurs from a rate determining step that is strongly dependent to one that is weakly dependent on catalyst concentration as concentration of the catalyst is increased. The following reaction scheme (Eq. 15) was proposed for this reaction.

$$NH_2OH + RCONH_2 \underset{k_{-1}[HA]}{\overset{k_1[HA]}{\rightleftharpoons}} HON(H)-\underset{R}{\overset{OH}{C}}-NH_2 \xrightarrow[k_3[HA]]{k_2} RCONHOH \qquad (15)$$

Formamide is more susceptible to hydroxylaminolysis than are esters below neutral pH (18). This is probably due to the greater basicity of amides (19); the pK_a of acetamide is about 0.0 and that of ethyl acetate is about -6.5. This difference in reactivity may, in suitable circumstances, allow analysis of a mixture of an amide and an ester by hydroxylaminolysis, the amide being determined at neutral pH and the total amide and ester at alkaline pH.

Thiol esters react quite rapidly at neutral pH with hydroxylamine (20). This is in sharp contrast to the slow reaction of oxygen esters with hydroxylamine, but is consistent with the relative reactivities of thiol and oxygen esters to other aminolysis reactions.

B. Analytical Applications

The ferric-hydroxamate method of analysis is carried out in three basic steps: (a) reaction of the substrate with hydroxylamine; (b) complexation of the resulting hydroxamic acid with ferric iron; and (c) measurement of the light absorption by the ferric-hydroxamate complex. These complexes usually have absorption maxima in the

range 500 to 550 nm, with molar absorptivities close to 10^3 $\underline{M}^{-1}$ cm^{-1}.

Feigl (21) first applied the ferric-hydroxamate method to analysis in spot tests for carboxylic acid derivatives. Soloway and Lipschitz (22) devised a spot test for amides and nitriles.* Lawlor (16) suggested that nickel (II) catalyzed hydroxamic acid formation from carboxylic acids might be useful as a spot test for the acids, though he did not describe the details of such a test. Buckles and Thelen (23) used the alkaline hydroxylaminolysis reaction in spot tests for a wide range of carboxylic acid esters, acid anhydrides, acid chlorides, amides, imides, and isocyanates. Positive tests were also obtained with formic and phthalic acids. These can possibly be attributed to impurities present in the sample but the possibility of some acid-catalyzed hydroxamic acid formation prior to the development of the ferric-hydroxamate complex should not be overlooked. An improved spot test for carboxylic acids in nonaqueous solutions has been suggested by Knight and Cleland (24). This method is based on conversion of acids to acid chlorides by the

---

*Nitriles react with hydroxylamine to form amidoximes which produce red colors with ferric ion (22).

$$R\text{-}C{\equiv}N + NH_2OH \rightleftharpoons R\text{-}\overset{\overset{NH}{\|}}{C}\text{-}NOH \rightleftharpoons R\text{-}\overset{\overset{NH_2}{|}}{C}{=}NOH$$

addition of thionyl chloride and subsequent conversion of the acid chlorides to the hydroxamic acid. The pyridine solvent used in this method aids in the dissolution of the acid, probably catalyzing the reaction, and aids in driving the reaction to the right.

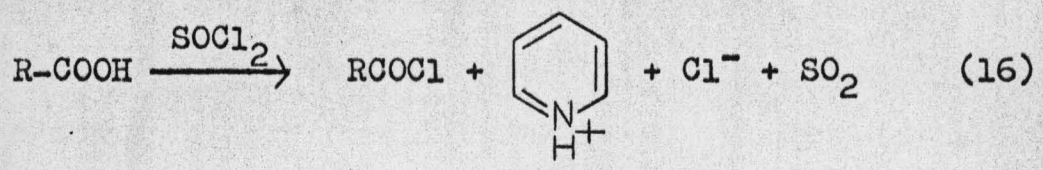

$$R\text{-}COOH \xrightarrow{SOCl_2} RCOCl + \text{(pyridinium)} + Cl^- + SO_2 \qquad (16)$$

A review of the sensitivity limits of the ferric-hydroxamate spot test for esters is given by Cheronis (25).

Aliphatic and aromatic esters of carboxylic acids have been quantitatively determined by alkaline hydroxylaminolysis (26-29). Esters of fatty acids have been determined by this method (30-32). Amides (26,29,33-37), acid chlorides (28), acid anhydrides (27,38), lactones (27), and imides have also been determined by the alkaline hydroxylaminolysis reaction. Phthalic acid esters have been determined in the presence of other esters (pH 7-8) (39).

A drawback to the alkaline reaction is that concurrent hydrolysis of the substrate may lead to substantially reduced yields, as shown by Notari for ethyl acetate (12).

Carboxylic acids have been measured indirectly by this method. The acid is esterified, and the ester is then converted to the hydroxamic acid. Duron and Nowotony (40) esterified fatty acids with boron trifluoride in methanol and measured the resulting methyl esters by the ferric-hydroxamate method. Tolbert and Kenner (41) measured

lactic acid via esterification with methanol-HCl followed by hydroxylaminolysis.

Indirect determination of alcohols by the ferric-hydroxamate method, first suggested by Hill (30), has been applied to some aliphatic alcohols by Gutnikov and Schenk (42). The alcohols were first acetylated and the acetate esters were then converted to the hydroxamic acids.

Hydroxamic acid formation has been widely used in biological studies to measure the amount of a particular acyl compound present. Acetylglycine (33), glutamic acid and asparagine (34), acetylphosphate (35), and glucono-lactone and galactolactone (43) have been determined by the neutral hydroxylaminolysis reaction. Acetylcholine (27), acetyl groups in pectin and carbohydrate polymers (44), lactone linkages in polysaccharides (45), sugar acids and reducing sugars (46), and D-glucono-δ-lactone (47,48) have been determined by the alkaline reaction.

Several pharmaceutically important compounds have been analyzed by the ferric-hydroxamate method. A summary of these is presented in Table I.

The relatively low molar absorptivity (about 10^3 $\underline{M}^{-1}$ cm^{-1}) of the ferric-hydroxamate complex limits this method to solutions of at least 0.0005 M in the carboxylic acid derivative. Hydroxamic acids have been measured by oxidizing two molecules of an arylhydroxamic acid (Eq. 17) and then using the liberated nitrite ion to diazotize a sulfanilamide molecule.

TABLE I

Pharmaceuticals Determined by the Ferric-Hydroxamate Method

Compound	Reaction Conditions	Functional Group	Reference
Panthenol	alkaline	lactone[a]	49
Penicillin	neutral	β-lactam	50,51
Chloramphenicol	alkaline	succinate ester	52
Chloramphenicol	alkaline	amide	53
Pilocarpine	alkaline	lactone	54,58
Lactic acid	alkaline	ester[b]	41
Di-(n-octyl) Sodium Sulfo-succinate	alkaline	ester	55

[a]formed by reaction of panthenol in HCl.

[b]acid esterified with methanolic-HCl.

$$2Ar\text{-}CONHOH \longrightarrow Ar\text{-}CONHOCO\text{-}Ar + NO_2^- \qquad (17)$$

The sulfanilamide is then coupled with N-1-naphthalene-diamine, the color of the coupled product being measured spectrophotometrically. Using this method concentrations of 10^{-6} to 10^{-5} M can be determined (56). This method is not generally used as a finish for the hydroxamic acid formed in a hydroxylaminolysis reaction since hydroxyl-amine, a reactant, can also be oxidized to produce nitrite ions.

Despite its limited sensitivity, the ferric-hydroxamate reaction provides a very useful general method for the analysis of carboxylic acid derivatives.

C. Research Plan

A commonly stated advantage of the ferric-hydroxamate method is that the hydrolysis products of the substrate (i.e., carboxylic acid and an alcohol, amine, halide, or another acid) do not interfere with the reaction. Thus an ester of a carboxylic acid can be determined in the presence of the parent acid, a very satisfactory circumstance. On the other hand, the non-reactivity of the acid precludes its own determination by this method.

Lawlor (16), while investigating a model enzyme system for phosphorylation (57), observed hydroxamic acid formation from acetate ion in the presence of nickel (II)

ions. This reaction may provide possible extension of the ferric-hydroxamate method. If the reaction occurs on a reasonable time scale, if the equilibrium is favorable, and if the reaction is general for carboxylic acids, then a colorimetric method for the analysis of carboxylic acids might be developed. The nickel (II) catalysis might conceivably occur with other substrates, suggesting the possibility of catalytic hydroxamic acid formation under mild conditions. Metal-ion catalysis might be viewed as a type of acid catalysis, so the present study was extended to include both nickel and hydrogen-ion catalysis of hydroxamic acid formation from carboxylic acids and some of their derivatives.

A major goal was, as noted, the exploration of possible extensions of the ferric-hydroxamate analytical method. In addition, observations have been made on the kinetics, equilibria, and mechanisms of these reactions, both to aid in analytical development and because these acyl transfer reactions are of considerable chemical interest.

II. EXPERIMENTAL

A. Materials

All inorganic chemicals, unless otherwise stated, were analytical reagent grade and were used without purification. Ferric perchlorate hexahydrate ($Fe(ClO_4)_3 \cdot 6H_2O$) and nickel perchlorate hexahydrate ($Ni(ClO_4)_2 \cdot 6H_2O$) were obtained from the G. F. Smith Co. and were used directly. Hydroxylamine perchlorate was prepared *in situ* by mixing equimolar quantities, in aqueous solutions, of silver perchlorate (G. F. Smith Co.) and hydroxylamine hydrochloride (Mallinckrodt Chemical Co.), and removing the precipitated silver chloride by filtration. The aqueous solution of hydroxylamine perchlorate was used immediately.

Ethyl acetate (Mallinckrodt Chemical Co.) was analytical grade and was used directly. Phenyl acetate (Aldrich Chemical Co.) was distilled at atmospheric pressure; b.p. 193-194° (Lit.: 193-195° (59)).

Acetohydroxamic acid was synthesized by the following modified procedure of Wise and Brandt (60). 56.1 g of potassium hydroxide, dissolved in 150 ml of methanol, was slowly added to 46.7 g of hydroxylamine hydrochloride which had been dissolved in 240 ml of methanol at reflux temperature; both solutions were at 40° before the addition. During the addition the mixture was cooled in

an ice bath to prevent excess temperature rise. The mixture was cooled in an ice-water bath for 10 minutes to precipitate potassium chloride, which was then removed by filtration. Ethyl acetate (30 g) was added to the reaction mixture and the resulting solution was allowed to stand at room temperature for four hours, when it was acidified with concentrated hydrochloric acid. The solvent was evaporated under reduced pressure, giving a syrupy residue, which was extracted with four 100-ml portions of boiling ethyl acetate. Crystals were obtained from the ethyl acetate solution upon cooling. The acetohydroxamic acid was recrystallized twice from ethyl acetate-methanol mixture (10:1); m.p. 89° (lit.: 89-91° (61)). Benzohydroxamic acid (Eastman Organic Chemicals) was recrystallized from hot water; m.p. 127-129° (lit.: 124-125° (62)).

Methanol (Mallinckrodt Chemical Co.), t-butanol, dioxane, and pyridine (all from Fisher Scientific Co.) were analytical grade reagents and were used directly.

Monochloroacetic acid (Mallinckrodt Chemical Co.) and succinic acid (Allied Chemical Co.) were analytical grade reagents and were used directly. Phenylacetic acid (Eastman Organic Chemicals) was recrystallized from Skellysolve^{R} B; m.p. 74-75° (lit.: 76-76.5° (63)). p-Methoxybenzoic acid (Merck Chemical Co.) was recrystallized from methanol-water mixture; m.p. 181-182° (lit.: 184° (64)). Diphenylacetic acid (Eastman Organic Chemicals)

was recrystallized from methanol-water mixture, m.p. 145-146° (lit.: 144-145° (65)). 3,5-Dinitrobenzoic acid (Fisher Scientific Co.) was recrystallized from methanol-water mixture; m.p. 204.5-206° (lit.: 205-207° (66)). Benzoic acid (Mallinckrodt Chemical Co.) was recrystallized twice from methanol; m.p. 121-122° (lit.: 122° (67)). Glycine (Fisher Scientific Co.) was recrystallized from methanol-water mixture; m.p. 225° d (lit.: 225-230° d (68)). o-Methoxybenzoic acid (Eastman Organic Chemicals) was used directly.

Benzhydrazide was synthesized by the method of Gatterman and Wieland (69). The product was recrystallized from hot water; m.p. 111-112° (lit.: 112° (70)). Acethydrazide was synthesized by the method of Curtius and Hofman (71). The product was recrystallized from ether; m.p. 65° (lit.: 67° (71)). Semicarbazide hydrochloride (Eastman Organic Chemicals) was recrystallized from methanol-water mixture; m.p. 175-180° d (lit.: 173° d (72)). Acetophenylhydrazide (Eastman Organic Chemicals) was recrystallized from methanol-water mixture; m.p. 127-128° (lit.: 128° (73)). Isonicotinic acid hydrazide (Pfizer Chemical Co.) was recrystallized from methanol; m.p. 169-170° (lit.: 171° (74)). p-Nitrobenzhydrazide (Eastman Organic Chemicals) was recrystallized from methanol; m.p. 209-210° (lit.: 210° (75)).

All water was redistilled from alkaline permanganate. Acetic acid stock solutions were prepared by diluting glacial acetic acid (Dupont Chemical Co.) with water and standardizing by titration with standard sodium hydroxide.

Ferric perchlorate stock solution (1.5 M) was prepared by dissolving 693.45 g of ferric perchlorate hexahydrate and 217 ml of 60% perchloric acid in enough water to make 1 liter. This solution was stored in the dark. Ferric perchlorate reagent solutions (0.15 M) were prepared as follows: 100.0 ml of ferric perchlorate stock solution were added to 500 ml of absolute methanol. This solution was then diluted to 1 liter with methanol, the final volume adjustment being made at 25°. Standard buffer solutions were prepared according to Bates (76). Phenyl acetate stock solutions in methanol were freshly prepared before use.

B. Apparatus

Spectral measurements were made with either a Cary model 14 or model 16 spectrophotometer fitted with thermostated cell compartments that maintained temperature constant to ±0.1°.

pH measurements at 25.0° were made with either a Radiometer pH meter model 25 with scale expander and equipped with a Sargent combination electrode S-30072-15, or an Orion model 801 pH meter* equipped with a Fisher high-temperature combination electrode 13-639-90. pH

---

*The Orion pH meter was graciously loaned by Prof. Joseph R. Robinson. I am also indebted to him for use of a high-temperature water bath.

measurements at 90.5° were made with the Orion model 801 pH meter and the Fisher high-temperature combination electrode 13-639-90. For these latter measurements, standard buffer solutions and the sample solution were equilibrated to 90.5° in a jacketed beaker prior to pH measurement. The beakers were covered with a Teflon^{R} disc to reduce evaporation.

Water bath temperatures at 25.0° were maintained to ±0.1° with a Sargent Thermonitor Electric Relay or with a "Temptrol 151" water bath (Precision Scientific Co.). Water bath temperatures at 90.5° were maintained to ±0.1° with a "Temptrol 151" water bath (Precision Scientific Co.) or with a "Dual-Purpose" water bath system equipped with a relay, heater, stirrer and circulator (American Instrument Co.) and regulated by a mercury column thermo-regulator (Bronwill Scientific Co.).

Melting points were determined on a Thomas-Hoover Capillary melting point apparatus.

Thermometers for use at 25.0° were calibrated against a thermometer carrying a National Bureau of Standards calibration certificate. Thermometers for use at 90.5° were calibrated against a reference thermometer which had been calibrated against a thermometer carrying an ASTM certificate.

C. Kinetic Measurements

1. Hydroxamic Acid Formation from Carboxylic Acids and Acid Hydrazides

Reaction mixtures were prepared by mixing appropriate aliquots of reactant stock solutions and adjusting pH with concentrated sodium hydroxide or hydrochloric acid solutions. Typical initial concentrations for these mixtures were 0.8 M hydroxylamine hydrochloride, 0.04 M nickel chloride, and 0.04 M acetic acid. When nickel was not present, the acetic acid concentration was raised to 0.4 M. Acid hydrazide concentrations were 0.005 M. After the solutions had been brought to volume, small adjustments in pH were made by dropwise addition of saturated sodium hydroxide solution or concentrated hydrochloric acid. Three ml portions of the reaction mixture were transferred to 5 ml ampules with a 10 ml glass syringe fitted with a 15 gauge needle. (All ampules, Kimble Neutraglas^{R}, were rinsed once with hot distilled water and dried before use.) The ampules were sealed.

To initiate the reaction the ampules were placed in a 90.5° water bath.* Samples were removed at recorded

---

*Elevated temperatures were needed because of the extremely slow reaction rate at 25°.

times and quenched in a dry ice-2-propanol bath. The ampules were then stored in a refrigerator freezer (-5 to -10°) until all of the samples were collected. They were then brought to 25.0°. 1.0 ml of the contents of an ampule was added to 20 ml of ferric perchlorate reagent solution contained in a foil-wrapped flask. After one hour, the absorbance at 530 nm, due to the ferric-hydroxamate complex, was measured.*

Rate constants for reactions at pH greater than 3 were calculated from initial velocity measurements, initial concentrations, and the rate equation. At pH less than 3, the reactions quickly reach equilibrium. For these reactions the rate constants were calculated from plots of log $(A_\infty - A_t)$, where A_t is the absorbance at time t and A_∞ is the absorbance at "infinity", against time. Since absorbances must be converted to concentrations in order to convert the initial slope dA_{530}/dt to initial rate dC/dt (Eq. 18), the molar absorptivities of acetohydroxamic and benzohydroxamic acids, under the analytical conditions, were determined using authentic samples of each hydroxamic acid ($\epsilon_{530} = 1.17 \times 10^3$ for acetohydroxamic acid and $\epsilon_{530} = 1.56 \times 10^3$ for benzohydroxamic acid).

---

*It has been shown by Notari and Munson (77) that the stability of the color of the ferric-hydroxamate solution is determined by the ratio $(Fe^{3+})_T/(NH_2OH)_T$ (subscript T denotes total concentration of all species), which should be at least 5. In the present work this ratio was 4, with the result that an initial period of instability is followed by a fairly stable color, hence the 1 hour waiting time.

$$\frac{dC}{dt} = \frac{dA}{dt}\left(\frac{1}{\epsilon b}\right)^{*} \qquad (18)$$

For reactions in which the product hydroxamic acid was different from these, the molar absorptivity of acetohydroxamic acid was used for aliphatics and that of benzohydroxamic acid for aromatics; this approximation will not be in error by more than a few percent since molar absorptivities of ferric-hydroxamate complexes are not very sensitive to acyl structure (28).

The succinic acid reactions were carried out in the same manner. All measurements were made in the first 2 or 3 percent of the reaction where the formation of a dihydroxamic acid is unlikely.

The acid hydrazide kinetics were studied similarly, all rate constants being calculated from plots of log $(A_\infty - A_t)$ against time where A_∞ represents the absorbance at "infinity" and A_t the absorbance at a measured time.

2. Phenyl Acetate Kinetics

a) Rate of Phenol Release. Reaction mixtures were prepared in volumetric flasks by mixing aliquots of reactant stock solutions and adjusting pH to the desired

---

*ϵ represents the molar absorptivity of the complex ($\underline{M}^{-1}$ cm^{-1}) and b is the cell path length (cm).

value with small volumes of saturated sodium hydroxide solution or concentrated hydrochloric acid. Three ml of the reaction mixture were pipeted into 1 cm square cells in the Cary model 14 recording spectrophotometer. The samples were allowed to equilibrate to the compartment temperature for 15 minutes. 0.025 ml of a methanolic phenyl acetate solution (0.071 M) was added to the sample cell and the absorbance at 275 nm was recorded as a function of time. Plots of log $(A_\infty - A_t)$ against time, or the method of Guggenheim (78), gave apparent first-order rate constants from the measured absorbance values.

b) Rate of Hydroxamic Acid Production. The pH of reaction mixtures was adjusted such that when the phenyl acetate stock solution was added and the solution was made up to volume, the final pH was 6.05. Typical concentration of phenyl acetate in the reaction mixture was 0.0065 M. Using this method, pH selection was usually reliable to $\pm$0.02 pH units and always to $\pm$0.05 pH units. The final solution was shaken well to insure dissolution of phenyl acetate and was poured into a 25 ml jacketed buret through the jacket of which 25.0° water was circulated. 1.0 ml samples each were run into 20 ml of 0.15 M ferric perchlorate solution at recorded times. One hour after sampling, the absorbances of the ferric perchlorate solutions were measured at 530 nm. First-order rate constants were obtained from plots of log $(A_\infty - A_t)$

against time. By using the jacketed buret to measure the reaction rates it is possible to measure rate constants of reactions having half-lives of 30 seconds. This would be impossible to do with sample removal by pipet.

3. Ethyl Acetate Kinetics

The ethyl acetate kinetics were measured in the same manner as the carboxylic acid kinetics. Initial concentrations of ethyl acetate were usually 0.4 M. Due to the vapor pressure of the ethyl acetate it was necessary to freeze the contents of the ampules before sealing them. Failure to do this resulted in imperfect seals. First-order rate constants were obtained from initial rates.

4. Acetohydroxamic Acid Hydrolysis

1.0 ml of an acetohydroxamic acid stock solution (0.15 M) was added to 99 ml of a buffer solution. 4.0 ml portions of this mixture were transferred to ampules with a 10 ml glass syringe equipped with a 15 gauge needle. The ampules were sealed and placed in a 90.5° water bath. They were withdrawn at intervals and placed in a dry ice-2-propanol bath to quench the reaction. Ampules were then stored in the refrigerator freezer until all samples were taken. The ampules were then brought to 25.0° and 3.0 ml of sample were added to 10 ml of 0.15 M ferric

perchlorate solution in a foil-wrapped flask. The absorbance at 530 nm was read after one hour. Apparent first-order rate constants were calculated from plots of log $(A_t - A_\infty)$ against time.

III. RESULTS

A. Nickel (II)-Catalyzed Hydroxamic Acid Formation from Acetic Acid and Other Carboxylic Acids

The experimental conditions used by Lawlor (16) included these initial reactant concentrations: sodium acetate, 1 M; hydroxylamine hydrochloride, 0.1 M, and nickel nitrate, 0.125 M. These conditions are not satisfactory for an analytical reaction for the acid because of the high concentration of substrate, sodium acetate, required for measurable reaction rates. The experimental conditions for the present study were therefore altered to reflect a more realistic system for analysis of the acid. The initial concentration adopted for study were: sodium acetate, 0.035 M; hydroxylamine hydrochloride, 0.8 M; and nickel chloride, 0.04 M.

The ratio of hydroxylamine to nickel (II) was found to be important in determining the maximum pH attainable in the system. As pH is increased in solutions containing nickel (II), insoluble nickel hydroxide complexes are formed. In the absence of hydroxylamine the precipitation from solutions containing 0.04 M nickel chloride is first observed at pH 3-4 as the pH is increased by the addition of sodium hydroxide. If hydroxylamine is present, the formation of soluble nickel-hydroxylamine complexes in

effect reduces the concentration of nickel (II) available for formation of the insoluble nickel hydroxides. In the presence of 0.8 M hydroxylamine hydrochloride (i.e., "total" hydroxylamine concentration is 0.8 M), the pH of these solutions can be raised to about 7 (25.0°) before precipitation is observed. At pH 7 and 25°, 90 percent of the hydroxylamine is in the base form and more than 90 percent of acetic acid will be in the anion form.

Rate constants for the nickel (II)-catalyzed reaction of hydroxylamine with acetic acid to give acetohydroxamic acid were obtained from initial rate measurements. Typical plots of absorbance against reaction time are shown in Figure 1. All total (analytical) concentrations are denoted by brackets with a subscript T. (E.g., $[NH_2OH]_T$ is the total molar hydroxylamine concentration, so $[NH_2OH]_T = [NH_2OH] + [NH_3OH^+]$). Only the first 3 to 5 percent of the reaction was followed in obtaining initial rates. The initial slopes, dA_{530}/dt, are converted to initial rates, dC/dt, by dividing the initial slope by the product of the molar absorptivity of the ferric hydroxamate, ϵ, and the cell path length, b. Apparent first-order rate constants are obtained by dividing the rate by the total concentration of the substrate, acetic acid. An apparent second-order rate constant is obtained by dividing the apparent first-order constant by the total hydroxylamine concentration.

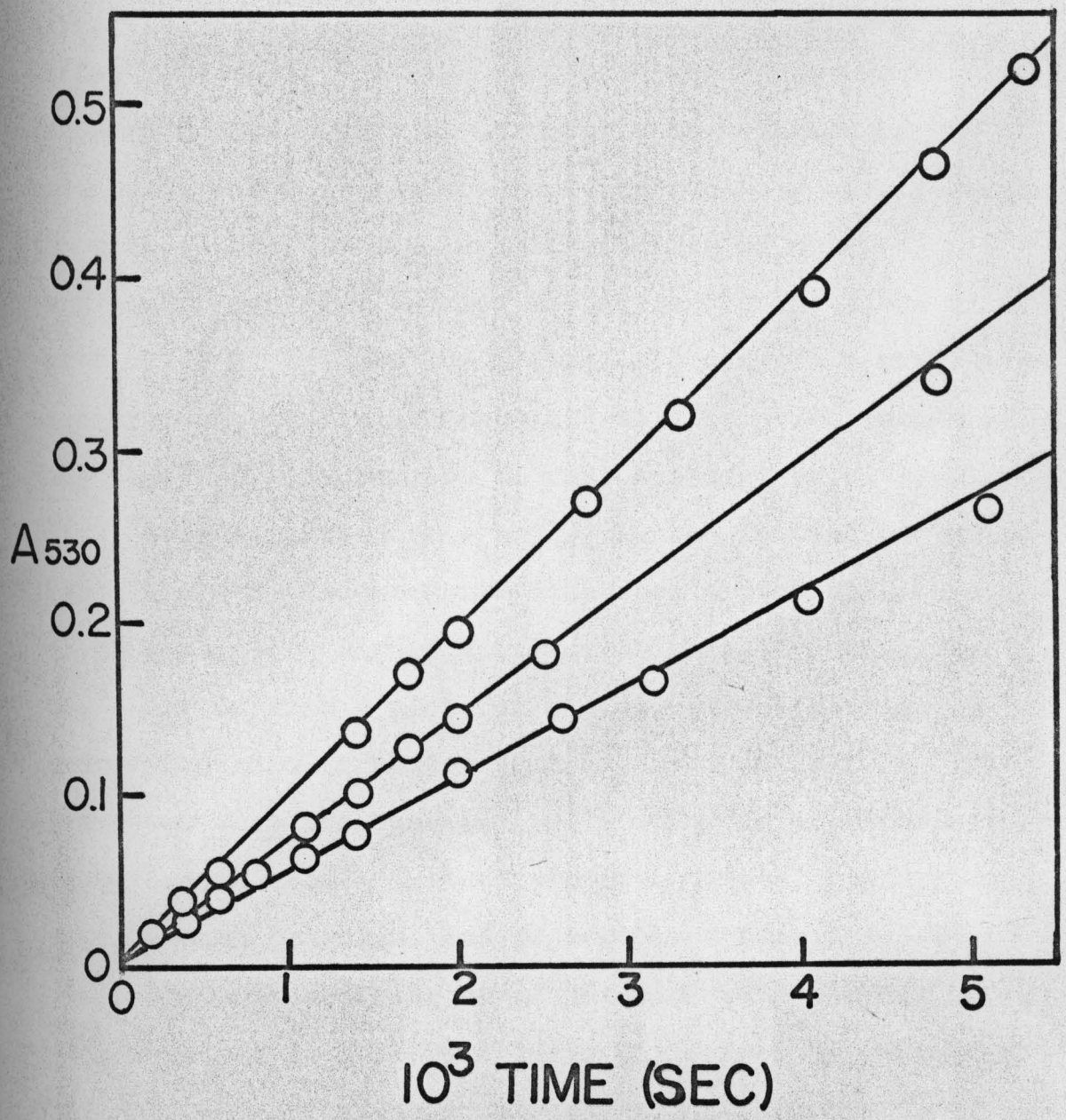

Figure 1. Initial rate plots for nickel (II)-catalyzed hydroxamic acid formation from acetic acid. $[NH_2OH]_T$ = 0.8 M, $[NiCl_2]_T$ = 0.04 M, μ = 1.0, T = 90.5°, pH 3.25 (90.5°), total acetic acid concentration from top to bottom, (M) 0.0345, 0.0258, 0.0172.

The order of a reaction with respect to a reactant can be determined from the general rate equation, $V = kC^n$, where V is the rate of the reaction, k is the nth-order rate constant, C is the concentration of the reactant, and n is the order of the reaction with respect to that reactant. The logarithmic form of this expression is $\log V = \log k + n \log C$. The slope of a plot of log V against log C (when all other concentrations are held substantially constant) will be n, the order of the reaction with respect to that reactant being considered. If V_o is the initial rate and C_o is the initial concentration, the rate measurements described above can be treated in this manner. Figure 2 (data in Table II) shows that the slope of such a plot for nickel (II)-catalyzed hydroxamic acid formation from acetic acid is 1.0. This indicates that the reaction is first order with respect to total acetic acid. In this experiment total hydroxylamine, total nickel chloride, and pH were kept constant. It is possible to find the order of reaction with respect to each reactant in turn by holding the concentrations of all but the reactant of interest essentially constant. Thus any variation in rate will depend only on variations in the concentration of that particular reactant. The data for the order of reaction with respect to total hydroxylamine are presented in Table III (Figure 3). The observed slope is 0.83. This deviation from unity is probably due to complexation of some of the hydroxylamine with nickel (II),

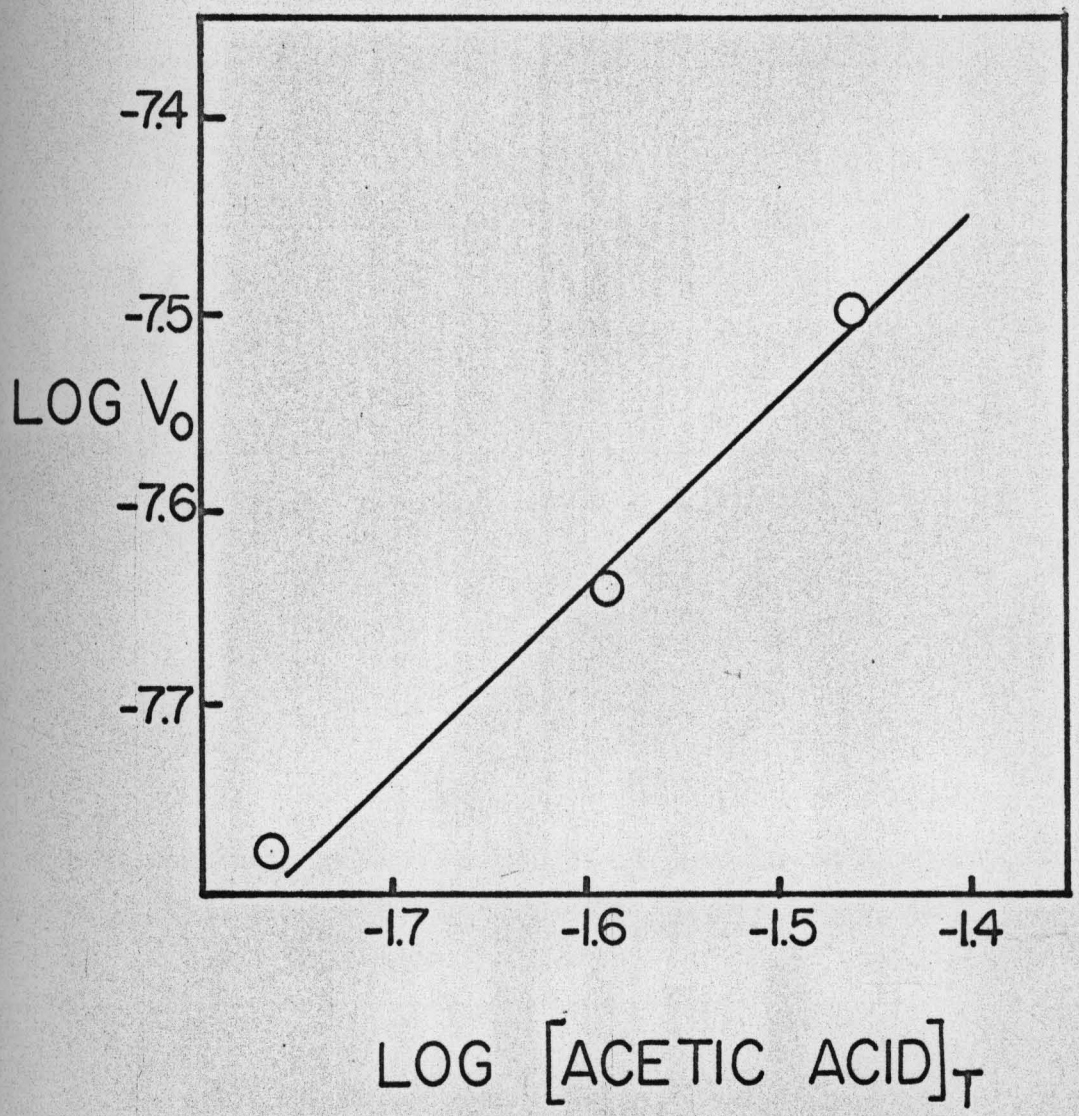

Figure 2. Log-log plot of initial rates as a function of total acetic acid concentration. The slope of the line is 1.0. Data from Table II.

TABLE II

Initial Rates for the Reaction of Hydroxylamine and Acetic Acid in the Presence of Nickel Chloride[a]

10^8 Initial Rate, V_o ($\underline{M}$ sec^{-1})	log V_o	10^2 [Acetic Acid]$_T$ ($\underline{M}$)	log [Acetic Acid]$_T$
3.26	- 7.49	3.45	- 1.46
2.38	- 7.64	2.58	- 1.59
1.65	- 7.78	1.72	- 1.76

[a] 90.5°; pH 5.25; μ = 1.0; 0.04 $\underline{M}$ $NiCl_2$; 0.80 $\underline{M}$ $NH_2OH \cdot HCl$.

TABLE III

Initial Rates for the Reaction of Acetic Acid with Hydroxylamine in the Presence of Nickel Chloride[a]

10^8 Initial Rate, V_o ($\underline{M}$ sec^{-1})	log V_o	[NH_2OH]$_T$ ($\underline{M}$)	log [NH_2OH]$_T$
0.53	- 6.27	0.40	- 0.40
0.76	- 6.12	0.60	- 0.23
0.93	- 6.03	0.80	- 0.10
1.16	- 5.94	1.00	0
1.31	- 5.88	1.20[b]	+ 0.08

[a] 90.5°; pH 5.15; μ = 1.2; 0.04 $\underline{M}$ $NiCl_2$; 0.045 $\underline{M}$ acetic acid.

[b] μ = 1.32.

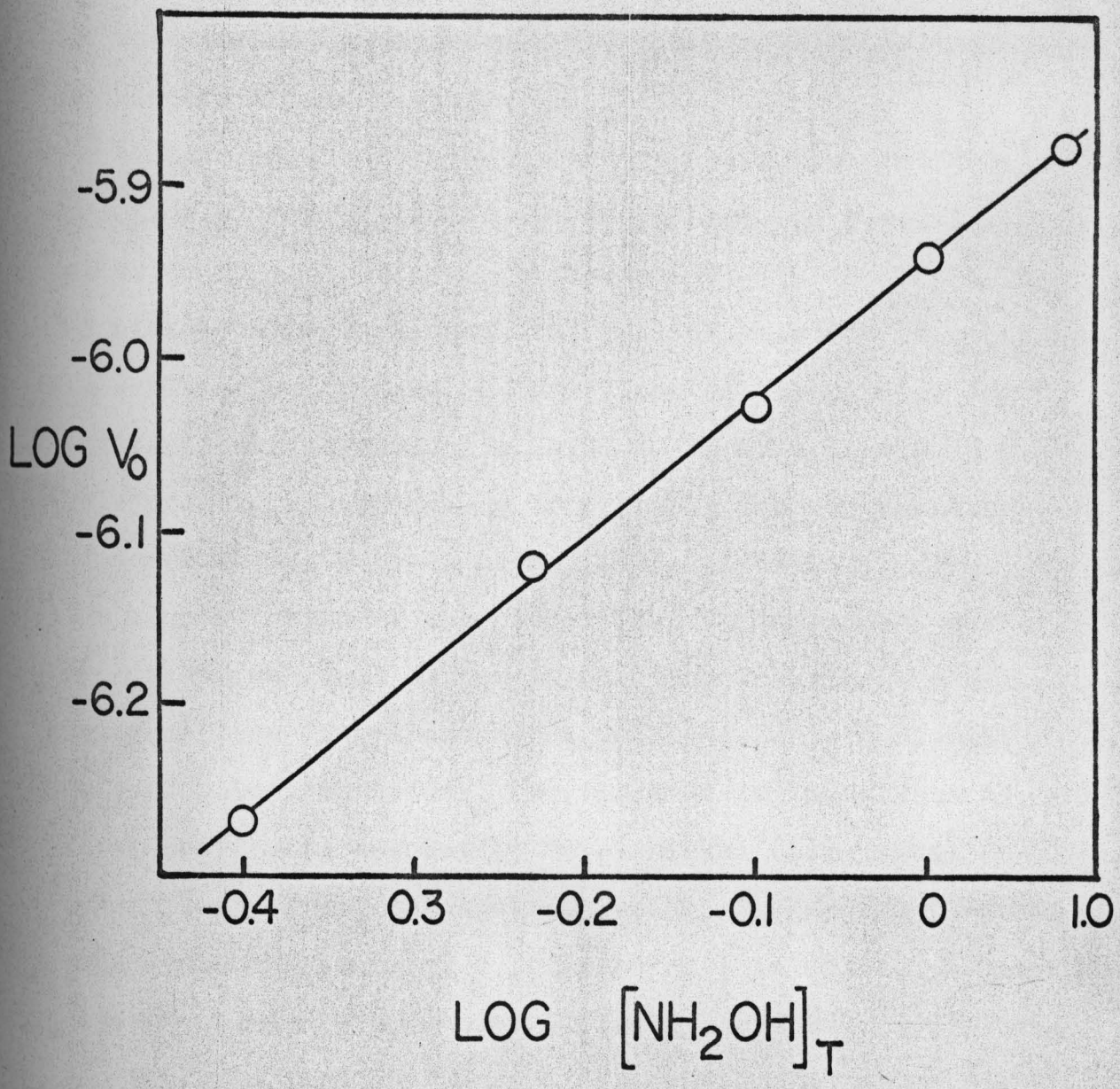

Figure 3. Log-log plot of initial rates as a function of total hydroxylamine concentration. Slope of the line is 0.83. Data from Table III.

so that the actual hydroxylamine concentration was less than the apparent concentration.

Plots of absorbance against reaction time for the reaction of hydroxylamine and acetic acid at several nickel chloride concentrations are shown in Figure 4. The effect of nickel concentration on the rate of reaction is presented in Table IV and Figure 5. The slope of the plot of log V_o (initial rate) against log $[NiCl_2]_T$ in this figure is 0.69. This fractional dependency is probably another manifestation of complexation between nickel (II) and hydroxylamine. As the concentration of the nickel (II) is increased, more hydroxylamine would be complexed, thus lowering the actual concentration of hydroxylamine available as a nucleophile. At this point, therefore, the reaction is thought to be first order with respect to total nickel (II), total hydroxylamine, and total acetic acid. The apparent second order rate constants as a function of total nickel chloride concentration are presented in Table V and Figure 6. The slope of the line in Figure 6, $k'_{Ni}/[NiCl_2]_T$, gives the apparent catalytic constant for nickel (II) (Eq. 19).

$$k'_{Ni} = k_{Ni} [NiCl_2]_T \qquad (19)$$

The value of k_{Ni} is 3.8×10^{-4} $\underline{M}^{-2}$ sec^{-1} for this set of experimental conditions of temperature, solvent, and ionic strength. When the reaction rate was measured in the

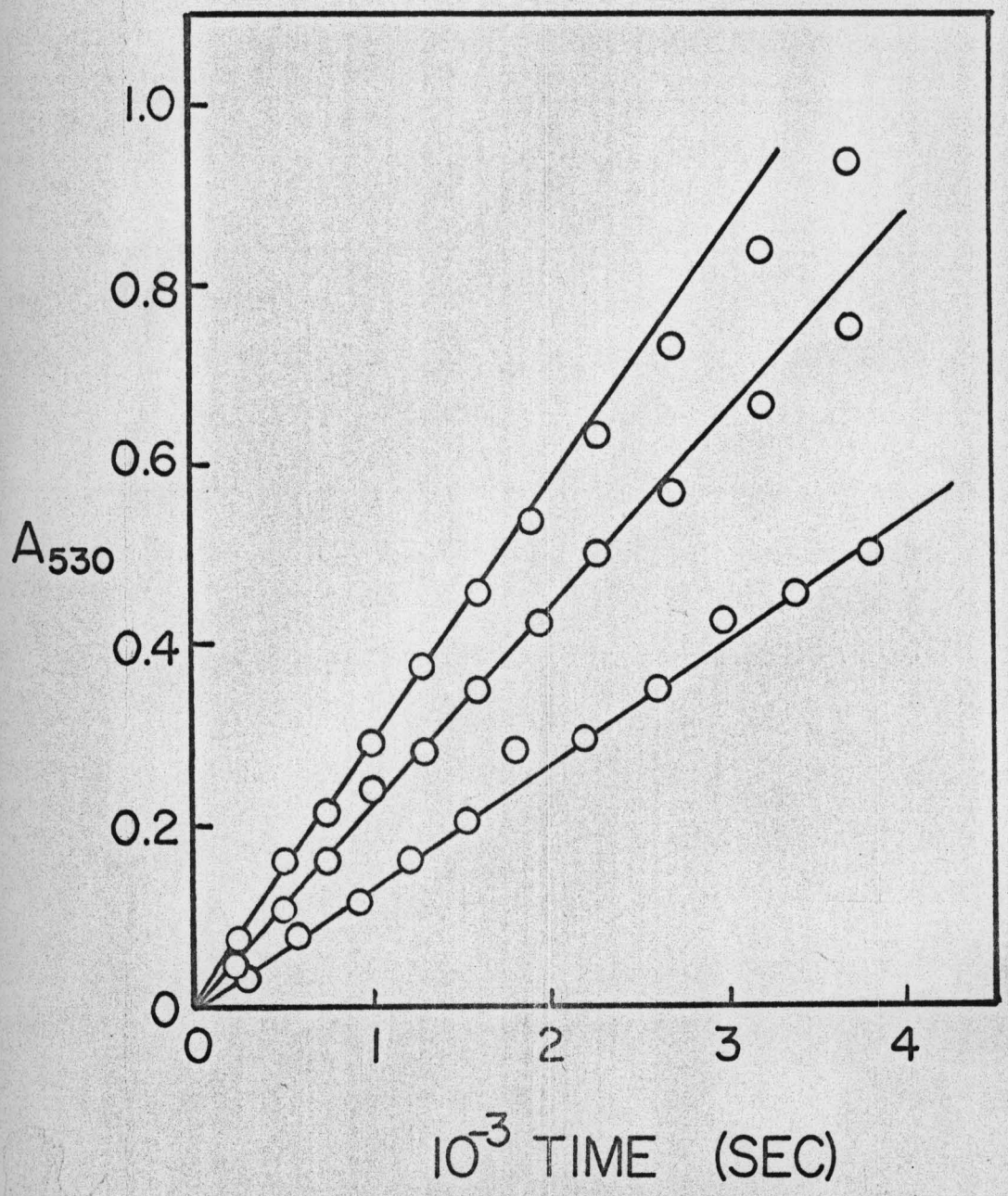

Figure 4. Initial rate plots for the reaction of hydroxylamine and acetic acid in the presence of $NiCl_2$; 0.80 M $NH_2OH \cdot HCl$; 0.045 M acetic acid; μ = 1.2; pH 5.15; T = 90.5°; $[NiCl_2]_T$ from top to bottom 0.12, 0.08, 0.04 M.

TABLE IV

Initial Rates and First Order Rate Constants for the Reaction of Hydroxylamine and Acetic Acid in the Presence of Nickel Chloride[a]

10^6 Initial Rate, V_o ($\underline{M}$ sec^{-1})	log V_o	10^5 k_{obs}[b] (sec^{-1})	$[NiCl_2]_T$	log $[NiCl_2]_T$
0.93	- 6.03	2.06	0.04	- 1.40
1.48	- 5.83	3.28	0.08	- 1.10
2.01	- 5.70	4.47	0.12	- 0.92

[a] 90.5°; pH 5.15; 0.80 $\underline{M}$ $NH_2OH \cdot HCl$; 0.045 $\underline{M}$ acetic acid; μ = 1.2.

[b] k_{obs} is an apparent first order rate constant.

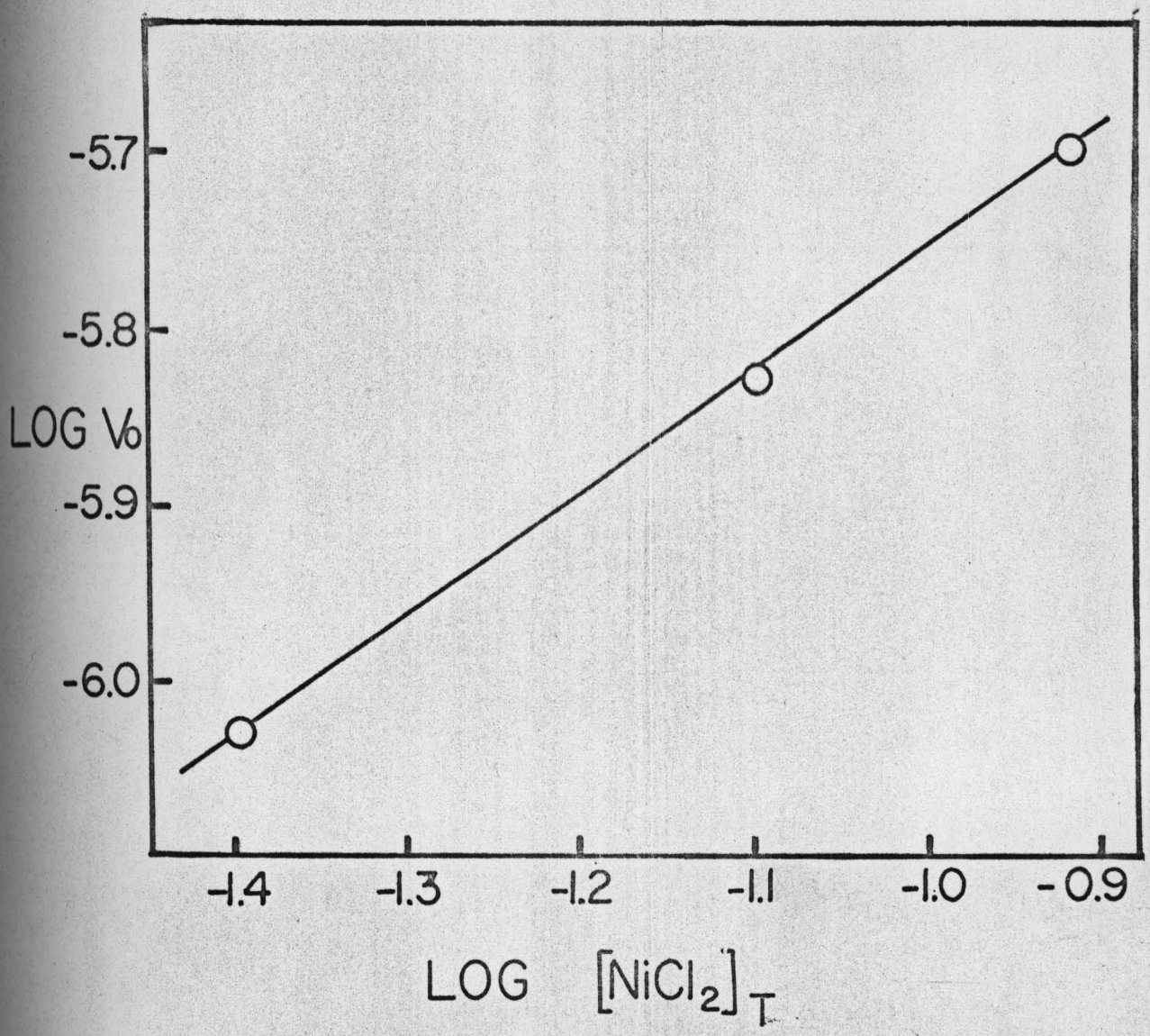

Figure 5. Log-log plot of initial rates for reaction of hydroxylamine and acetic acid in the presence of nickel chloride against total nickel chloride concentration. Data from Table IV.

TABLE V

Second-Order Rate Constants for the Reaction of Hydroxylamine and Acetic Acid in the Presence of Nickel Chloride[a]

$NiCl_2$ (M)	10^5 k_{obs} (sec^{-1})[b]	10^5 k' ($\underline{M}^{-1}$ sec^{-1})[c]
0.04	2.06	2.58
0.08	3.28	4.10
0.12	4.47	5.60

[a] 90.5°; pH 5.15; 0.80 $\underline{M}$ $NH_2OH \cdot HCl$; 0.045 $\underline{M}$ acetic acid; μ = 1.2.

[b] From Table IV.

[c] $k' = k_{obs}/[NH_2OH]_T$

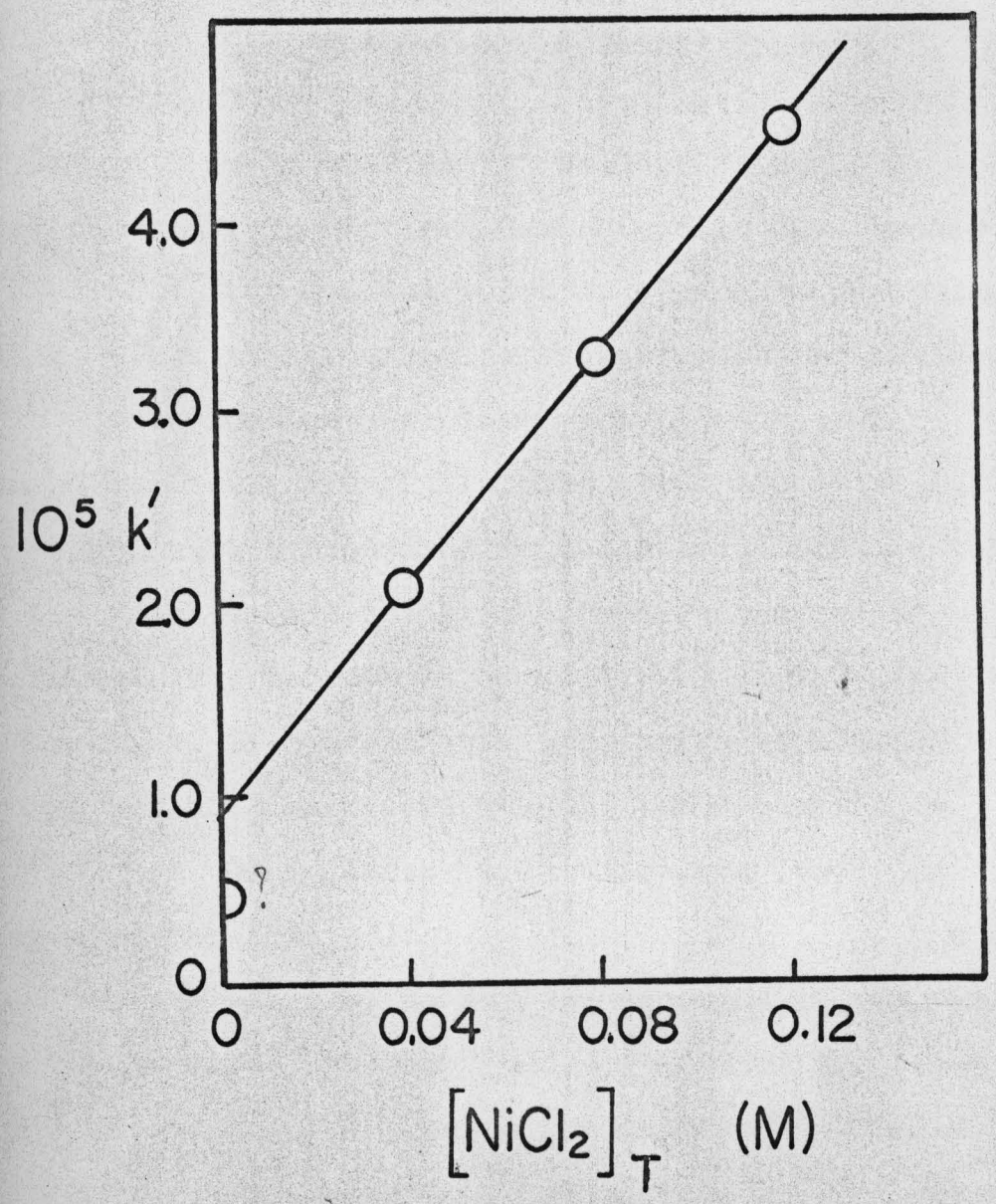

Figure 6. Plot of apparent second-order rate constants for the reaction of hydroxylamine and acetic acid in the presence of various $NiCl_2$ concentrations. Data from Table V. k' is defined by $k' = V/[HOAc]_T [NH_2OH]_T$.

absence of nickel (II), a finite rate constant was obtained (note also the non-zero extrapolated intercept in Figure 6). This suggests the presence of another reaction that occurs without nickel (II) catalysis. The intercept of Figure 6 would be expected to pass through the experimental rate constant determined in the absence of nickel (II), but the intercept is above the experimental point. This higher value is probably another manifestation of complexation between nickel and hydroxylamine. Although the pH and total hydroxylamine concentration are held constant, more hydroxylamine is complexed with nickel (II) as the total nickel chloride concentration is increased. Therefore, the concentration of free hydroxylamine, the nucleophile, is not constant and varies with nickel concentration. Each experimental point (except at [Ni(II)] = 0) in Figure 6 is therefore lower than if corrected for this effect.

The pH-rate profile for the nickel (II)-catalyzed hydroxamic acid formation from acetic acid is presented in Table VI and Figure 7, where the logarithm of the apparent second-order rate constants are plotted as a function of pH. The solid line is drawn from the rate equation,

$$V = k_1^{Ni}[HOAc][NH_2OH][H^+] + k_2^{Ni}[HOAc][NH_2OH] + k_3^{Ni}[OAc^-][NH_2OH][Ni^{+2}] \quad (20)$$

TABLE VI

Apparent Second-Order Rate Constants for the Reaction of Hydroxylamine and Acetic Acid in the Presence of Nickel Chloride[a]

pH (90.5°)	10^5 k' ($\underline{M}^{-1}$ sec^{-1})[b]	log k'
3.20	0.45	- 5.35
3.82	0.59	- 5.23
4.04	0.76	- 5.12
4.50	1.33	- 4.89
4.68	1.95	- 4.71
4.93	2.37	- 4.63
5.21	2.45	- 4.61
5.28	2.48	- 4.61
5.45	2.72	- 4.57
5.83	2.83	- 4.55

[a] 90.5°; 0.04 $\underline{M}$ $NiCl_2$; 0.80 $\underline{M}$ $NH_2OH \cdot HCl$; 0.035 $\underline{M}$ acetic acid; μ = 1.0.

[b] $k' = V/[HOAc]_T [NH_2OH]_T$

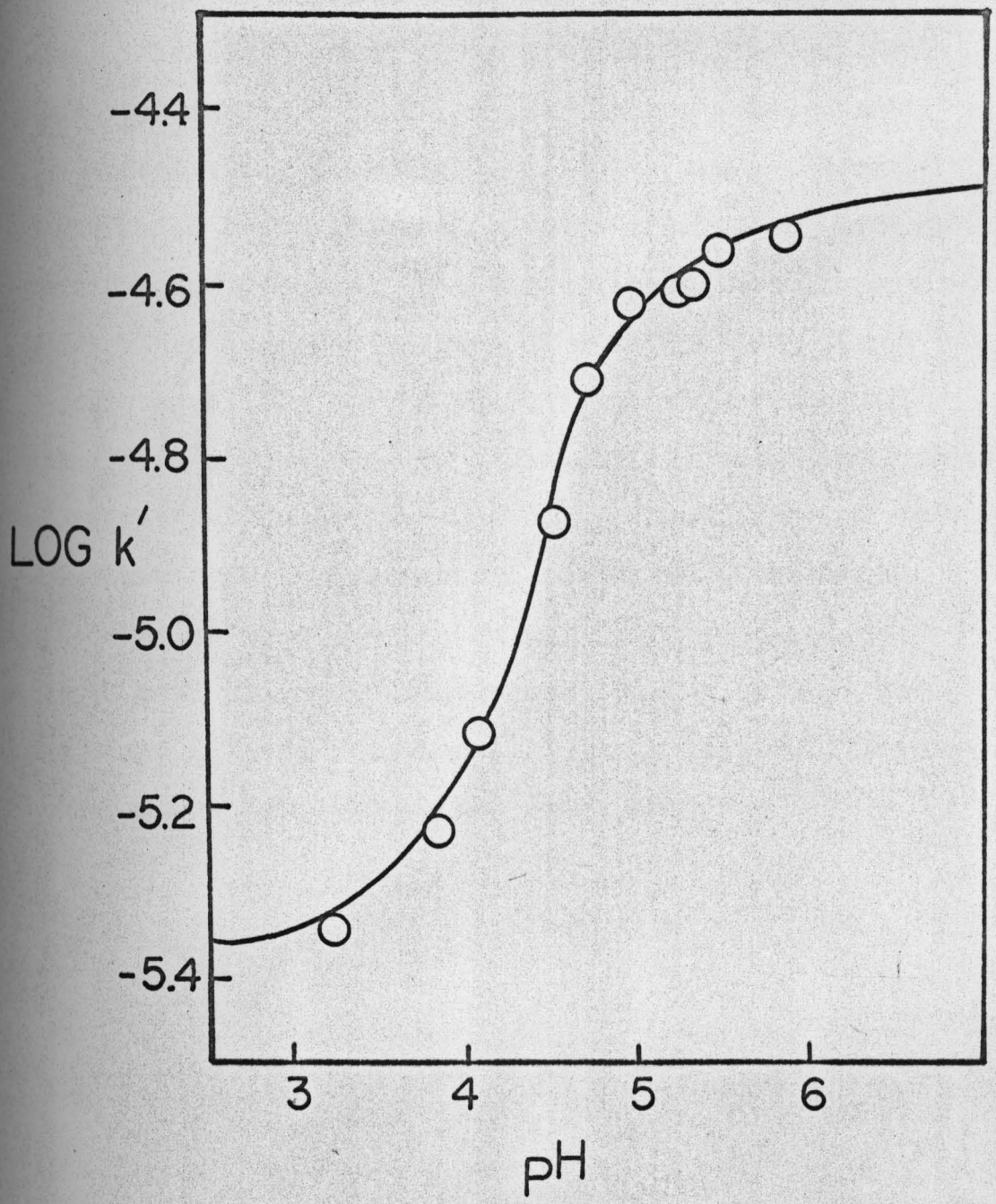

Figure 7. pH-rate profile for the reaction of hydroxylamine and acetic acid in the presence of nickel chloride. Data from Table VI. Solid line drawn according to experimental rate equation (Eq. 26).

Acetic acid is represented as HOAc and acetate ion as OAc^-. The first term, corresponding to hydrogen ion-catalyzed reaction of hydroxylamine and acetic acid, and the second term, corresponding to the non-catalyzed reaction of hydroxylamine and acetic acid, are arrived at through consideration of the reaction of acetic acid and hydroxylamine in the absence of nickel (II). These reactions will be discussed in the next section. The third term corresponds to a nickel (II) catalyzed reaction of hydroxylamine and acetate ion. Through the pH region where the rate is increasing, acetic acid undergoes dissociation to the anion form. The dissociations of acetic acid and hydroxylammonium ion are written in Equation (21) and Equation (22), with the equilibrium constants being given in Equations (23) and (24).

$$CH_3\text{-}COOH \rightleftharpoons CH_3COO^- + H^+ \qquad (21)$$

$$NH_3OH^+ \rightleftharpoons NH_2OH + H^+ \qquad (22)$$

$$K_{HOAc} = \frac{[H^+][OAc^-]}{[HOAc]} \equiv K_1 \qquad (23)$$

$$K_{NH_3OH^+} = \frac{[H^+][NH_2OH]}{[NH_3OH^+]} \equiv K_2 \qquad (24)$$

Substitution of Equations (23) and (24) into Equation (20) leads to,

$$\frac{V}{[HOAc]_T} = k_{obs} = \frac{k_1^{Ni}K_2[H^+]^2[NH_2OH]_T}{([H^+] + K_1)([H^+] + K_2)} + \frac{k_2^{Ni}K_2[H^+][NH_2OH]_T}{([H^+] + K_1)([H^+] + K_2)} + \frac{k_3^{Ni}K_1K_2[NiCl_2]_T\,[NH_2OH]_T}{([H^+] + K_1)([H^+] + K_2)} \qquad (25)$$

with $[NH_2OH]_T$ and $[NiCl_2]_T$ representing total concentrations of hydroxylamine and nickel chloride. k_{obs} is the apparent first-order rate constant. Note that in this treatment $[Ni^{+2}]$ is assumed to be equal to $[NiCl_2]_T$. Dividing Equation (25) by $[NH_2OH]_T$ gives an expression for the apparent second-order rate constant (Eq. 26).

$$k' = \frac{k_1^{Ni}K_2[H^+]^2}{([H^+] + K_1)([H^+] + K_2)} + \frac{k_2^{Ni}K_2[H^+]}{([H^+] + K_1)([H^+] + K_2)} + \frac{k_3^{Ni}K_1K_2[NiCl_2]_T}{([H^+] + K_1)([H^+] + K_2)} \qquad (26)$$

The theoretical line in Figure 7 is calculated from Equation (26) using the following values for the constants.

$$k_1 = 9.0 \times 10^{-2}\ \underline{M}^{-2}\ sec^{-1}$$

$$k_2 = 2.5 \times 10^{-5}\ \underline{M}^{-1}\ sec^{-1}$$

$$k_3 = 7.2 \times 10^{-4}\ \underline{M}^{-2}\ sec^{-1}$$

$$K_1 = 6.0 \times 10^{-5}\ \underline{M}$$

$$K_2 = 5.0 \times 10^{-6}\ \underline{M}$$

The dissociation constants for acetic acid and hydroxylammonium ion were treated as adjustable parameters because of the probable effect of complexation with nickel (II) on the apparent equilibrium constants. The values of K_1 and K_2 in the presence of nickel (II) could be independently determined from a knowledge of the stability constants of nickel (II) complexes of acetic acid and hydroxylamine. This type of study, in this very complicated system, would add little to the present work, and would be a major digression. It is for this reason that K_1 and K_2, in the presence of nickel (II), were treated as adjustable parameters. These acid dissociation constants were, however, determined for these conditions (μ = 1.0, 90.5°) in the absence of nickel; their values are $K_1 = 2.46 \times 10^{-5}$ $\underline{M}$ and $K_2 = 7.40 \times 10^{-6}$ $\underline{M}$.

Lawlor (16) reported a bell-shaped pH-rate profile for the reaction of hydroxylamine and acetic acid in the presence of nickel (II), the rate maximum being at pH 5.5. Figure 8 and Table VII shows the pH-rate profile for the

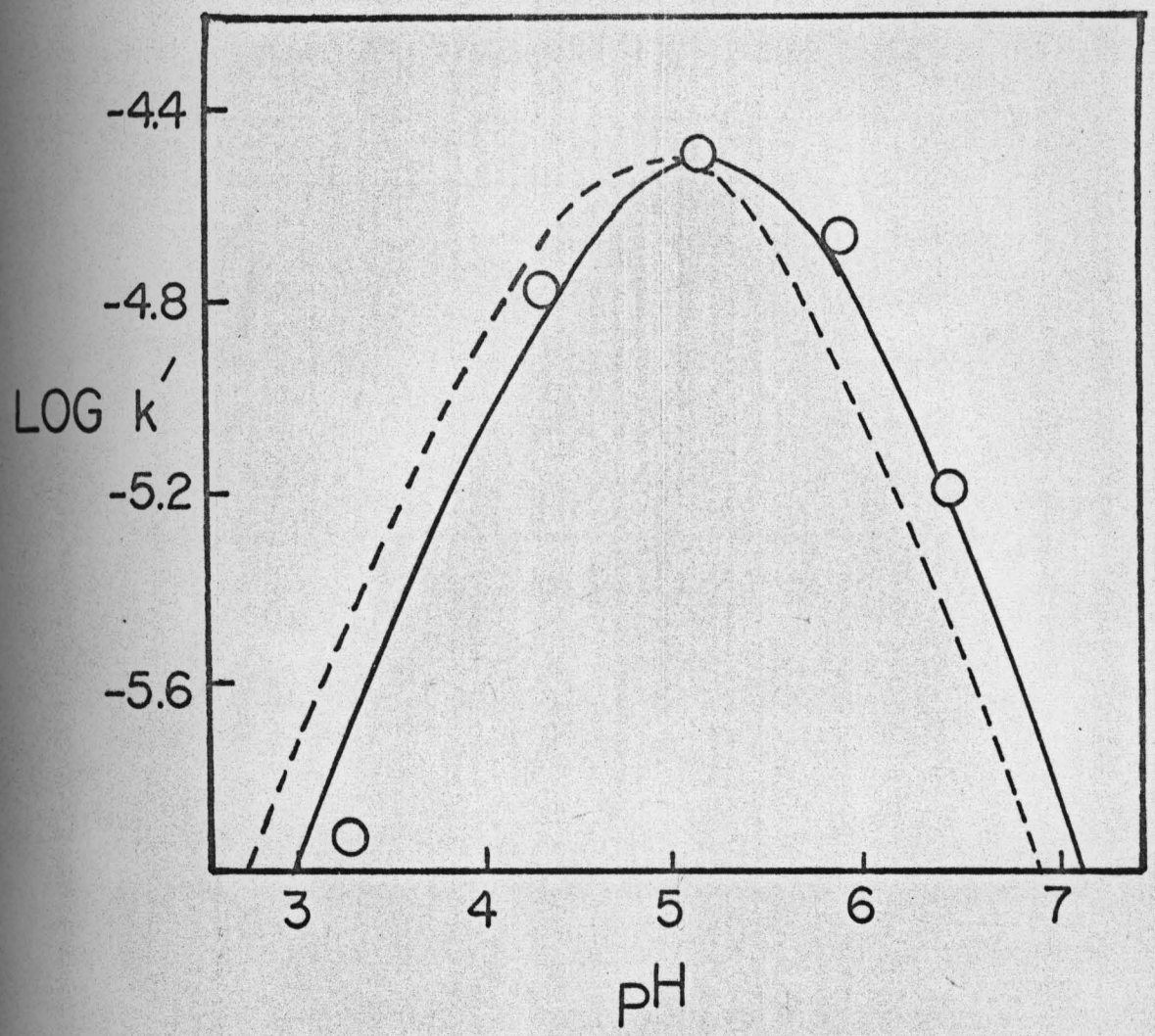

Figure 8. pH-rate profile for reaction of acetic acid with hydroxylamine in the presence of nickel chloride; 0.1 M $NH_2OH \cdot HCl$; 0.125 M $NiCl_2$; 1.1 M acetic acid. Data from Table VII. (Lawlor's (16) conditions)

TABLE VII

Apparent Second-Order Rate Constants for the Reaction of Hydroxylamine and Acetic Acid in the Presence of Nickel (II) Using Lawlor's (16) Conditions[a]

pH (90.5°)	10^5 k' ($\underline{M}^{-1}$ sec^{-1})[b]	log k'
3.28	0.138	- 5.86
4.28	1.67	- 4.78
5.12	3.22	- 4.49
5.88	2.22	- 4.65
6.45	0.635	- 5.20

[a] 90.5°; 0.1 $\underline{M}$ $NH_2OH \cdot HCl$; 0.125 $\underline{M}$ $NiCl_2$; 1.1 $\underline{M}$ acetic acid.

[b] Acid catalyzed reaction contribution has been subtracted.

reaction of hydroxylamine and acetic acid as determined in the present study using Lawlor's conditions of concentrations. The dashed line is calculated from the rate equation given in Equation (27) which was first suggested by Lawlor to account for his observations.

$$V = k_o[HOAc][NH_2OH][NiCl_2]_T \qquad (27)$$

This equation is chosen because the decrease in concentration of hydroxylamine base would cause the decreasing rate

as pH is lowered and the decrease in free acetic acid causes the decreasing rate as pH is raised. Hence, at some intermediate pH, the product $[HOAc][NH_2OH]$ will have a maximum value. Substituting Equations (23) and (24) into Equation (27) gives:

$$k' = \frac{V}{[HOAc]_T\,[NH_2OH]_T} = \frac{k_o K_2 [H^+][NiCl_2]_T}{([H^+] + K_1)([H^+] + K_2)} \qquad (28)$$

Experimentally determined values for K_1 and K_2 (90.5°) in the absence of nickel (II), $K_1 = 2.46 \times 10^{-5}$ M and $K_2 = 7.40 \times 10^{-6}$ M, were used in calculating the dashed line. The solid line was drawn by shifting the calculated line slightly to the right. This is equivalent to adjusting the values of K_1 and K_2 such that they satisfy Equation (29), where $-\log K = pK$.

$$\frac{pK_1 + pK_2}{2} = 5.15 \qquad (29)$$

Spectra for the reaction mixture from the determination of the sigmoid pH-rate profile are shown in Figure 9 and spectra of reaction mixtures from the study with Lawlor's conditions are shown in Figure 10. The differences in these spectra will be discussed later.

Other metals were screened as potential catalysts. Cobalt (II) was comparable with nickel (II) in its

Figure 9. Spectra of nickel-hydroxylamine complexes; 0.80 M $NH_2OH \cdot HCl$; 0.04 M $NiCl_2$; 0.04 M acetic acid; 25.0°; A, pH 6.70; B, pH 5.44; C, pH 4.29.

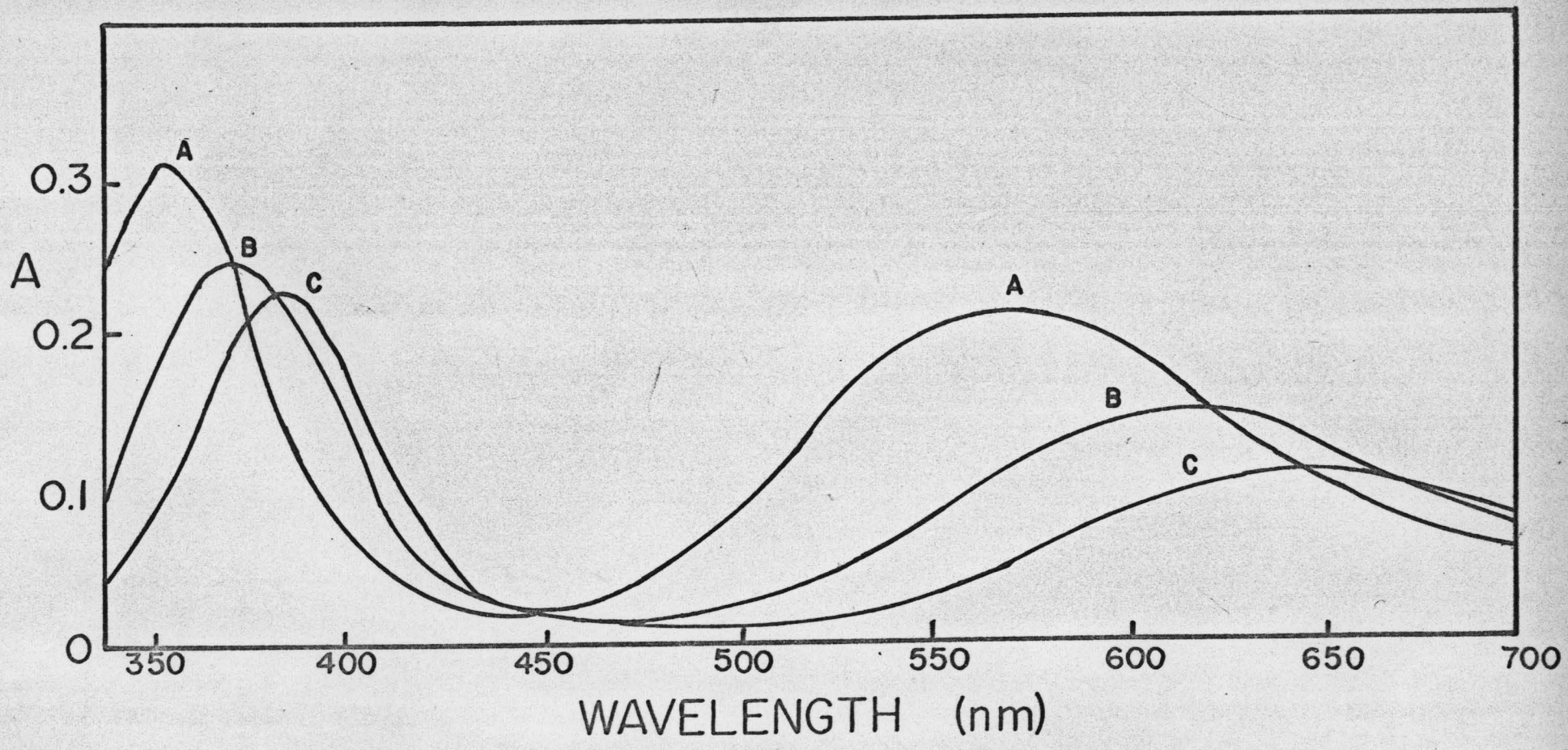
A
0.3
0.2
0.1
0
A
B
C
A
B
C
350
400
450
500
550
600
650
700
WAVELENGTH (nm)

Figure 10. Spectra of nickel-hydroxylamine complexes using Lawlor's (16) conditions; 0.10 M $NH_2OH \cdot HCl$; 0.125 M $NiCl_2$; 1.1 M acetic acid; 25.0°; A, pH 6.10; B, pH 5.10; C, pH 3.62.

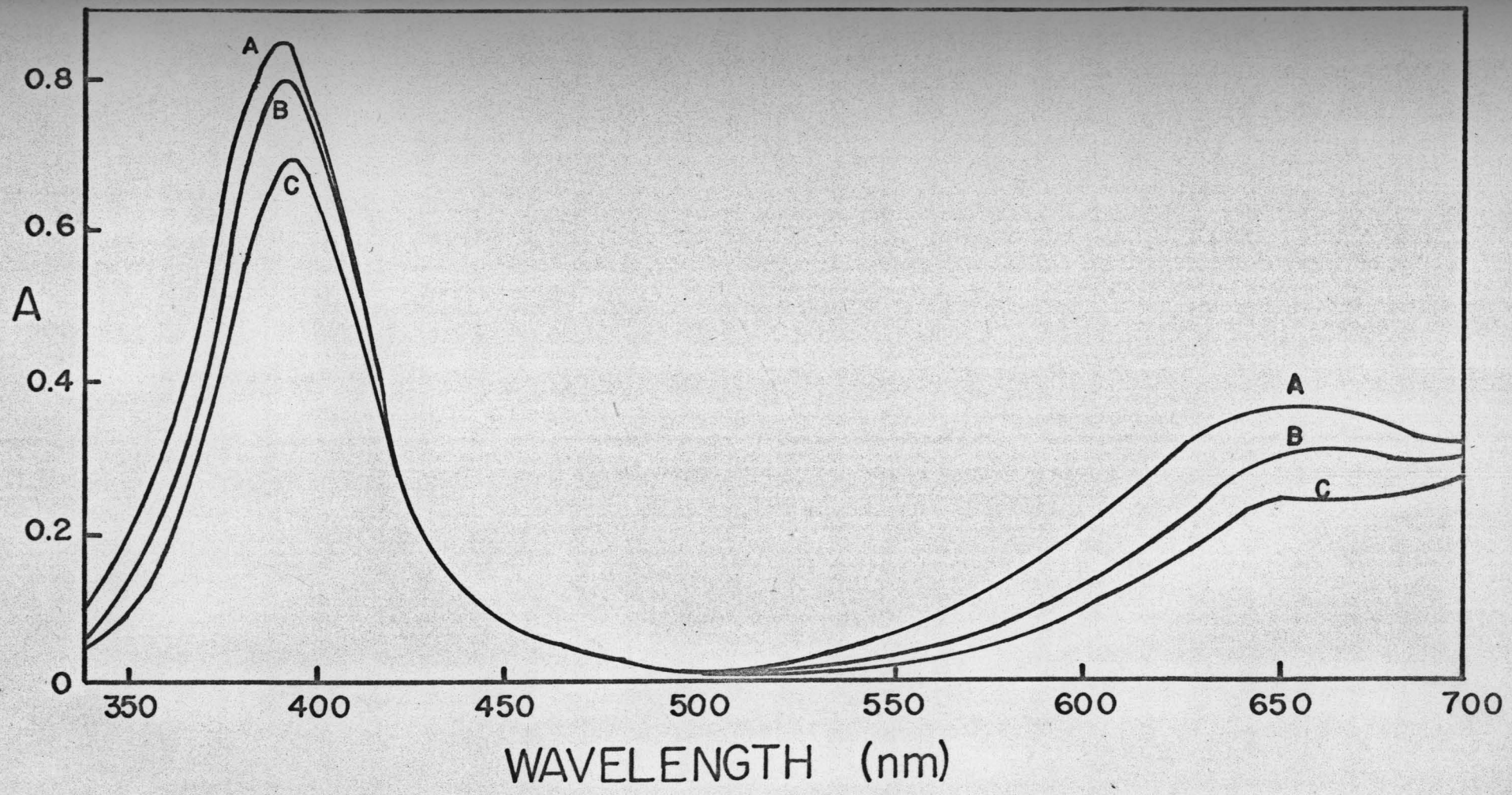
A
0.8
0.6
0.4
0.2
0
A
B
C
A
B
C
350
400
450
500
550
600
650
700
WAVELENGTH (nm)

catalytic efficiency. Cupric ions were not tested because of evolution of gas from a solution of cupric ions and hydroxylamine as sodium hydroxide was added. Ferrous and ferric ions formed insoluble hydroxides at about pH 4 even in the presence of hydroxylamine. Similar solubility problems were encountered with beryllium. Because of the solubility and catalytic properties of the nickel (II) ion, attention was focused on nickel (II) catalysis for the rest of the study.

Several solvents were investigated for rate enhancement effects. A summary of these effects on the nickel (II)-catalyzed reaction of hydroxylamine and acetic acid is shown in Table VIII. The effect of complete replacement of all anions with perchlorate ions is also shown in Table VIII. Dioxane was the most effective solvent for increasing the rate of reaction. A limit to the amount of dioxane that can be incorporated is determined by solubilities of all the reactants. There was no attempt made in this study to define this limit. Replacement of all chloride ions with perchlorate ions gave more than a two-fold increase in rate. However, the procedure for generating hydroxylammonium perchlorate makes this rate enhancement experimentally unattractive. A commercial source of hydroxylammonium perchlorate would greatly simplify the above experiment.

TABLE VIII

Effect of Solvent Additives on the Rate of Nickel (II)-Catalyzed Reaction of Acetic Acid and Hydroxylamine[a]

Additive	Additive Concentration	K_{REL}[b]
None	0	1.00
25% (v/v) Methanol	6.14	1.48
25% (v/v) t-Butanol	4.68	1.59
25% (v/v) Dioxane	2.92	1.91
25% (v/v) Pyridine	3.09	1.12
Perchlorate salt[d]	1.0	2.44

[a] 90.5°; pH 6.15[c]; 0.80 M $NH_2OH \cdot HCl$; 0.04 M $NiCl_2$; 0.045 M acetic acid; μ = 1.0

[b] Rate relative to that with no additive

[c] pH measurements were made at 25.0° and are apparent pH values.

[d] ClO_4^- replacing Cl^-

The rates of nickel (II)-catalyzed hydroxamic acid formation, under a single set of experimental conditions, from other carboxylic acids are presented in Table IX. The aromatic acids were less reactive than the aliphatic acids. The presence of an ortho substituent on the aromatic acids caused a further 10-fold decrease in rate. Glycine (aminoacetic acid) gave no detectable reaction under these conditions.

An initial rate method of analysis for acetic acid by Nickel (II)-catalyzed hydroxamic acid formation was developed using the results obtained in this study. A plot of absorbances against reaction times for this reaction is shown in Figure 11. A plot of the logarithm of the initial rates against logarithm of total acetic acid is presented in Figure 12 (Table X). This method appears to be satisfactory for acetic acid concentrations of at least 10^{-4} M. However, 5 cm cells must be used in measuring absorbances for these low concentrations. Data are presented in Table XI indicating that initial slopes, dA/dt, are reproducibly measured at substrate concentrations of 10^{-2} M. It should be pointed out that a 20-fold dilution of the sample reaction mixture was employed in the development of the ferric hydroxamate color. This was necessary because of the high concentration of hydroxylamine present. (See Section II-C-1 for a comment on the effects of hydroxylamine on color development.) If the dilution

TABLE IX

Relative Rate for the Nickel (II)-Catalyzed Reaction of Hydroxylamine and RCOOH[a]

R	K_{REL}
CH_3-	1.00
$ClCH_2$-	1.20
$C_6H_5CH_2$-	0.58
$(C_6H_5)_2CH$-	0.06
C_6H_5-	0.02
p-CH_3O-C_6H_5-	0.02
3,5-$(NO_2)_2$-C_6H_5-	0.03
o-CH_3O-C_6H_5-	0.003
NH_2-CH_2-	nil

[a] 90.5°; pH 6.00 (25.0°)[b]; 0.8 M $NH_2OH \cdot HCl$; 0.04 M $NiCl_2$; 25% (v/v) dioxane; 0.045 M RCOOH.

[b] pH measured at 25.0° and is an apparent pH.

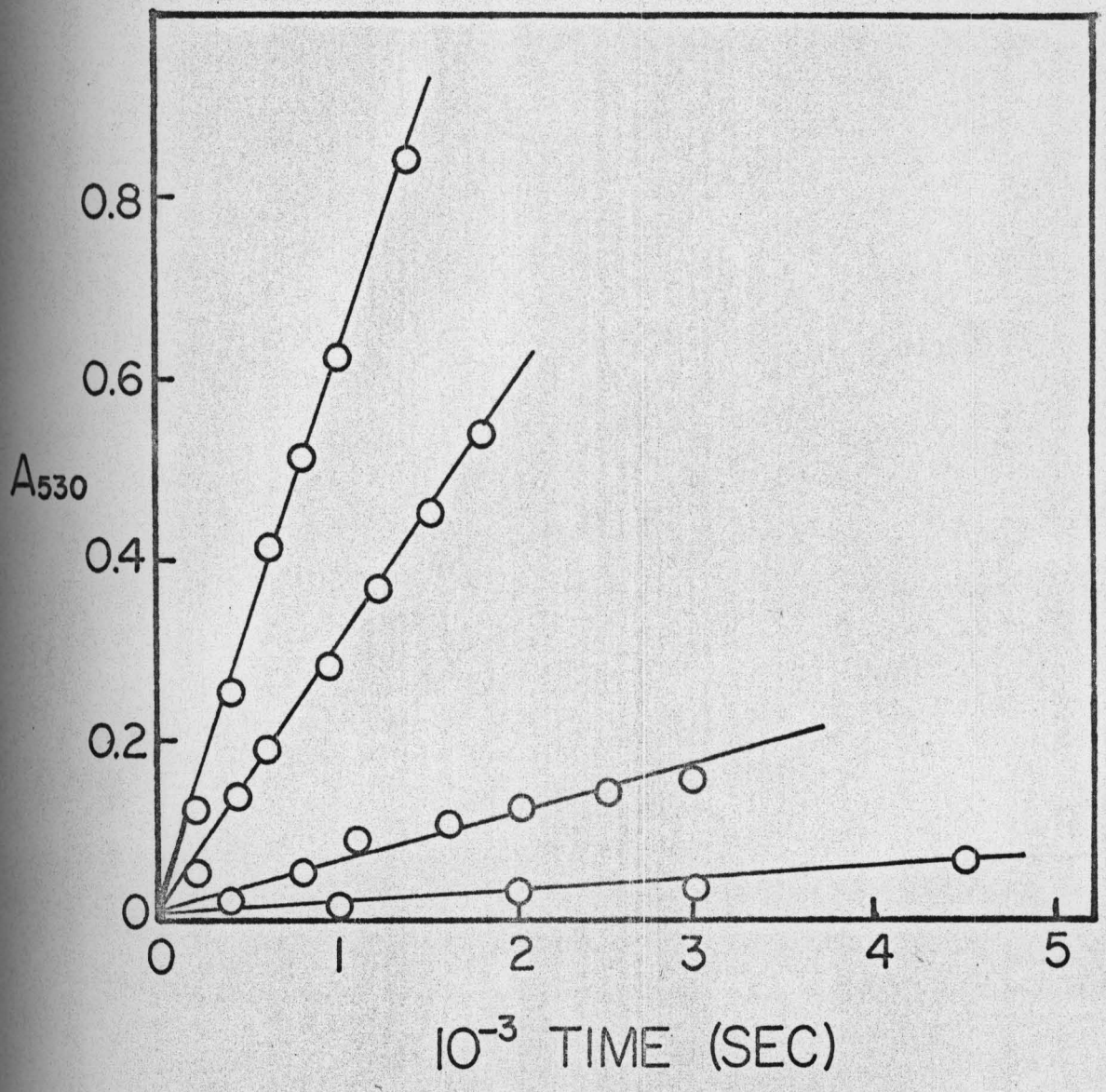

Figure 11. Plot of absorbances against time for hydroxamic acid formation from acetic acid in the presence of nickel chloride. Reaction conditions listed in Table X.

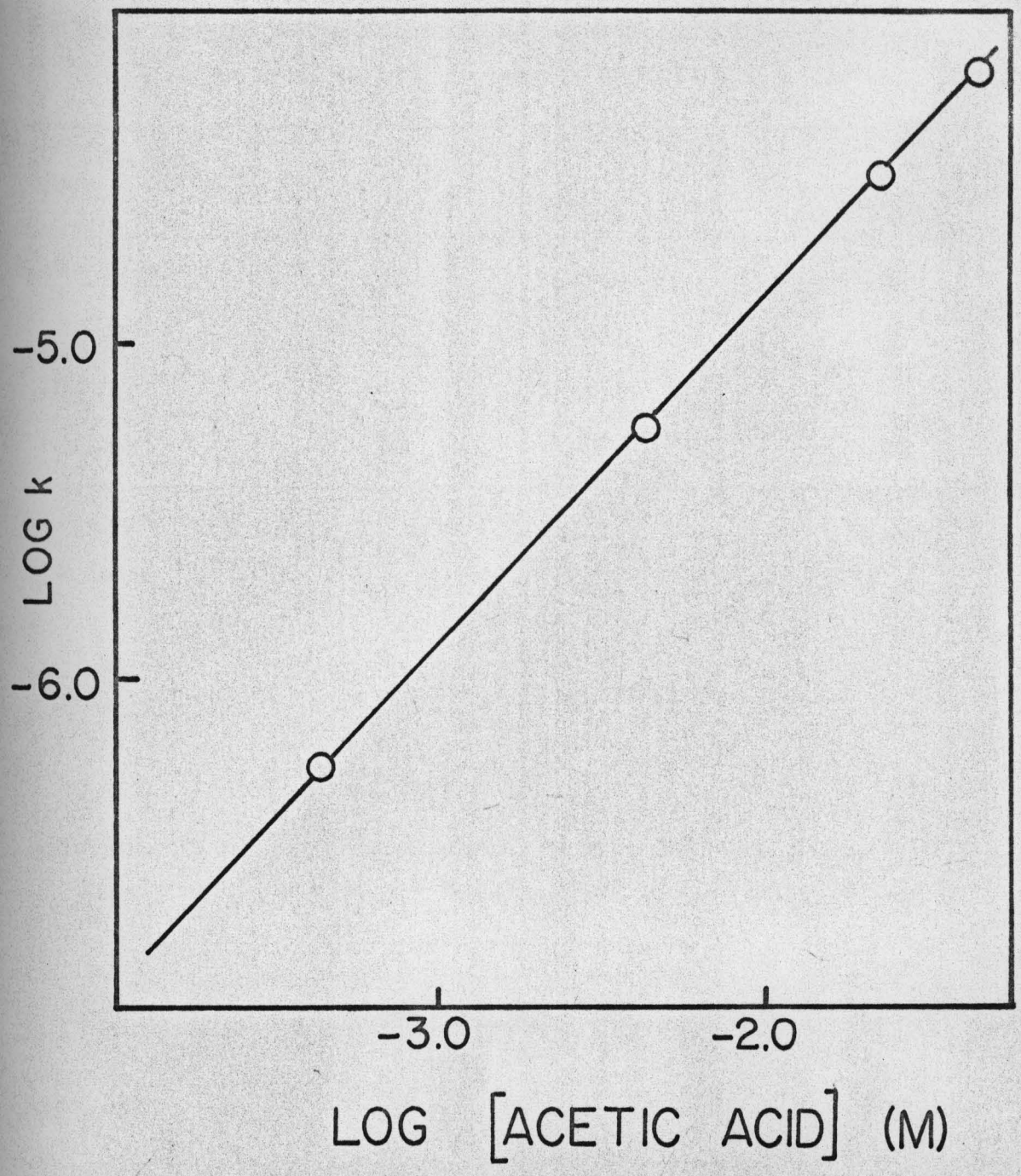

Figure 12. Plot of log initial slope against log [acetic acid]$_T$ for the nickel (II)-catalyzed hydroxamic acid formation from acetic acid. Data from Table X.

TABLE X

Initial Slopes as a Function of Acetic Acid Concentration for Nickel (II)-Catalyzed Hydroxamic Acid Formation

10^4 Initial Slope, dA/dt (sec^{-1})	log dA/dt	10^2 $[HOAc]_T$ (M)	log $[HOAc]_T$
0.054	- 5.37	0.044	- 3.36
0.58	- 4.23	0.441	- 2.36
3.12	- 3.51	2.20	- 1.66
6.37	- 3.20	4.41	- 1.36

[a]95.0°; 1.0 M $NH_2OH \cdot HCl$; 0.1 M $NiCl_2$; 25% (v/v) dioxane; pH 6.15 (25.0°).

TABLE XI

Measurement of Initial Slopes, dA/dt, for the Nickel (II)-Catalyzed Reaction of Acetic Acid and Hydroxylamine[a]

10^4 dA/dt (sec^{-1})[b]	Trial
3.12	1
3.14	2
3.19	3
3.10	4
3.18	5

[a]90.5°; pH 6.15 (measured at 25.0°); 1.0 M $NH_2OH \cdot HCl$; 0.1 M $NiCl_2$; 25% (v/v) dioxane.

[b]Mean 3.15; standard deviation 0.026; range 0.09.

step could be eliminated, perhaps by selective destruction of the hydroxylamine, one order of magnitude in the sensitivity could be gained. A suggested analytical procedure for the analysis of acetic acid will be presented later.

A spot test for carboxylic acids utilizing nickel (II)-catalyzed hydroxamic acid formation was devised and tested. The results of the spot tests are given in Table XII. A detailed description of the procedure used and the scope of the test will be given later.

B. Hydrogen Ion-Catalyzed Hydroxamic Acid Formation from Acetic Acid

The results shown in Figure 6 suggest that a reaction takes place under these conditions that does not require nickel catalysis. The following study attempts to elucidate the nature of this reaction. The conditions used are similar to the nickel study except that higher acetic acid concentrations (0.4 M) were necessary to obtain measurable reaction rates. All reaction rate constants at pH greater than 3 were obtained from initial slope measurements. In the initial 5 percent of the overall reaction, the reverse reaction, hydrolysis of aceto-hydroxamic acid, does not occur significantly. Data presented in the next section show that the rate of hydrolysis of acetohydroxamic acid is much slower than its

TABLE XII

Results with the Nickel-Catalyzed Ferric Hydroxamate Spot Test[a]

Compound	Reaction Time 30 min	60 min
A. Simple aliphatic carboxylic acids		
1. acetic	+	
2. propionic	+	
3. n-butyric	+	
4. chloroacetic	-	+
5. malonic	+	
6. succinic	+	
7. glutaric	+	
8. phenylacetic	+	
9. hydrocinnamic[b]	-	-
B. Aromatic carboxylic acids		
1. benzoic	-	-
2. p-nitrobenzoic[b]	-	-
3. phthalic	-	-
4. isonicotinic	-	-
C. α-Aminocarboxylic acids		
1. glycine	-	-
2. leucine	-	-
3. proline	-	-
4. glutamic acid	-	-
D. Miscellaneous		
1. Unsaturated acids		
a. maleic	-	-
b. cinnamic[b]	+	
c. fumaric	-	-
d. crotonic	-	+
2. α-Hydroxy acids		
a. citric	-	+
b. methyllactic	-	+
c. tartaric	-	-
d. lactic	-	+
E. Other carboxylate derivatives		
1. methyl acetate	+	
2. methyl benzoate	+	
3. acetamide	+	

[a] + indicates positive test; - indicates negative test. Compounds giving a positive test at 30 minutes were not tested at 60 minutes.

[b] Acid was not fully soluble at 0.1 M.

formation from acetic acid (e.g., $k_f \sim 10^{-6}$ $\underline{M}^{-1}$ sec^{-1} and $k_r \sim 10^{-8}$ $\underline{M}^{-1}$ sec^{-1} at pH 5.0). Therefore the observed rate constants obtained from initial slopes are the rate constants for the forward reaction only (Eq. 30).

$$CH_3COOH + NH_2OH \underset{k_r}{\overset{k_f}{\rightleftharpoons}} CH_3CONHOH + H_2O \qquad (30)$$

Some typical plots of absorbance against time are shown in Figure 13. At pH values less than 3, the reactions reached equilibrium quite rapidly. This circumstance required that the rate constants be obtained from plots of log ($A_\infty - A_t$) against time. Since the observed rate constant, k_{obs}, is equal to the sum of the rate constants for the forward and reverse reaction (Eq. 31), it is necessary to isolate the forward rate constant in order to make comparisons with the rate constants obtained from the initial slopes.

$$k_{obs} = k_f + k_r \qquad (31)$$

A typical plot of absorbance against time for the reaction at low pH is shown in Figure 14. The first order plot for this reaction is presented in Figure 15. Reactions at lower pH values (0.5 to 1.0) gave very low yields of hydroxamic acid at equilibrium.

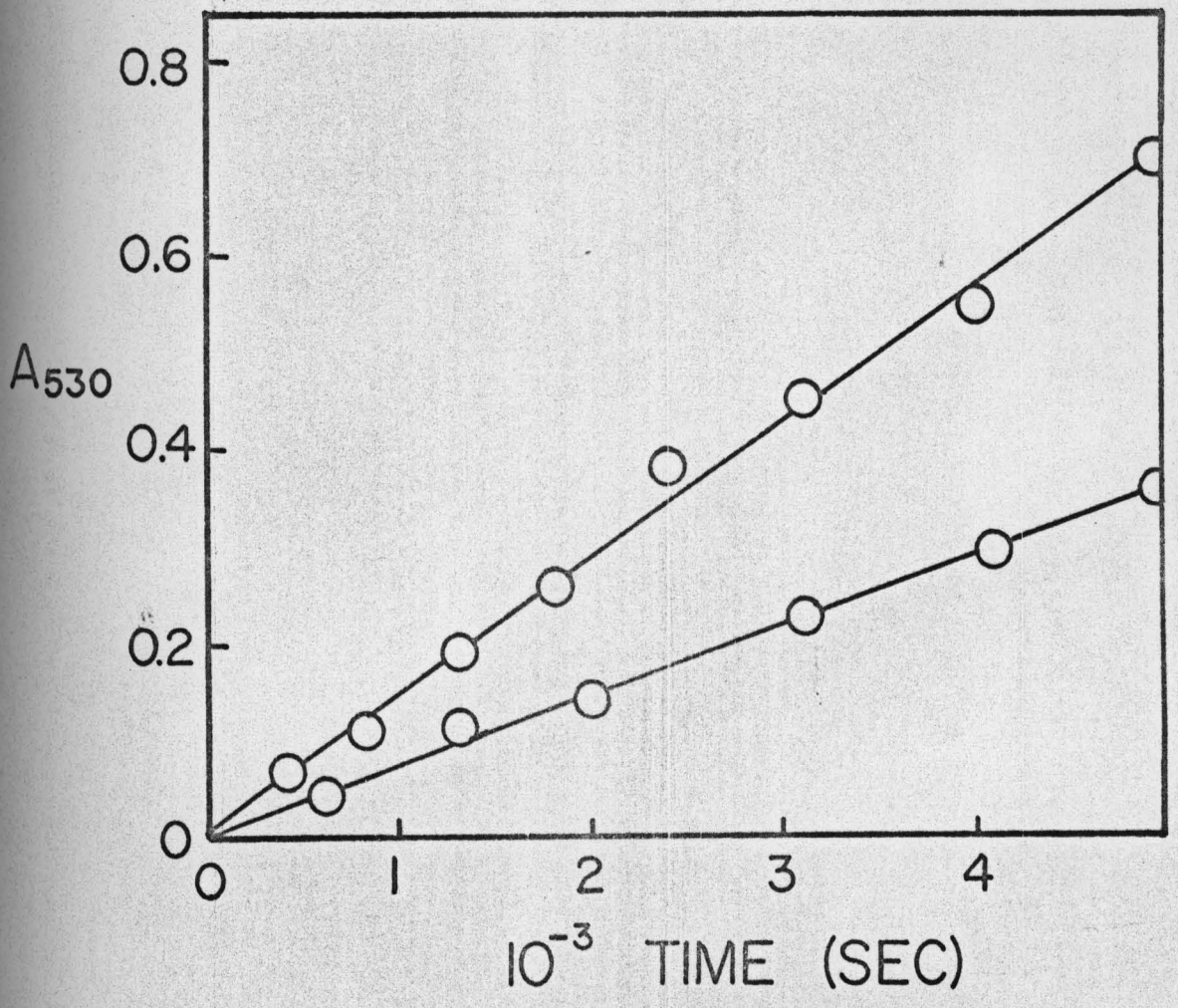

Figure 13. Some typical plots of absorbance against time for the reaction of acetic acid and hydroxylamine in the absence of nickel; 0.8 M $NH_2OH \cdot HCl$; μ = 1.2; pH 3.80 (90.5°); acetic acid, top line 0.39 M, bottom line 0.195 M; 2 cm cells.

Figure 14. A typical plot of absorbance against reaction time for hydroxamic acid formation from acetic acid; 90.5°; pH 1.55; 0.8 M $NH_2OH \cdot HCl$; 0.85 M acetic acid; μ = 1.2; 2 cm cells.

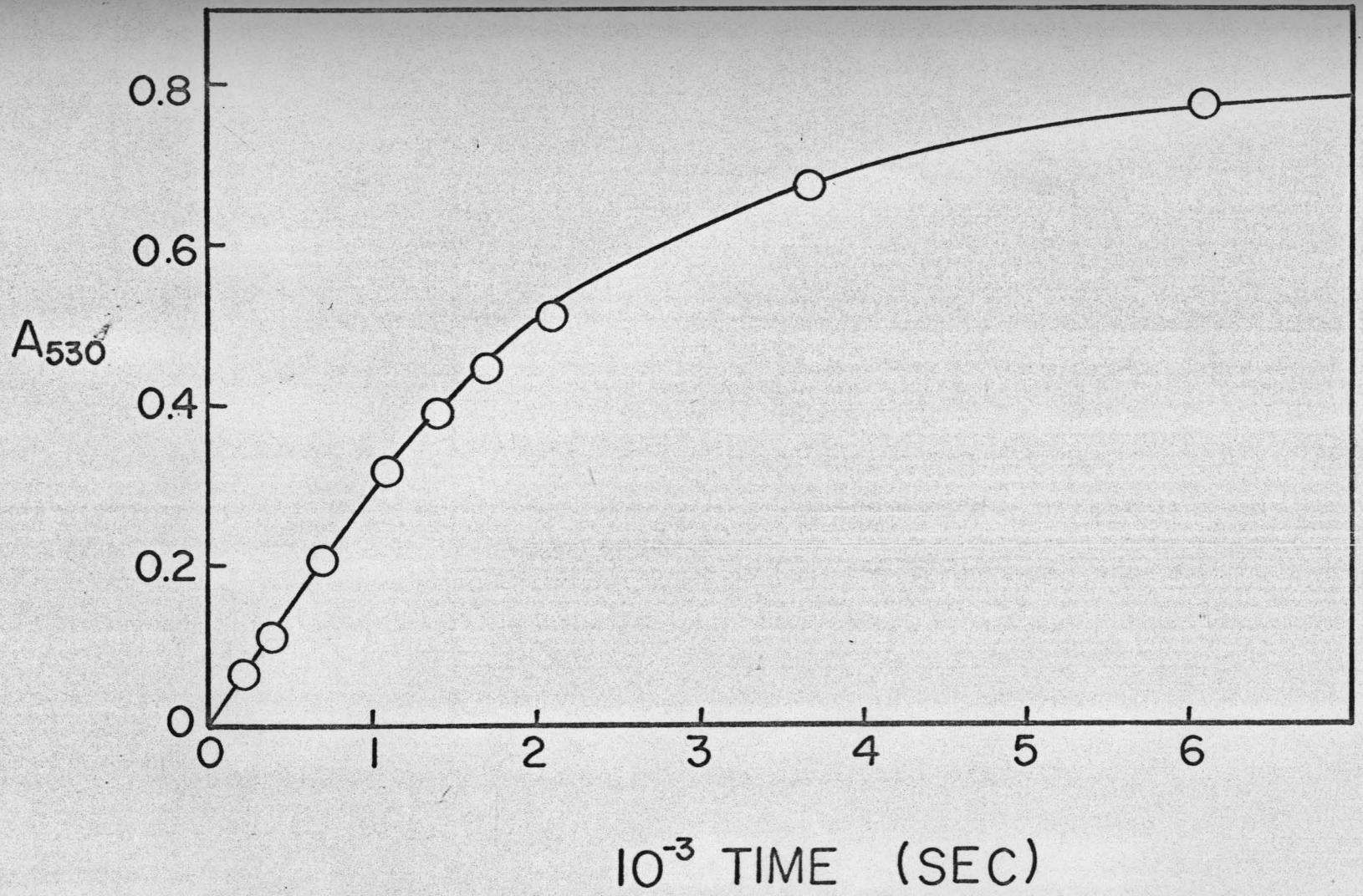
0.8
0.6
A_{530}
0.4
0.2
0
0
1
2
3
4
5
6
10^{-3} TIME (SEC)

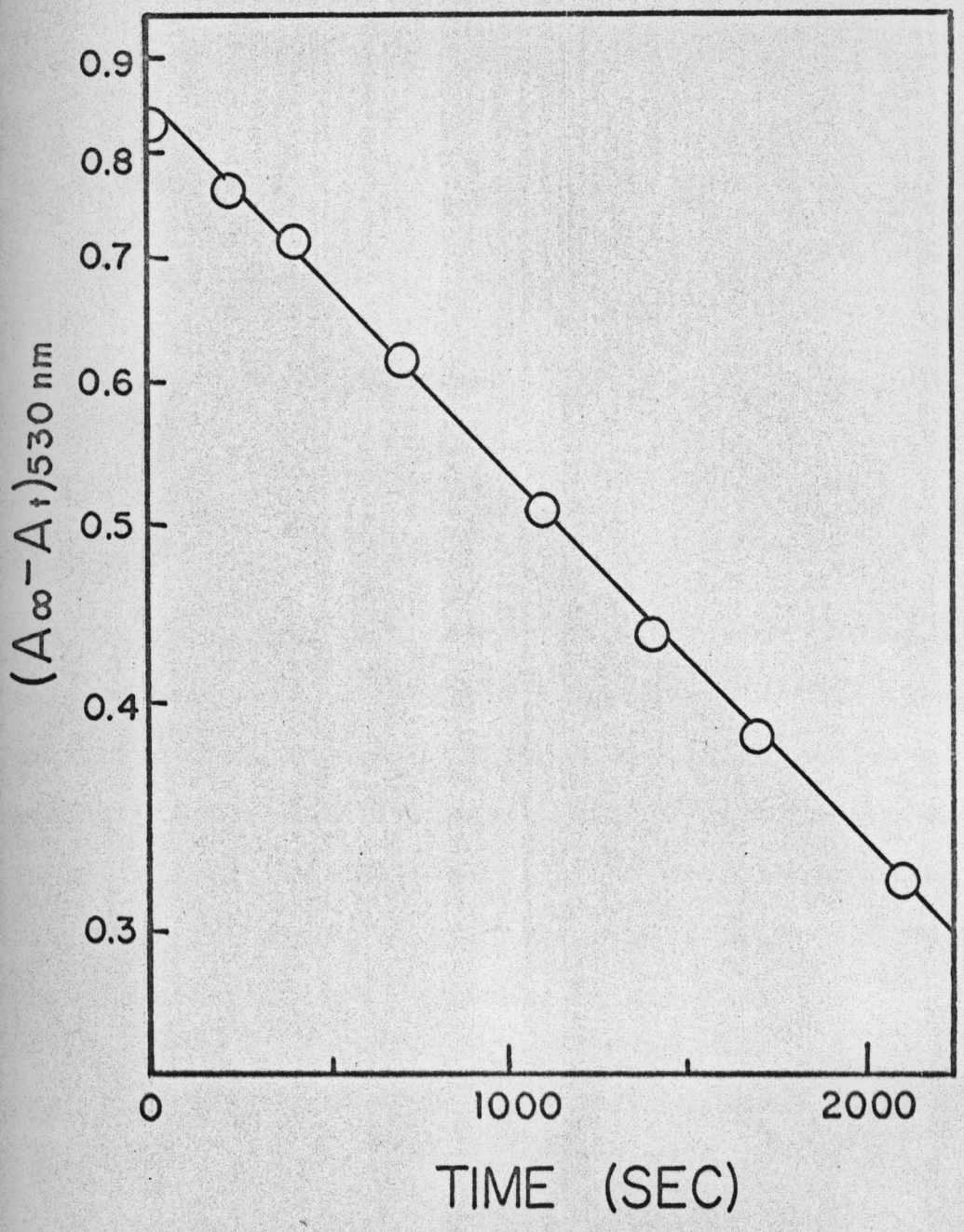

Figure 15. A typical apparent first-order plot (log $(A_\infty - A_t)$ against time) for hydroxamic acid formation from acetic acid; 90.5°; pH 1.55; 0.8 M $NH_2OH \cdot HCl$; 0.85 M acetic acid; μ = 1.2; 2 cm cells; k_{obs} = 2.303 (slope).

An expression for k_f can be derived from the following considerations. The equilibrium constant for the reaction,

$$\begin{array}{ccc} \text{acetic acid} & \overset{k_f}{\underset{k_r}{\rightleftharpoons}} & \text{acetohydroxamic acid} \\ + & & + \\ \text{hydroxylamine} & & H_2O \end{array} \qquad (32)$$

can be written as in Equation (33),

$$K = \frac{[CH_3CONHOH]_{\infty,T}\,[H_2O]}{[HOAc]_{\infty,T}\,[NH_2OH]_{\infty,T}} \qquad (33)$$

where the subscript ∞,T denotes total concentration of the bracketed compound at "infinity" time, or in this case, equilibrium. No assumptions about the ionic states of the reactants involved in hydroxamic acid formation are made in this definition, so these equilibrium constants are pH dependent. The hypothetical rate equation for the reaction of acetic acid and hydroxylamine is given as:

$$\frac{d[CH_3CONHOH]_T}{dt} = k_f[HOAc][NH_2OH] - k_r[CH_3CONHOH][H_2O] \qquad (34)$$

The equilibrium constant is further interpreted as,

$$K = \frac{k_f}{k_r} \qquad (35)$$

Since the experimentally determined rate constant found from plots of log $(A_\infty - A_t)$ against time for the appearance of acetohydroxamic acid, denoted as H.A., is k_{obs}, the experimental rate equation takes the form,

$$V = k_{obs}([HA]_\infty - [HA]_t) \qquad (36)$$

The hypothetical rate equation written in the same form is,

$$V = k_f[HOAc][NH_2OH] - k_r[H.A.][H_2O] \qquad (37)$$

Furthermore, we have the mass-balance equation,

$$[HOAc] + [H.A.] = [HOAc]_\infty + [H.A.]_\infty \qquad (38)$$

Combining Equations (33), (35), and (38) and solving for [HOAc] gives Equation (39).

$$[HOAc] = \frac{k_r[H.A.]_\infty[H_2O]}{k_f[NH_2OH]_\infty} + [H.A.]_\infty - [H.A.] \qquad (39)$$

Since only a very small fraction of the total hydroxylamine is consumed in the reaction, $[NH_2OH]$ is assumed to equal $[NH_2OH]_T$. Substituting Equation (39) into Equation (37) leads to Equation (40).

$$V = (k_f[NH_2OH]_T + k_r[H_2O])([H.A.]_\infty - [H.A.]) \qquad (40)$$

Comparing Equation (40) with Equation (36) shows that

$$k_{obs} = k_f[NH_2OH]_T + k_r[H_2O] \qquad (41)$$

Since $K = k_f/k_r$ (Eq. 35), Equation (41) can be rewritten as,

$$k_f = \frac{k_{obs}}{[NH_2OH]_T + \frac{[H_2O]}{K}} \qquad (42)$$

All quantities on the right-hand side of Equation (42) are known or can be measured directly. The reverse reaction rate constant, k_r, can be calculated from Equation (35).

Hydroxamic acid formation from acetic acid is shown to be first-order in total acetic acid concentration (Figure 16 and Table XIII) and first-order in total hydroxylamine concentration (Figure 17 and Table XIV) at pH 3.50 (measured at 25.0°).

The pH rate profile for hydroxamic acid formation from acetic acid is shown in Figure 18 (Table XV). The solid line is calculated from the rate equation (Eq. 43).

$$V = k_1^H[HOAc][NH_2OH][H^+]^2 + k_2^H[HOAc][NH_2OH][H^+] + k_3^H[HOAc][NH_2OH] \qquad (43)$$

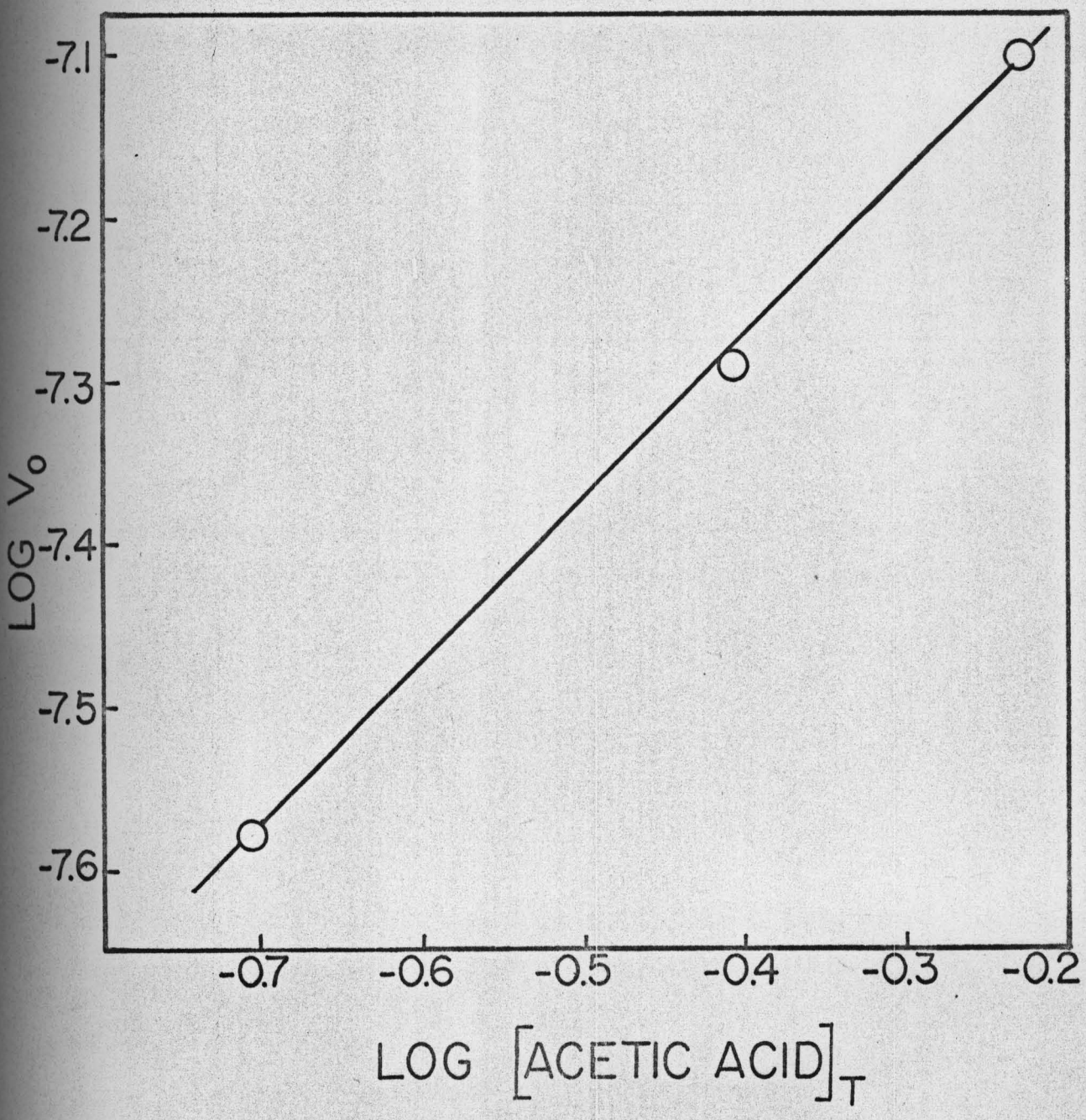

Figure 16. Plot of log V_o against log [acetic acid]$_T$ for hydroxamic acid formation from acetic acid. Slope of line is 1.0. Data from Table XIII.

TABLE XIII

Rate of Reaction for Hydroxamic Acid Formation from Acetic Acid; Order of Reaction with Respect to Total Acetic Acid Concentration[a]

10^8 Initial Rate, V_o ($\underline{M}$ sec^{-1})	log V_o	$[HOAc]_T$ ($\underline{M}$)	log $[HOAc]_T$
8.0	- 7.10	0.585	- 0.233
5.1	- 7.29	0.390	- 0.408
2.7	- 7.58	0.195	- 0.710

[a] 90.5°; 0.80 $\underline{M}$ $NH_2OH \cdot HCl$; μ = 1.4; pH 3.50 (measured at 25.0°).

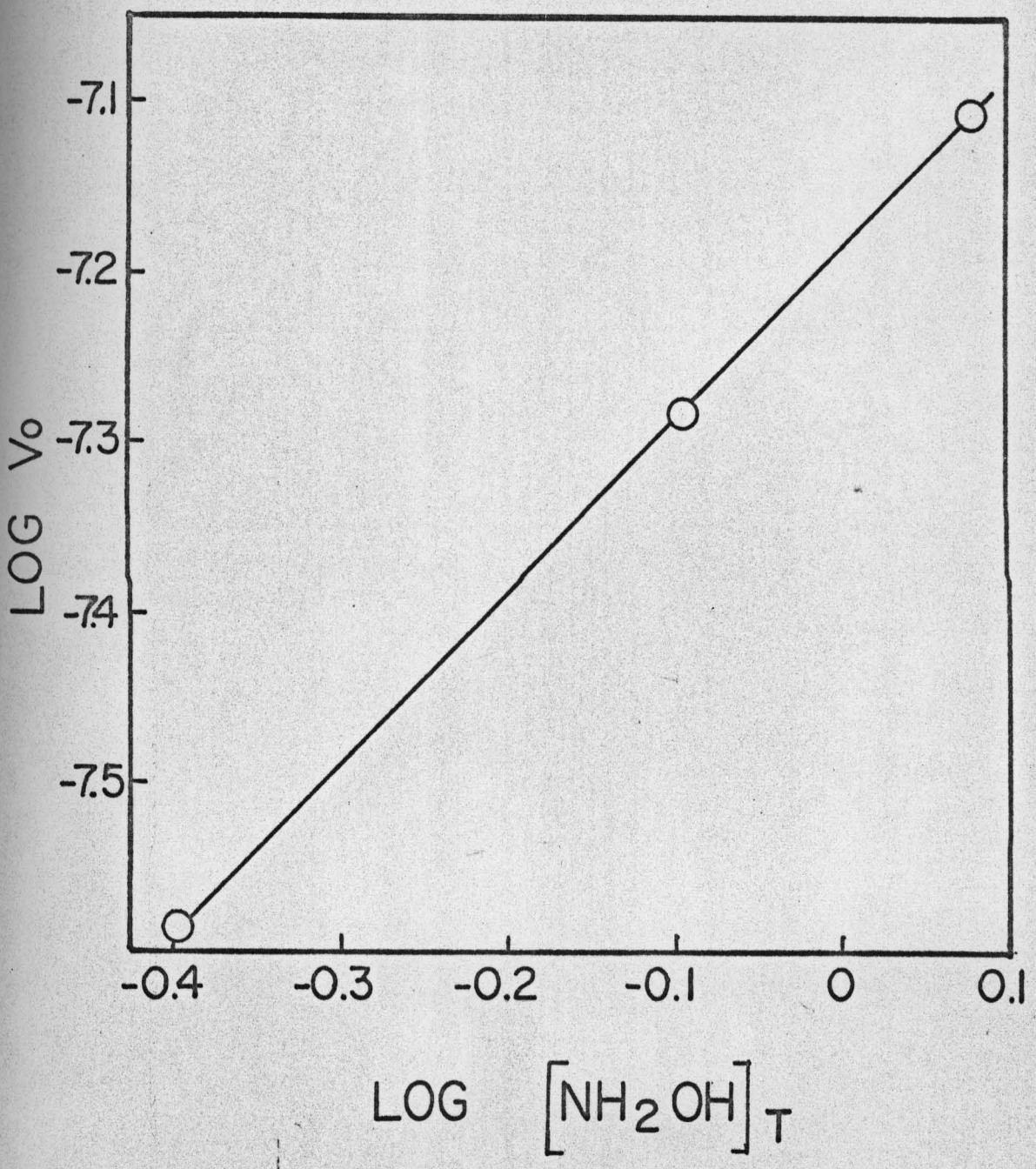

Figure 17. Plot of log V_o against log $[NH_2OH]_T$ for hydroxamic acid formation from acetic acid. Slope of line is 1.0. Data from Table XIV.

TABLE XIV

Rate of Reaction of Hydroxamic Acid Formation from Acetic Acid, Showing Order of Reaction with Respect to Total Hydroxylamine Concentration[a]

10^8 Initial Rate, V_o ($\underline{M}$ sec^{-1})	log V_o	$[NH_2OH]_T$ ($\underline{M}$)	log $[NH_2OH]_T$
7.75	- 7.11	1.20	+ 0.079
5.20	- 7.28	0.80	- 0.096
2.56	- 7.59	0.40	- 0.395

[a] 90.5°; 0.39 $\underline{M}$ acetic acid; μ = 1.60; pH 3.50 (measured at 25.0°).

Figure 18. pH-rate profile for hydroxamic acid formation from acetic acid; 90.5°; μ = 1.2; ○ 0.80 M $NH_2OH \cdot HCl$; 0.40 M acetic acid; ◐ 0.40 M $NH_2OH \cdot HCl$; 0.40 M acetic acid; ● 0.80 M $NH_2OH \cdot HCl$, 0.86 M acetic acid; □ 0.80 M $NH_2OH \cdot HCl$, 0.195 M acetic acid. Data from Table XV.

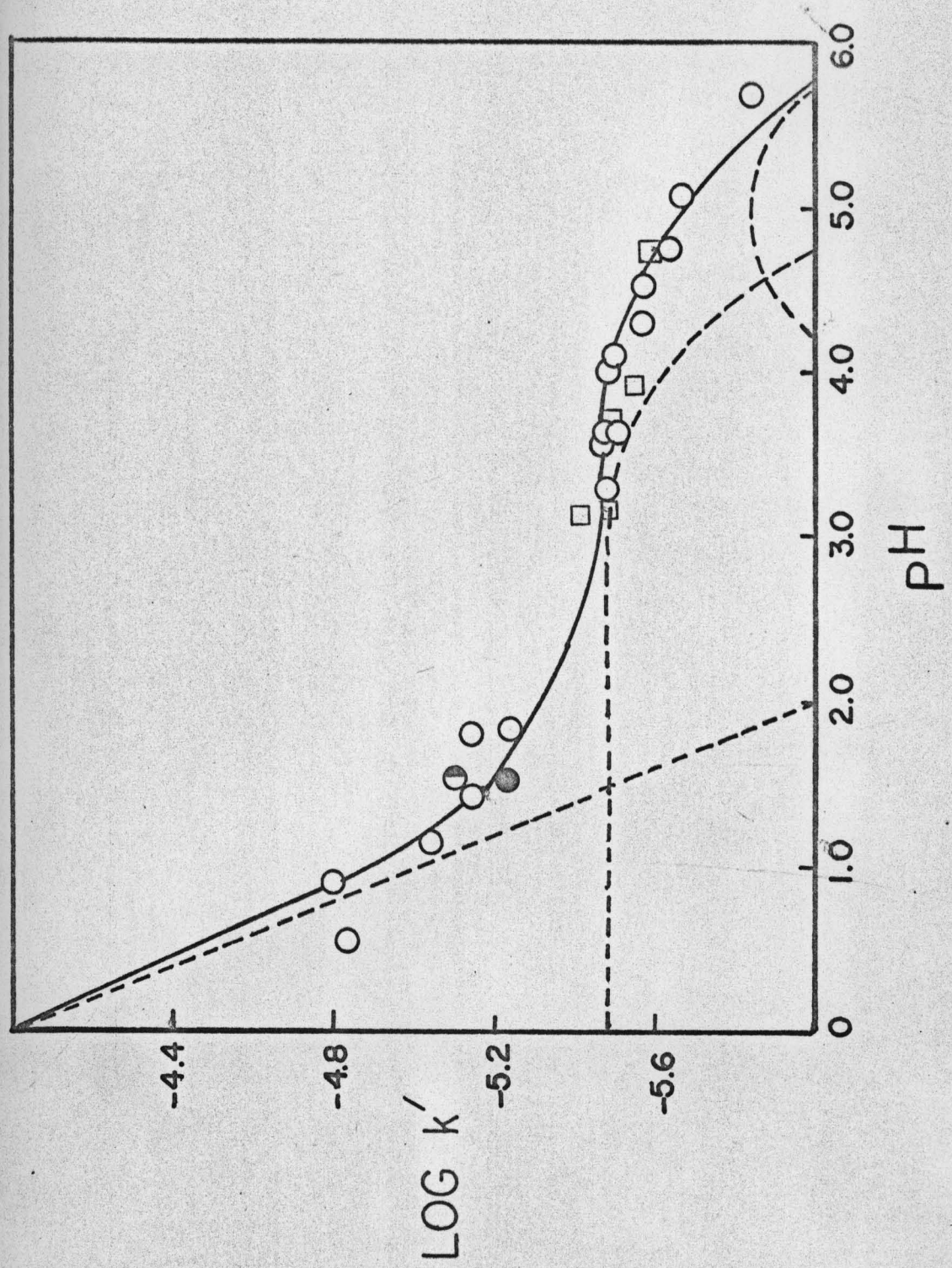

TABLE XV

Apparent Second-Order Rate Constants for the Reaction of Acetic Acid with Hydroxylamine[a]

pH	10^6 k'[b] (M^{-1} sec^{-1})	log k'
0.54	14.6	- 4.84
0.92	15.7	- 4.80
1.18	8.95	- 5.05
1.42	6.90	- 5.16
1.53[c]	7.75	- 5.11
1.55[d]	5.65	- 5.25
1.80	7.06	- 5.15
1.83	5.73	- 5.25
3.23[e]	3.58	- 5.45
3.28	3.32	- 5.48
3.57	3.28	- 5.48
3.63	3.22	- 5.49
3.64	3.10	- 5.51
3.78[e]	3.16	- 5.50
3.78	3.12	- 5.51
4.02[e]	2.76	- 5.56
4.03	3.22	- 5.49
4.10	3.10	- 5.51
4.30	2.63	- 5.58
4.53	2.60	- 5.58
4.77	2.29	- 5.64
4.80[e]	2.38	- 5.62
5.09	2.12	- 5.67
5.68	1.40	- 5.85

[a] 90.5°; μ = 1.2; 0.80 M $NH_2OH \cdot HCl$; 0.40 M acetic acid.

[b] $k' = k_{obs}/[NH_2OH]_T$.

[c] 0.40 M $NH_2OH \cdot HCl$; 0.40 M acetic acid.

[d] 0.80 M $NH_2OH \cdot HCl$; 0.86 M acetic acid.

[e] 0.80 M $NH_2OH \cdot HCl$; 0.195 M acetic acid.

The third term (k_3^H) corresponds to the uncatalyzed reaction of acetic acid and hydroxylamine, while the second term (k_2^H) describes the acid-catalyzed reaction of acetic acid and hydroxylamine. The first term (k_1^H) corresponds to an acid-catalyzed reaction that involves two hydrogen ions. Since the hydroxylamine concentration (i.e., free base concentration) is decreasing in the same proportion as the hydrogen ion concentration is increasing, this term appears to be kinetically first order in hydrogen ion. For the same reason, the second term appears to be independent of hydrogen ion concentration below pH 3.5.

Substitution of concentration terms in Equation (43) in terms of total concentrations and dissociation constants, as defined earlier, leads to Equation (44).

$$k_f' = \frac{V}{[HOAc]_T\,[NH_2OH]_T} = \frac{k_1^H K_2 [H^+]^3}{([H^+] + K_1)([H^+] + K_2)} + \frac{k_2^H K_2 [H^+]^2}{([H^+] + K_1)([H^+] + K_2)} + \frac{k_3^H K_2 [H^+]}{([H^+] + K_1)([H^+] + K_2)} \tag{44}$$

Experimentally determined dissociation constants for acetic acid (K_1 = 2.5 x 10^{-5} M, 90.5°) and hydroxylammonium ion (K_2 = 7.4 x 10^{-6} M, 90.5°) were used in calculation of the theoretical line. The individual rate constants, k_1^H, k_2^H, and k_3^H, were treated as adjustable parameters with the final values being 14.5 M^{-3} sec^{-1}, 0.45 M^{-2} sec^{-1}, and

1.2×10^{-5} $\underline{M}^{-1}$ sec^{-1}, respectively. The dashed lines give the contribution of each individual rate term. The point indicated by a half-filled circle was determined with 0.4 $\underline{M}$ hydroxylamine hydrochloride, one-half the concentration that was used for determining the other points. The completely filled circle indicates the rate constant determined with 0.86 $\underline{M}$ acetic acid, about twice the concentration used in determining the other rate constants. Within the experimental uncertainties of these measurements, the agreement of these points with the others indicates no significant general acid catalysis in this region. The squares indicate rate constants obtained using 0.195 $\underline{M}$ acetic acid, one-half the usual concentration. Data could not be collected between pH 2 and 3 due to the lack of a suitable, non-interfering buffer.

C. Hydrolysis of Acetohydroxamic Acid

Typical plots of absorbance at 530 nm against reaction time for the hydrolysis of acetohydroxamic acid are shown in Figure 19. The absorbances were measured using a methanol spectral blank, hence the non-zero "infinity" value. Proper blank corrections yield zero "infinity" values. All reactions were followed to completion. First-order plots for the same reactions are presented in Figure 20. Since these reactions go essentially to completion, $[H.A.]_\infty = 0$, an apparent second-order rate constant can be calculated by dividing the first-order

Figure 19. Plots of absorbance at 530 nm as a function of time; 90.5°; μ = 1.2; acetohydroxamic acid, 0.0015 M; 2 cm cells; top line, pH 1.68; bottom line, pH 0.73.

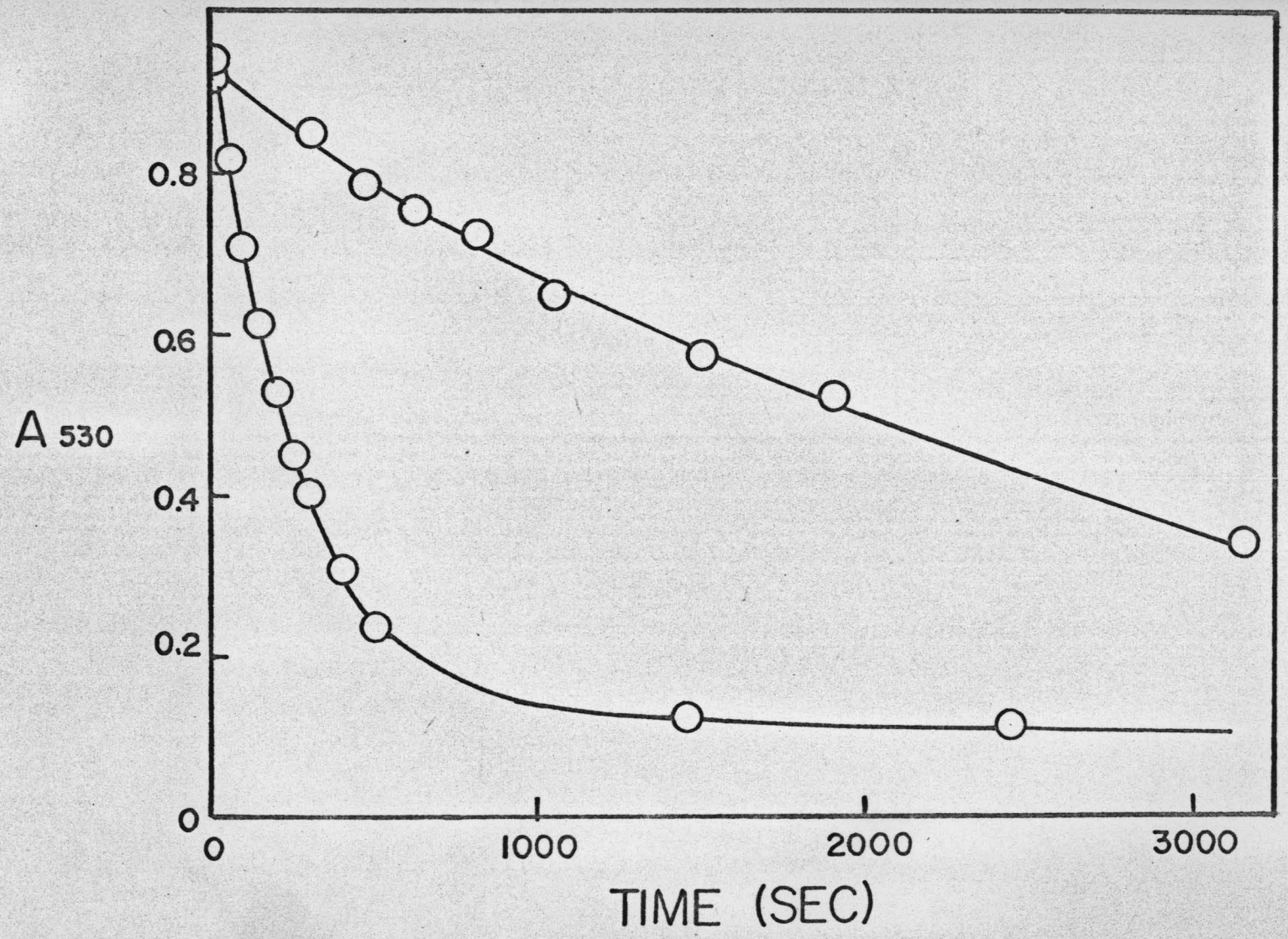
A 530
0.8
0.6
0.4
0.2
0
0
1000
2000
3000
TIME (SEC)

Figure 20. First-order plots for the hydrolysis of acetohydroxamic acid; 90.5°; μ = 1.2; top line pH 1.68; bottom line pH 0.73.

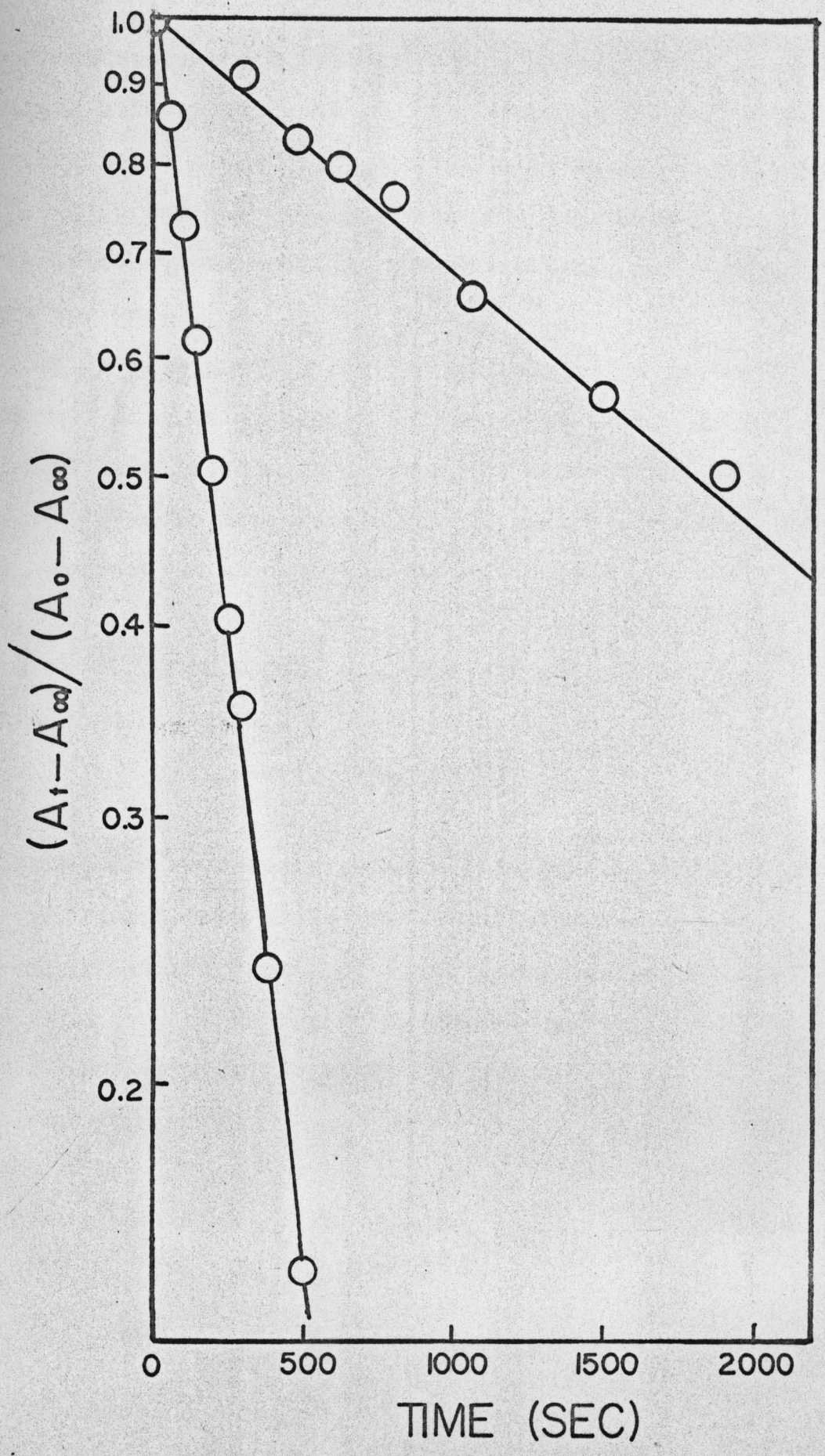
1.0
0.9
0.8
0.7
0.6
0.5
0.4
0.3
0.2
$(A_t - A_\infty)/(A_0 - A_\infty)$
0
500
1000
1500
2000
TIME (SEC)

rate constant by the concentration of water, 55.5 M. Rate constants between pH 2 and 10 were measured at two buffer concentrations, either 0.05 M and 0.1 M, or 0.1 M and 0.2 M. Reported rate constants were obtained by extrapolation to zero buffer concentration. The buffer effect was small.

The pH-rate profile for the hydrolysis of acetohydroxamic acid is presented in Figure 21 (Table XVI). The solid line is calculated from the theoretical rate equation given in Equation (45) with acetohydroxamic acid being represented as H.A. and its anion by A^-.

$$V = k_a[H.A.][H_2O][H^+] + k_b[H.A.][H_2O][OH^-] + k_c[A^-][H_2O][OH^-] \quad (45)$$

The first term represents an acid-catalyzed hydrolysis of acetohydroxamic acid while the second term represents a base-catalyzed hydrolysis of acetohydroxamic acid. The third term represents a base-catalyzed hydrolysis of the anion of acetohydroxamic acid. Equation (45) can be rewritten as,

$$k_r' = \frac{k_{obs}}{[H_2O]} = k_a[H^+] + \frac{k\,K_w}{[H^+]\,K_a} + \frac{k_c\,K_a\,K_w}{[H^+](1 + K_a)} \quad (46)$$

Figure 21. pH-rate profile for the hydrolysis of acetohydroxamic acid; 90.5°; μ = 1.2; solid line drawn from experimental rate equation (Eq. 46). Data from Table XVI.

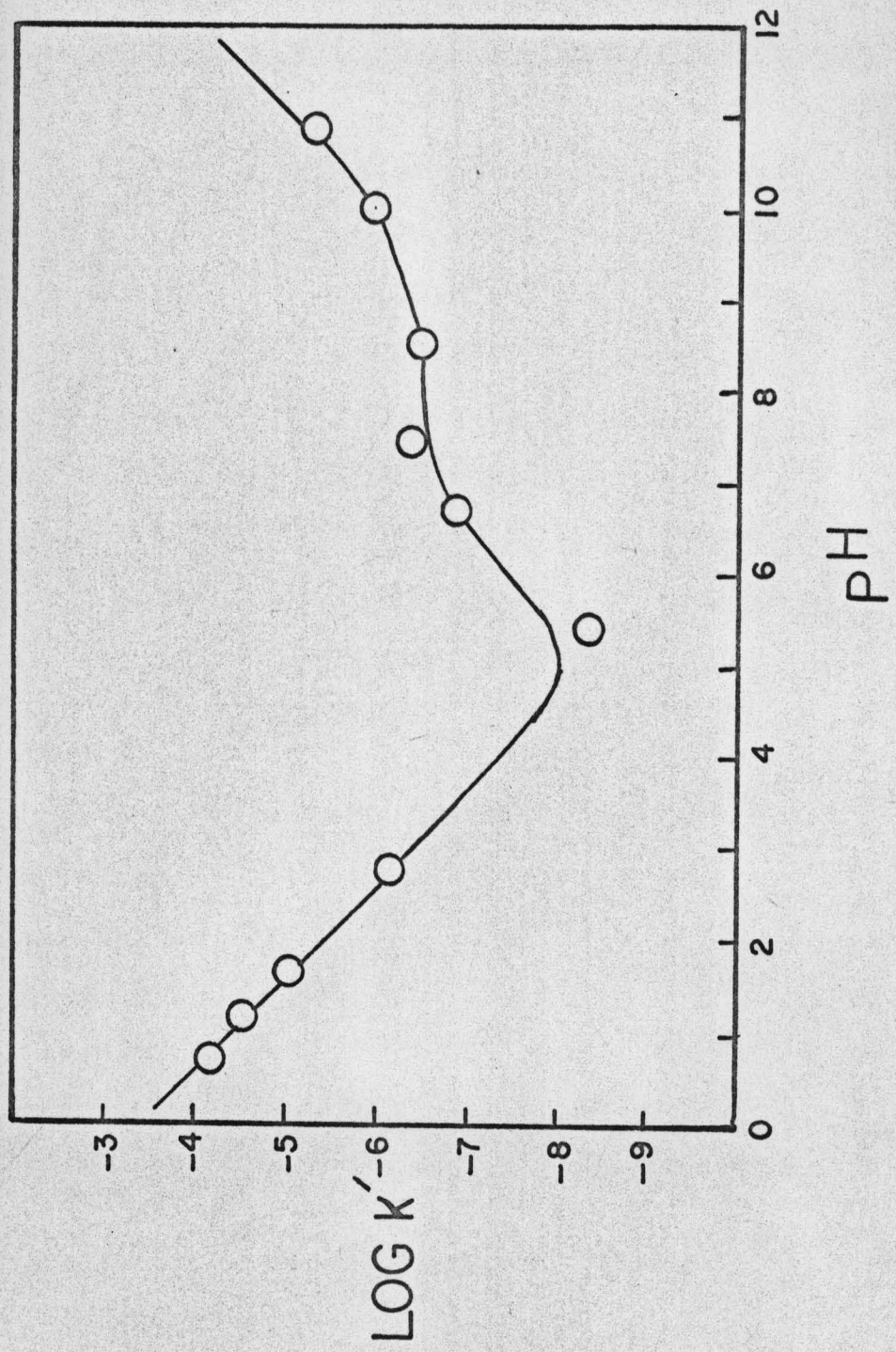

TABLE XVI

Apparent Second-Order Rate Constants for the Hydrolysis of Acetohydroxamic Acid[a]

pH (90.5°)	k(M^{-1} sec^{-1})[b]	log k
0.73	6.60×10^{-5}	- 4.18
1.15	2.96×10^{-5}	- 4.53
1.68	0.76×10^{-5}	- 5.12
2.70[c]	7.00×10^{-7}	- 6.16
5.35[d]	4.70×10^{-9}	- 8.33
6.71[e]	1.35×10^{-7}	- 6.87
7.40[e]	3.62×10^{-7}	- 6.44
8.45[f]	3.50×10^{-7}	- 6.44
9.94	1.17×10^{-6}	- 5.93
10.80	4.32×10^{-6}	- 5.36

[a] 90.5°; μ = 1.20

[b] $k = k_{obs}/[H_2O]$ where water is taken to be 55.5 M

[c] glycine buffer

[d] phthalate buffer

[e] phosphate buffer

[f] borate buffer

where K_w is the autoprotolysis constant of water and K_a, the dissociation constant of acetohydroxamic acid, is treated as an adjustable parameter. $K_w = 3.55 \times 10^{-14}$ was used in calculating the theoretical line.*

Rate constants for the hydrolysis of acetohydroxamic acid can also be calculated from the rate constant for the forward reaction and the equilibrium constant (Eq. 35). Some calculated rate constants are plotted in Figure 22 (Table XVII) along with rate constants calculated directly from the hydrolysis of acetohydroxamic acid (Table XVI). Hydrolysis rate constants obtained from studies of hydroxamic acid formation from acetic acid in the presence of nickel (II) are also plotted.

Whenever acetohydroxamic acid formation from acetic acid was followed to equilibrium it was possible to calculate the equilibrium constant for the formation of acetohydroxamic acid from Equation (33). The final hydroxamic acid concentrations were calculated directly from absorbance values and the molar absorptivity of the ferric hydroxamate complex. Since the yields were always small (less than one percent based on initial substrate concentration), [HOAc] and [NH_2OH] were taken to be the same as the initial concentrations. Water concentration

---

*This value is extrapolated at 90.5° from data presented by Harned and Hamer (79).

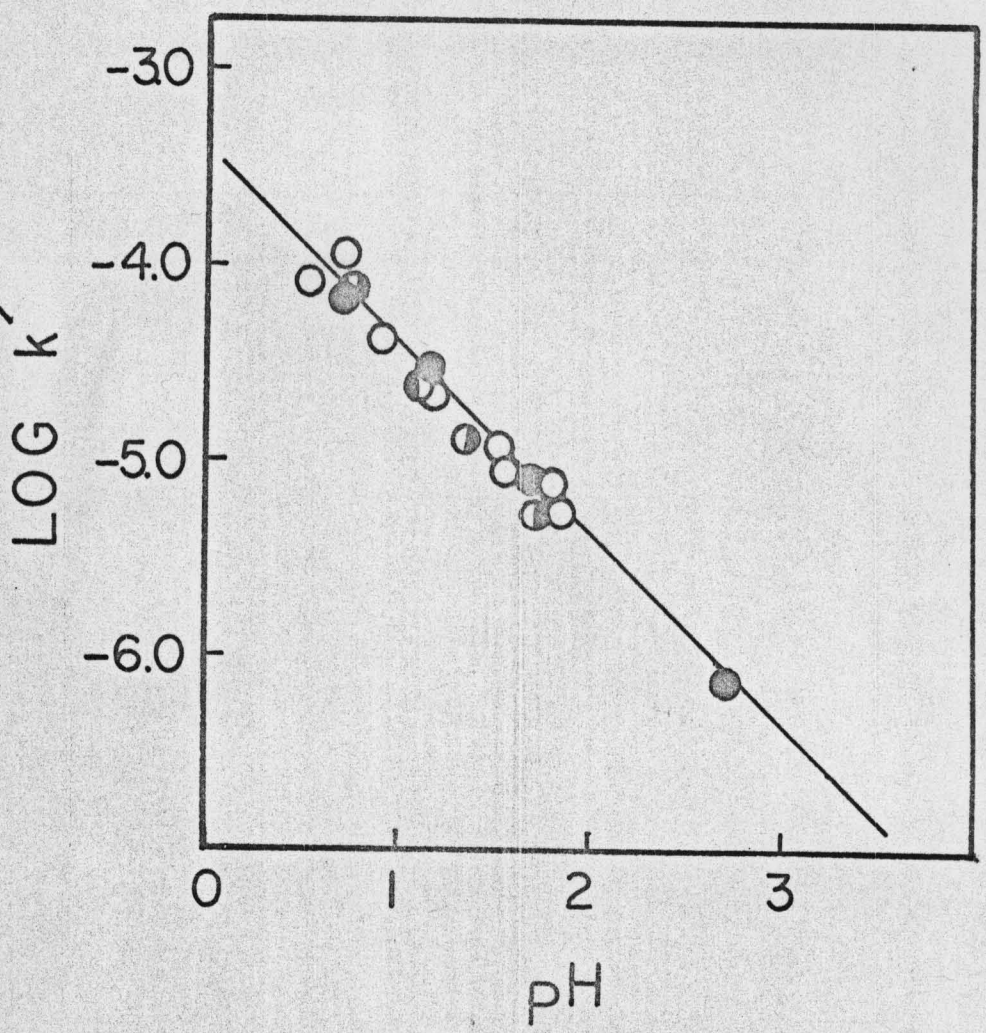

Figure 22. Partial pH-rate profile for the hydrolysis of acetohydroxamic acid; line drawn from Equation (46): filled circles represent experimental points for hydrolysis study; open circles represent rate constants calculated from reaction of acetic acid and hydroxylamine; half-filled circles represent rate constants calculated from reaction of acetic acid and hydroxylamine in the presence of 0.04 M $NiCl_2$. Data from Tables XVI and XVII.

TABLE XVII

Hydrolysis Rate Constants for Acetohydroxamic Acid Calculated from the Rate of Acetohydroxamic Acid Formation[a]

pH (90.5°)	10^5 k ($\underline{M}^{-1}$ sec^{-1})	log k
0.54	8.15	- 4.09
0.73	11.4	- 3.94
0.92	4.02	- 4.40
1.18	2.06	- 4.69
1.42	1.33	- 4.88
1.53	1.14	- 4.94
1.55	0.83	- 5.08
1.80	0.77	- 5.11
1.83	0.49	- 5.31
0.73[b]	6.65	- 4.18
1.12[b]	2.54	- 4.59
1.34[b]	1.31	- 4.88
1.83[b]	0.77	- 5.11

[a] 90.5°; μ = 1.2

[b] 0.04 $\underline{M}$ $NiCl_2$

was taken as 55.5 M. These experimentally determined equilibrium constants (see Table XVIII) are plotted as a function of pH in Figure 23. The solid line was calculated from the equation for the equilibrium constant (Eq. 35) and the theoretical rate equations for the formation (k_f) and the hydrolysis (k_r) of acetohydroxamic acid (Equations 44 and 46), and the rate constants that were used to generate the lines in Figures 18 and 21. The agreement is reasonable considering some experimental difficulties. Equilibrium constants were not experimentally obtainable for pH's greater than 4.5 because of the slowness of the reaction and the concurrent decomposition of hydroxylamine. Equilibrium constants at low pH (less than 0.75), were difficult to determine because of the low yields of hydroxamic acid.

D. Hydrogen Ion-Catalyzed Hydroxamic Acid Formation from Succinic Acid

Hydroxamic acid formation from a dicarboxylic acid, succinic acid, was studied in order to determine the effect of the neighboring carboxylate group on the reaction. Higuchi, et al. (80,81) suggested that aminolysis of dicarboxylic acids such as succinic acid proceeds through a cyclic anhydride intermediate. The primary purpose of these experiments is to determine the approximate relative reactivities of acetic acid and succinic acid in acid-catalyzed hydroxamic acid formation.

TABLE XVIII

Equilibrium Constants for the Formation of Acetohydroxamic Acids[a]

pH (90.5°)	K	log K
0.54	0.18	- 0.75
0.58	0.22	- 0.66
0.76	0.31	- 0.51
0.92	0.39	- 0.41
1.18	0.44	- 0.36
1.42	0.52	- 0.28
1.53	0.95	- 0.02
1.55	0.55	- 0.25
1.80	0.91	- 0.04
1.83	1.08	+ 0.03
2.55	2.34	+ 0.37
2.86	14.2	+ 1.15
4.03	30.8	+ 1.49
0.73[b]	0.30	- 0.52
1.12[b]	0.42	- 0.38
1.34[b]	0.56	- 0.25
1.83[b]	1.06	+ 0.25

[a] 90.5°; μ = 1.2

[b] $[NiCl_2]_T$ = 0.04 M

Figure 23. Equilibrium constants for the formation of acetohydroxamic acid from acetic acid; solid line calculated from $K = k_f/k_r$ where k_f is the rate constant for the formation of acetohydroxamic acid and k_r is the rate constant for the hydrolysis of acetohydroxamic acid. Data from Table XVIII.

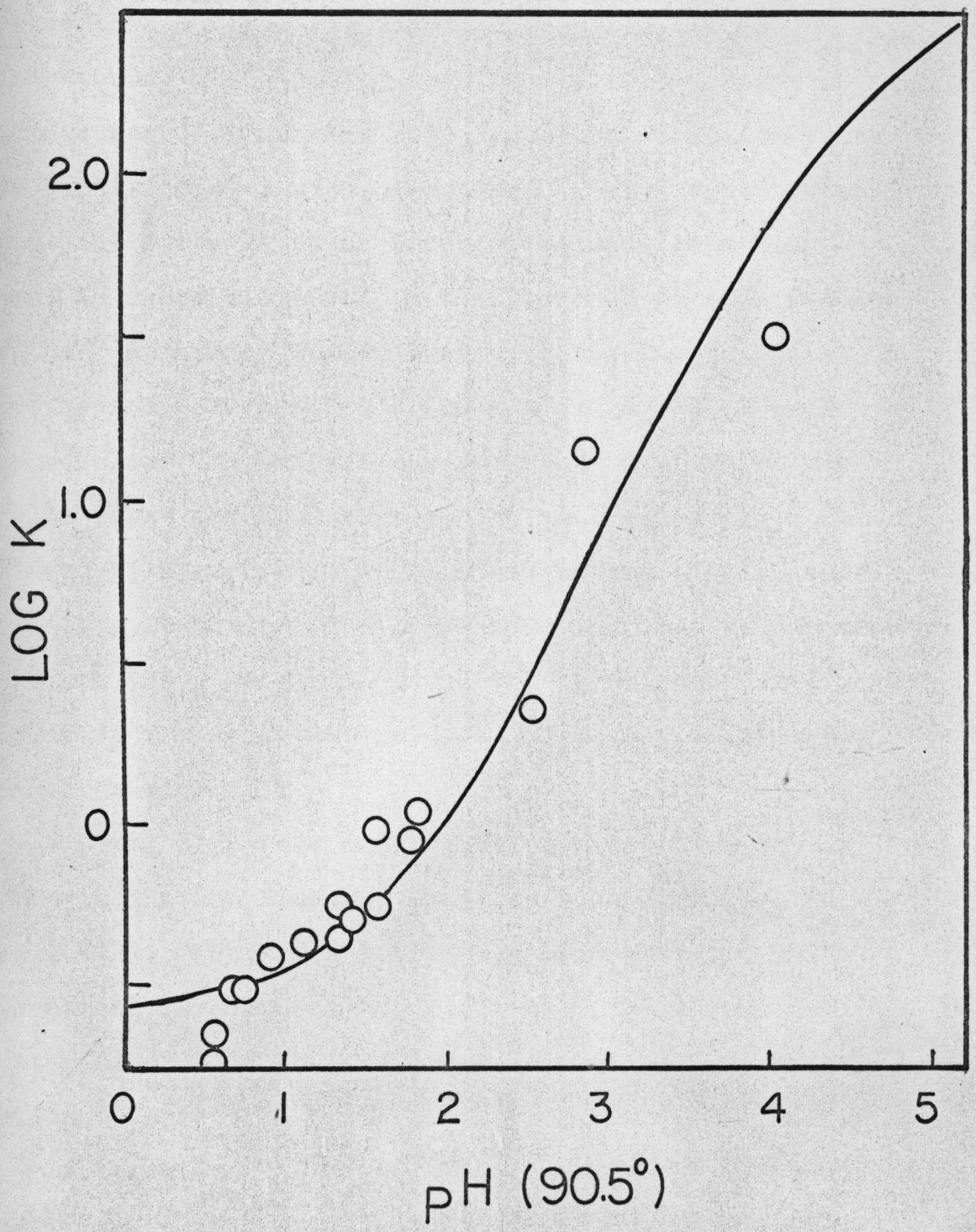
2.0
1.0
0
LOG K
0
1
2
3
4
5
pH (90.5°)

Some typical plots of absorbance against time for hydroxamic acid formation from succinic acid are shown in Figure 24. Rate constants for these reactions at pH greater than 3 were determined from initial slope measurements, since during the first 2 or 3 percent of the reaction dihydroxamic acid formation is unlikely. Rate constants at low pH, less than 2, were not obtainable due to the presence of an interfering side reaction. Figure 25 shows a typical plot of absorbance against time for the reaction of succinic acid and hydroxylamine at low pH. The initial reaction appears to be followed by a second, slower reaction. The probable reaction sequence here is first the formation of the monohydroxamic acid followed by a much slower formation of the dihydroxamic acid. The formation of N-hydroxysuccinimide, as reported by Notari (14), as a side reaction, is not suspected here because of the reported speed of its formation from the monohydroxamic acid.

A partial pH-rate profile for the reaction of hydroxylamine and succinic acid is shown in Figure 26 (Table XIX). The solid lines drawn are not based on theoretical rate equations. The straight line on the right-hand side of the graph has a slope of 1.0. The important feature of these data is that the rate constants are similar in magnitude to those obtained in the study of acetic acid. This similarity will be discussed later with regard to possible anhydride intermediates.

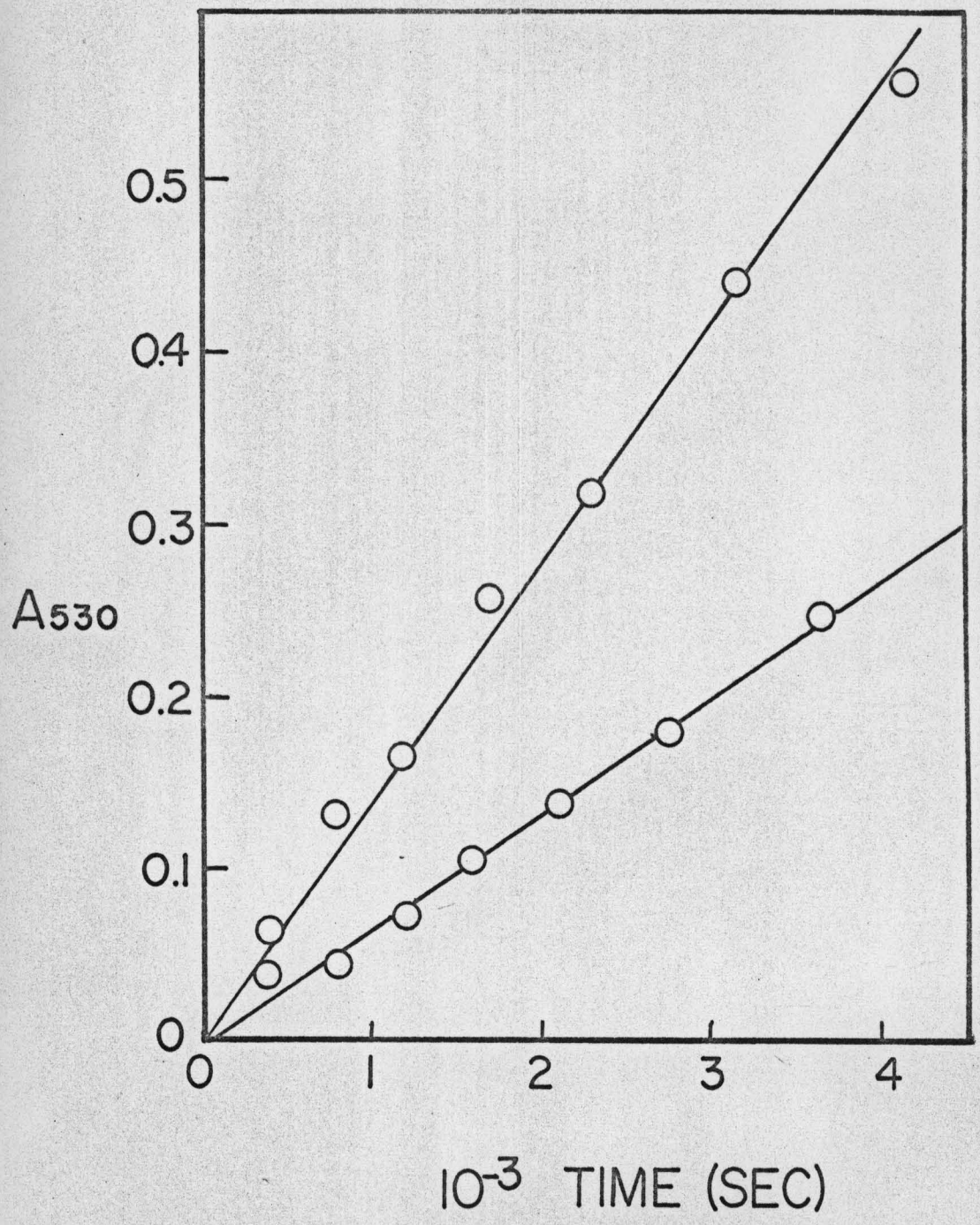

Figure 24. Typical plots of absorbance against reaction time for hydroxamic acid formation from succinic acid; 90.5°; μ = 2.0; 0.80 M $NH_2OH \cdot HCl$; 0.40 M succinic acid; 2 cm cells; top line, pH 6.18; bottom line, pH 6.53.

Figure 25. Plot of absorbance against time for reaction of hydroxylamine and succinic acid; 90.5°; pH 1.08; 0.80 M $NH_2OH \cdot HCl$; 0.40 M succinic acid; μ = 2.0; 2 cm cells.

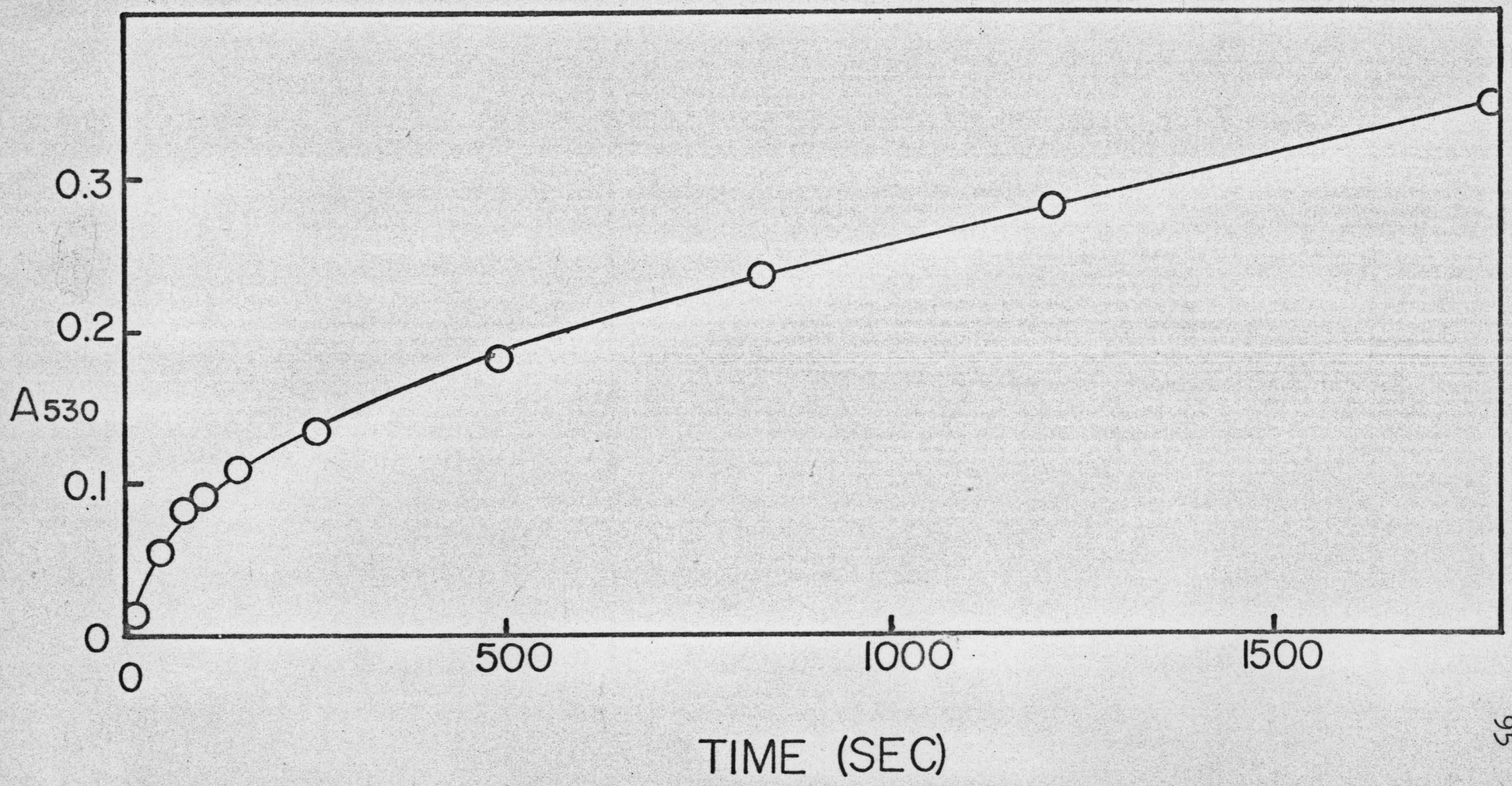
0.3
0.2
A530
0.1
0
0
500
1000
1500
TIME (SEC)

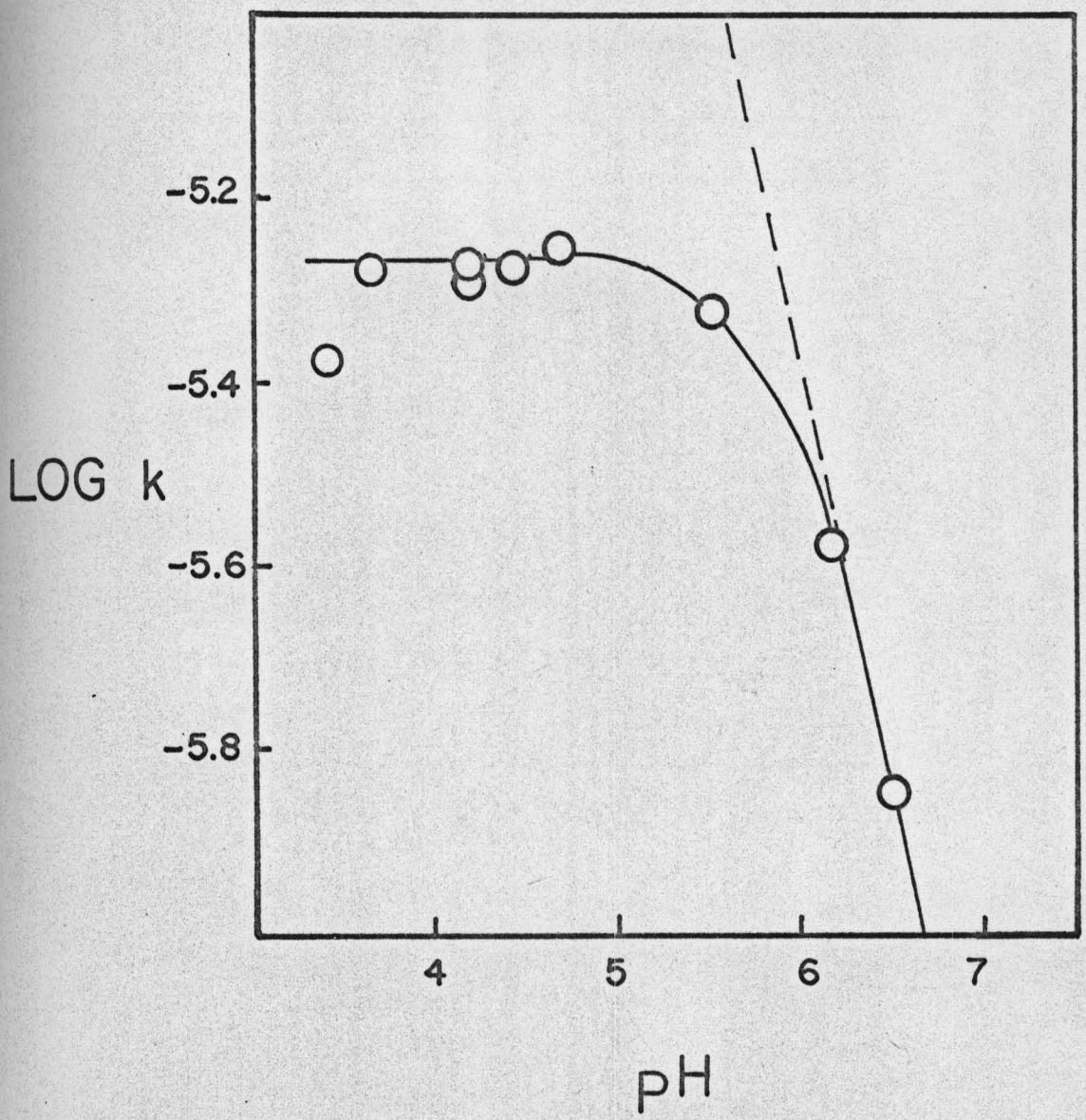

Figure 26. pH-rate profile for hydroxamic acid formation from succinic acid. Data from Table XIX.

TABLE XIX

Apparent Second-Order Rate Constants for the Reaction of Succinic Acid and Hydroxylamine[a]

pH	10^6 k' ($\underline{M}^{-1}$ sec^{-1})	log k'
3.41[b]	4.18	- 5.38
3.66	5.25	- 5.28
4.20	5.35	- 5.27
4.23[b]	5.12	- 5.29
4.43	5.22	- 5.28
4.68[b]	5.44	- 5.26
5.55[b]	4.82	- 5.32
6.18	2.62	- 5.58
6.53	1.40	- 5.85

[a] 90.5°; 0.80 $\underline{M}$ $NH_2OH \cdot HCl$; 0.40 $\underline{M}$ succinic acid; $\mu = 2.0$

[b] $\mu = 1.0$

E. Reactions of Phenyl Acetate with Hydroxylamine

Phenyl esters of acetic acid have been shown by Jencks (7,8) to react in a two-step reaction. The first step is O-acetylation of the hydroxylamine, followed by conversion of the O-acetylhydroxylamine, VI, to the N-acetylhydroxylamine (hydroxamic acid), VII (Eqs. 47 and 48).

$$CH_3COO\text{-}C_6H_5 + NH_2OH \longrightarrow CH_3COONH_2 + C_6H_5\text{-}OH \qquad (47)$$

VI

$$CH_3COONH_2 \xrightarrow{NH_2OH} CH_3\text{-}CONHOH \qquad (48)$$

VII

Phenyl acetate, chosen here as a substrate for the study of possible nickel (II) catalysis of the reaction of hydroxylamine and an aromatic ester, is sufficiently labile to permit kinetic studies at 25.0°. The progress of the first step of the reaction (Eq. 47) can be monitored by measuring the absorbance change at 275 nm, which is due to the release of phenol. The second step of the reaction (Eq. 48) can be followed by measuring the absorbance of the ferric-hydroxamate complex at 530 nm. (O-acetyl-hydroxylamine does not give a color with ferric iron.) Typical plots of absorbance against time for phenol release

and hydroxamic acid formation are shown in Figure 27. Some typical first-order plots for phenol release and hydroxamic acid formation are presented in Figures 28 and 29.

A plot of the apparent first-order rate constants against total hydroxylamine concentration for phenol release (Figure 30 and Table XX) shows a distinct upward curvature, suggesting a higher-than-first-order dependence on total hydroxylamine concentration. A simple rate equation that could account for the curvature is of the form,

$$V = k'[ESTER][NH_2OH] + k''[ESTER][NH_2OH]^2 \qquad (49)$$

The second term, being second order in hydroxylamine, could arise from catalysis by hydroxylamine. Converting Equation (49), in the usual way, into an expression containing total hydroxylamine concentration and solving for the observed first-order rate constant (k_{obs}) gives,

$$\frac{V}{[ESTER]} = k_{obs} = k'\left(\frac{K_a}{K_a + [H^+]}\right)[NH_2OH]_T + k''\left(\frac{K_a}{K_a + [H^+]}\right)^2[NH_2OH]_T^2 \qquad (50)$$

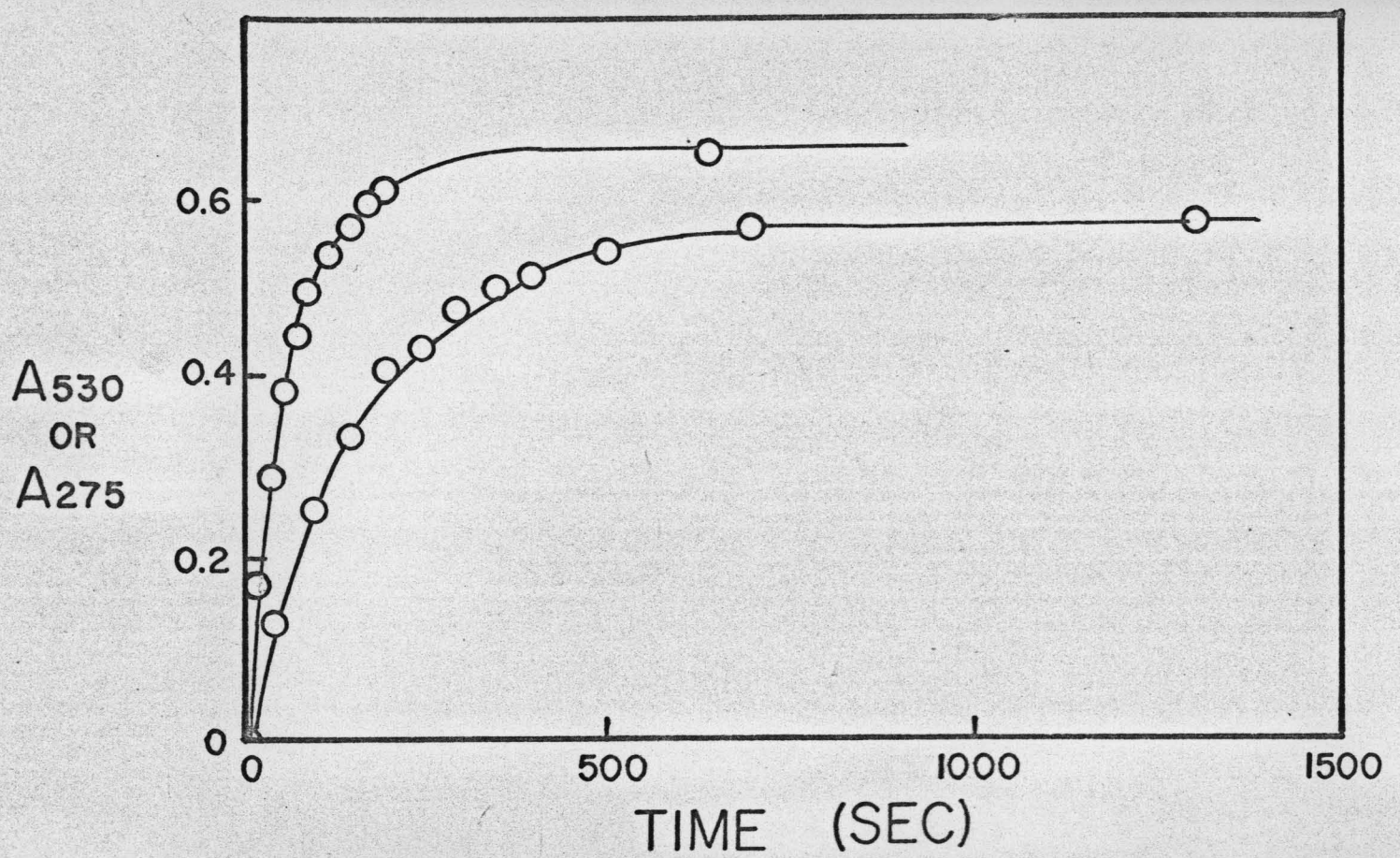

Figure 27. Plots of absorbance against reaction time for the reaction of phenyl acetate with hydroxylamine; 0.64 M $NH_2OH \cdot HCl$; 25.0°; μ = 1.0; top line, phenol release, absorbance measured at 275 nm, 1 cm cells, pH 6.05, phenyl acetate 0.00059 M; bottom line, hydroxamic acid production, absorbance measured at 530 nm; 2 cm cells; pH 6.10; phenyl acetate 0.0065 M.

Figure 28. First-order plots for phenol release from the reaction of phenyl acetate with hydroxylamine; 25.0°; μ = 1.0; total hydroxylamine concentration from top to bottom, 0.32, 0.448, 0.64 M; pH 6.06.

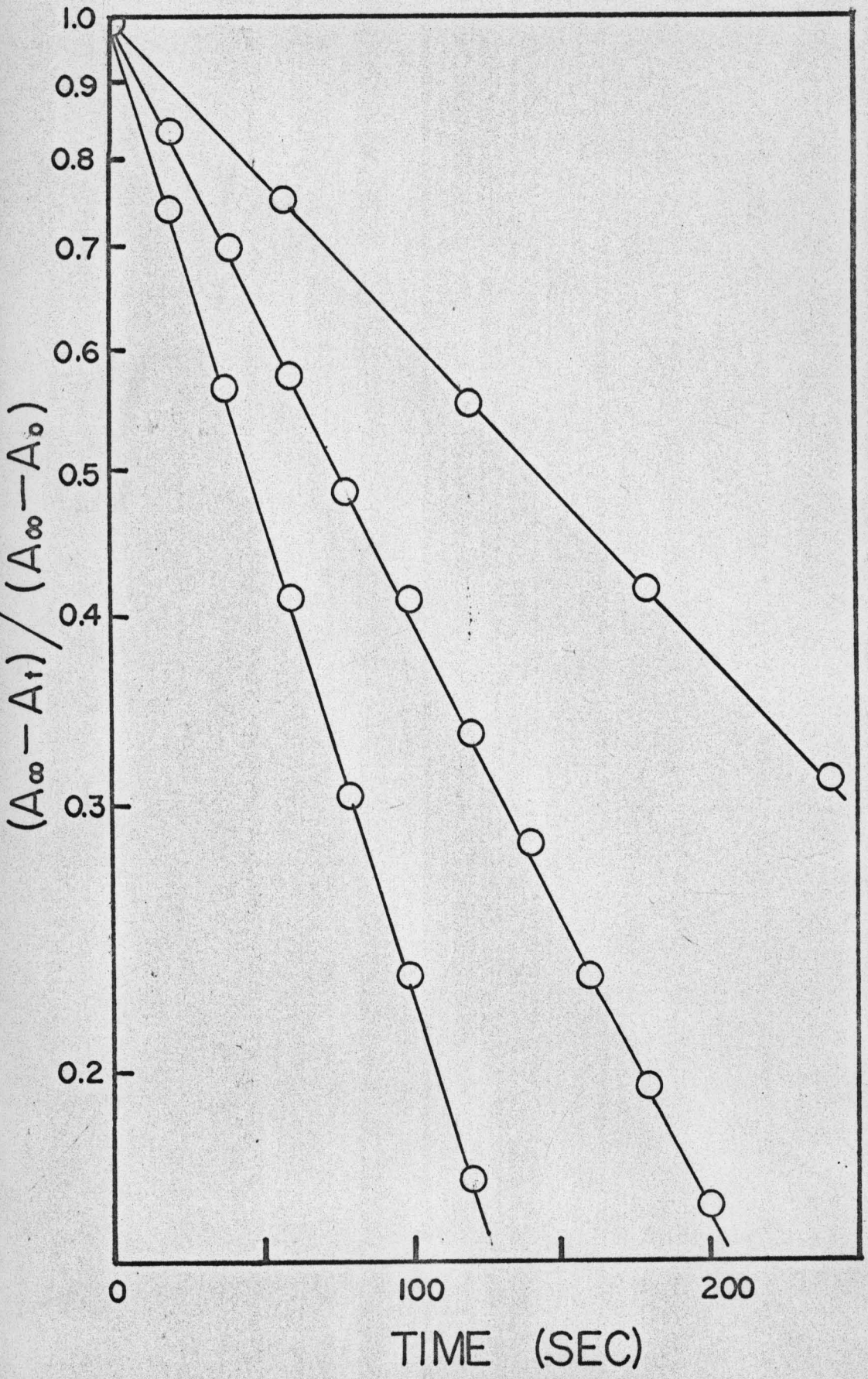
1.0
0.9
0.8
0.7
0.6
0.5
0.4
0.3
0.2
$(A_\infty - A_t) / (A_\infty - A_0)$
0
100
200
TIME (SEC)

Figure 29. First-order plots for hydroxamic acid production from the reaction of phenyl acetate and hydroxylamine; 25.0°; μ = 1.0; total hydroxylamine concentration from top to bottom, 0.256, 0.448, 0.640 M; pH = 6.10.

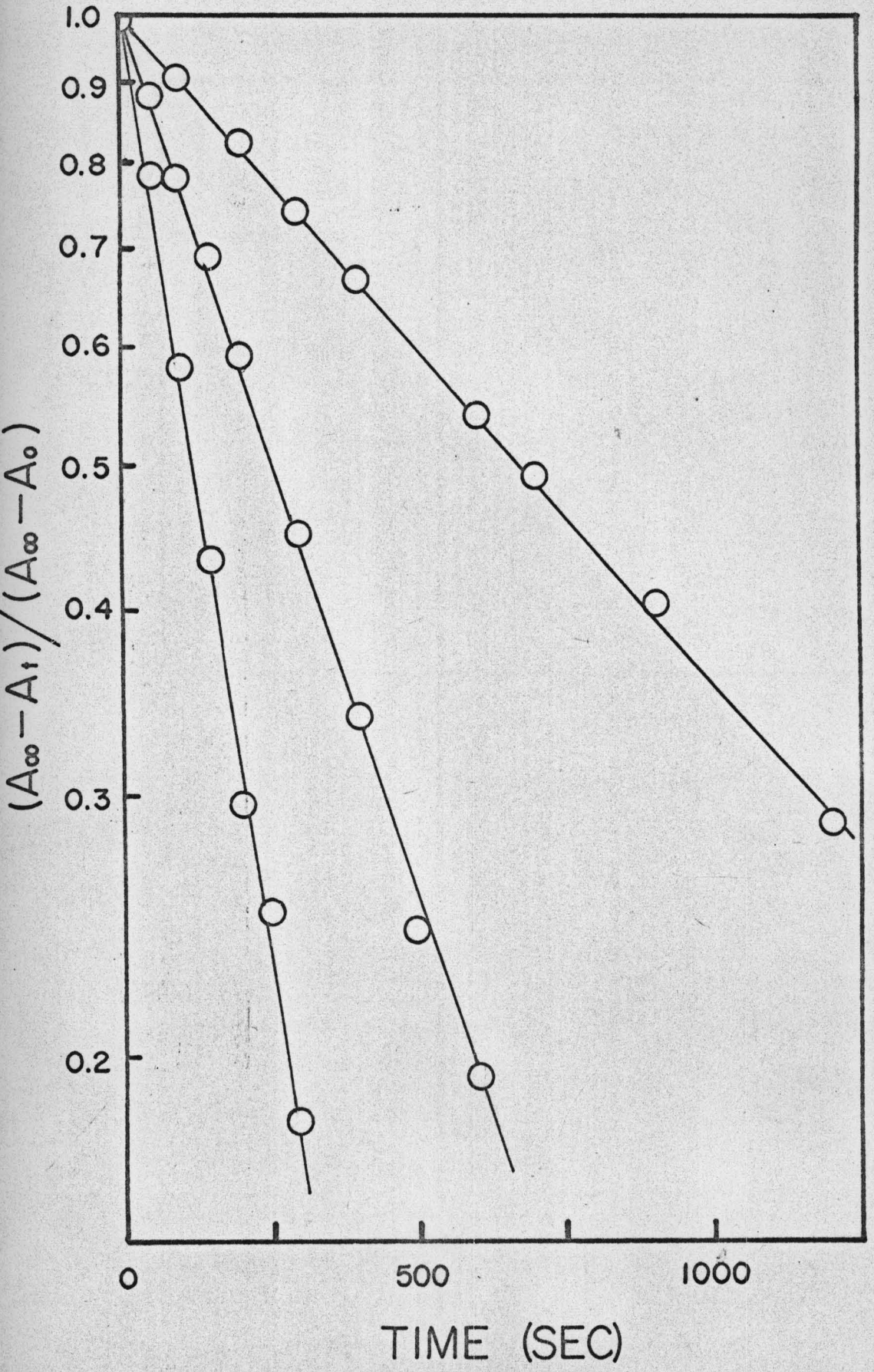
1.0
0.9
0.8
0.7
0.6
0.5
0.4
0.3
0.2
$(A_\infty - A_t)/(A_\infty - A_0)$
0
500
1000
TIME (SEC)

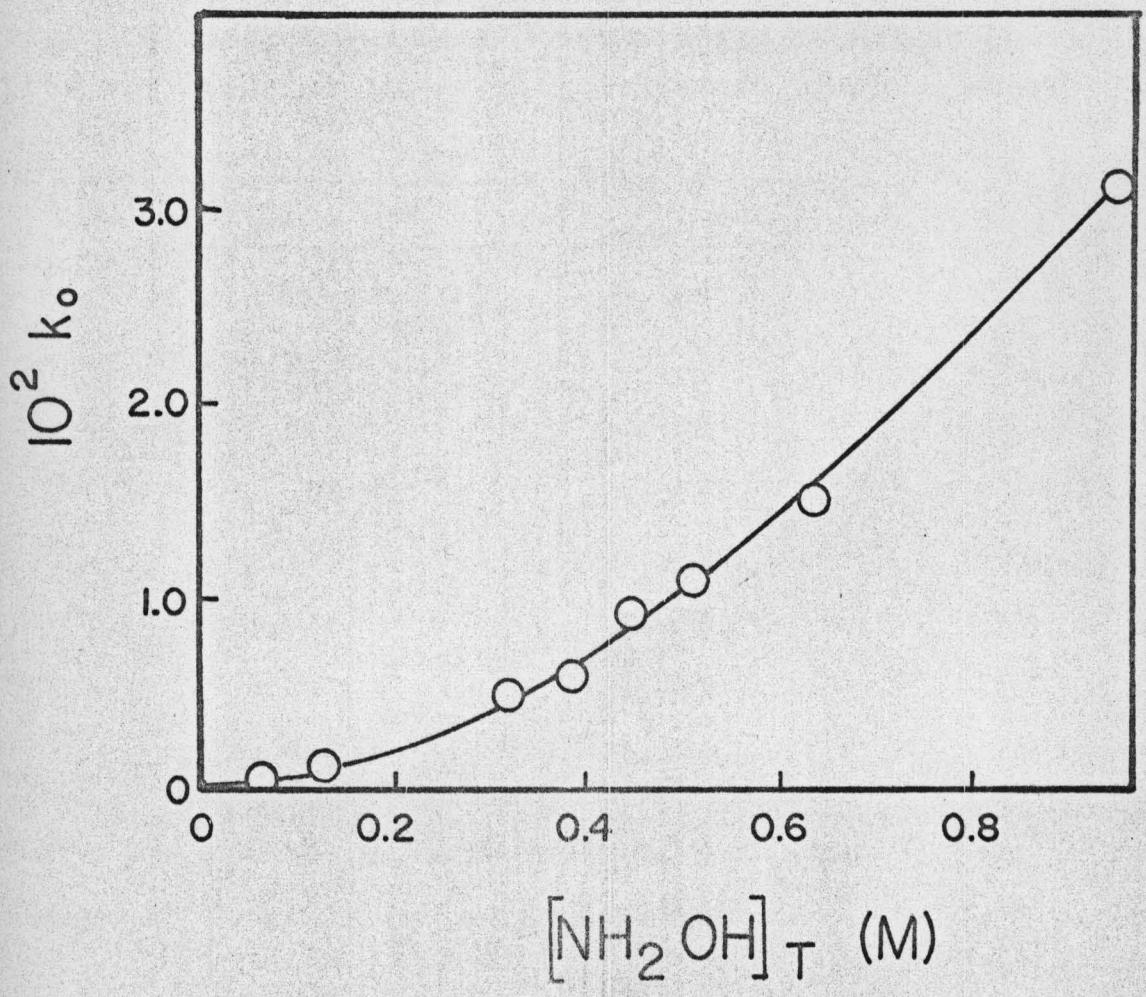

Figure 30. Plot of apparent first-order rate constants as a function of total hydroxylamine concentration for phenol release from the reaction of phenyl acetate and hydroxylamine. Data from Table XX.

TABLE XX

Apparent First-Order Rate Constants for Phenol Release from the Reaction of Phenyl Acetate and Hydroxylamine[a]

$[NH_2OH]_T$ (M)	$10^2 k_{obs}$ (sec^{-1})[b]
0.064	0.048
0.128	0.111
0.320	0.488
0.384	0.589
0.448	0.908
0.512	1.085
0.640	1.498
0.960	3.13

[a] 25.0°; μ = 1.0; pH 6.06; 0.083% (v/v) methanol

[b] average of at least two determinations

where K_a is the dissociation constant for the hydroxylammonium ion. Dividing both sides of Equation (50) by $[NH_2OH]_T$ leads to Equation (51), which is of the form of an equation for a straight line.

$$\frac{k_{obs}}{[NH_2OH]_T} = k'\left(\frac{K_a}{K_a + [H^+]}\right) + k''\left(\frac{K_a}{K_a + [H^+]}\right)^2[NH_2OH]_T \qquad (51)$$

Figure 31 (Table XXI) shows plots of $k_{obs}/[NH_2OH]_T$ against $[NH_2OH]_T$ for phenol release and for hydroxamic acid formation from phenyl acetate in the absence of nickel (II). Both the intercept, $k'\left(\frac{K_a}{K_a + [H^+]}\right)$, and the slope, $k''\left(\frac{K_a}{K_a + [H^+]}\right)^2$, are smaller for hydroxamic acid production than for phenol release. When the same plots are made for the reaction in the presence of nickel (II), the slopes and intercepts for phenol release and hydroxamic acid formation are essentially the same (Figure 32 and Table XXII). Comparing Figures 31 and 32 shows that the intercept of the phenol release plot for the reaction in the presence of nickel (II) is essentially the same as in the absence of nickel (II); however, the slope is less than in the absence of nickel.

In the reactions without nickel (II) the first step of the reaction sequence, phenol release or O-acetylhydroxylamine production, is faster than hydroxamic acid formation. Hence, the second step, hydroxamic acid

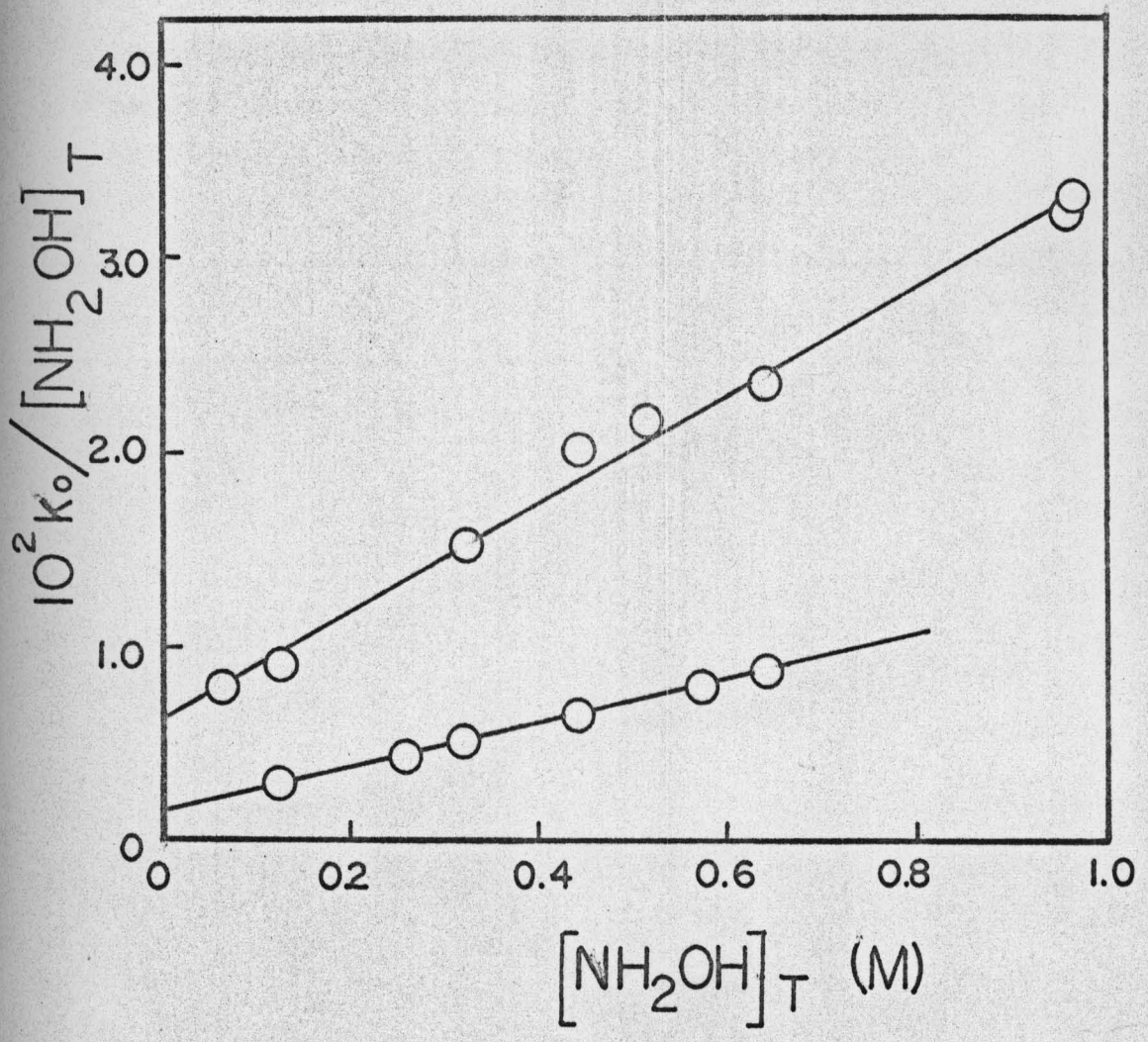

Figure 31. Apparent second-order rate constants for phenol production and hydroxamic acid formation from phenyl acetate plotted as a function of total hydroxylamine concentration. Top line, phenol production; Bottom line, hydroxamic acid formation. Data from Table XXI.

TABLE XXI

Apparent Second-Order Rate Constants for Phenol Production and Hydroxamic Acid Formation from the Reaction of Phenyl Acetate and Hydroxylamine[a]

	$[NH_2OH]_T$	$\frac{10^2 k\ (sec^{-1})}{[NH_2OH]_T}$
A. Phenol Production		
	0.064	0.75
	0.128	0.87
	0.320	1.53
	0.384	1.54
	0.448	2.02
	0.512	2.15
	0.640	2.34
	0.960	3.24
	0.960	3.30
B. Hydroxamic Acid Formation		
	0.128	0.261
	0.256	0.404
	0.320	0.497
	0.448	0.640
	0.576	0.756
	0.640	0.861

[a] 25.0°; μ = 1.0; pH 6.05

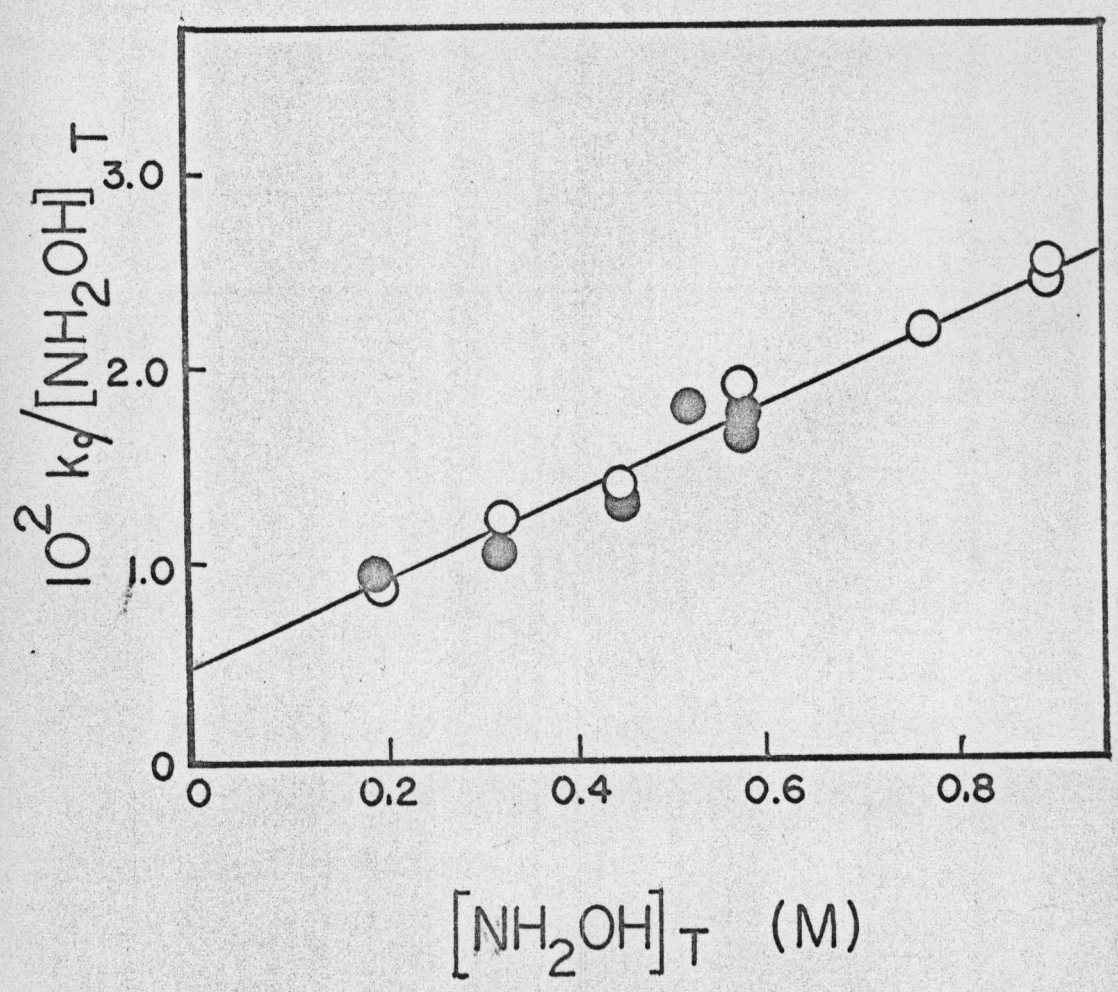

Figure 32. Apparent second-order rate constants for phenol production and hydroxamic acid formation from phenyl acetate in the presence of nickel (II) plotted as a function of total hydroxylamine concentration; open circles, phenol production; filled circles, hydroxamic acid production. Data from Table XXII.

TABLE XXII

Apparent Second-Order Rate Constants for Phenol Production and Hydroxamic Acid Formation from the Reaction of Phenyl Acetate and Hydroxylamine in the Presence of Nickel Chloride[a]

	$[NH_2OH]_T$	$\frac{10^2 k\ (sec^{-1})}{[NH_2OH]_T}$
A. Phenol Production		
	0.192	0.859
	0.320	1.201
	0.448	1.439
	0.576	1.898
	0.768	2.153
	0.896	2.537
	0.896	2.392
B. Hydroxamic Acid Formation		
	0.192	0.91
	0.320	1.05
	0.448	1.36
	0.448	1.28
	0.512	1.80
	0.576	1.63
	0.576	1.72

[a] 25.0°; pH 6.05; μ = 1.0; 0.04 M $NiCl_2$

formation from O-acetylhydroxylamine, appears to be the rate determining step for the overall formation of hydroxamic acid from phenyl acetate. In the presence of nickel (II) the apparent second-order rate constants for phenol release are the same as those for hydroxamic acid formation. Also, the rate constants for the formation of hydroxamic acid are greater for the reaction in the presence of nickel (II) than in its absence. These data lead to two possible explanations for the nickel catalysis of hydroxamic acid formation: a) the first step of the reaction, O-acetylhydroxylamine formation, is made rate limiting as a result of catalysis of the second step of the reaction; or, b) there is a direct nickel (II)-catalyzed N-acetylation (Eq. 52) in addition to O-acetylation.

$$CH_3COO\text{-}C_6H_5 + NH_2OH \longrightarrow CH_3CONHOH + C_6H_5\text{-}OH \qquad (52)$$

A test to differentiate between these mechanisms is to measure the rate of phenol release in the presence and absence of nickel (II). If the second mechanism, b, is operative, then nickel must also catalyze phenol release since a phenol molecule is released for every hydroxamic acid molecule produced by N-acetylation. It should be noted that under these conditions of temperature and pH, there was no detectable spontaneous hydrolysis of phenyl acetate in either the presence or absence of nickel (II)

over the time scale of these reactions.

The individual rate constants k' and k" can be obtained from the intercept and slope of plots of $k_{obs}/[NH_2OH]_T$ against $[NH_2OH]_T$. Note that the intercept of Equation (51) is a function of pH. Denoting the intercept as I, the expression for the intercept can be rewritten as,

$$[H^+] = \frac{k_1 K_a}{I} - K_a \qquad (53)$$

By determining the intercept of the plot of $k_{obs}/[NH_2OH]_T$ against $[NH_2OH]_T$ at several pH values, it is possible to obtain values for k' and K_a. From Equation (53), a plot of hydrogen ion concentration against the reciprocal of the intercept gives an intercept of K_a and a slope of $k_1 K_a$. Using the value of K_a determined here, k" can be determined from the slope of Equation (51) (Eq. 54).

$$\text{Slope} = k''\left(\frac{K_a}{K_a + [H^+]}\right)^2 \qquad (54)$$

Figure 33 (Table XXIII) shows a plot of $k_{obs}/[NH_2OH]_T$ against $[NH_2OH]_T$ for a series of pH values for phenol release from phenyl acetate in the absence of nickel (II). A plot of the reciprocal of the intercept against hydrogen ion concentration for these data is presented in Figure 34 (Table XXIV). This graph gives an intercept, $-K_a$, of

Figure 33. Plots of $k_{obs}/[NH_2OH]_T$ against $[NH_2OH]_T$ for phenol release from phenyl acetate in the absence of nickel (II); top line, pH 6.50; middle line, pH 6.00; bottom line, pH 5.50. Data from Table XXIII. Lines are "least squares" lines.

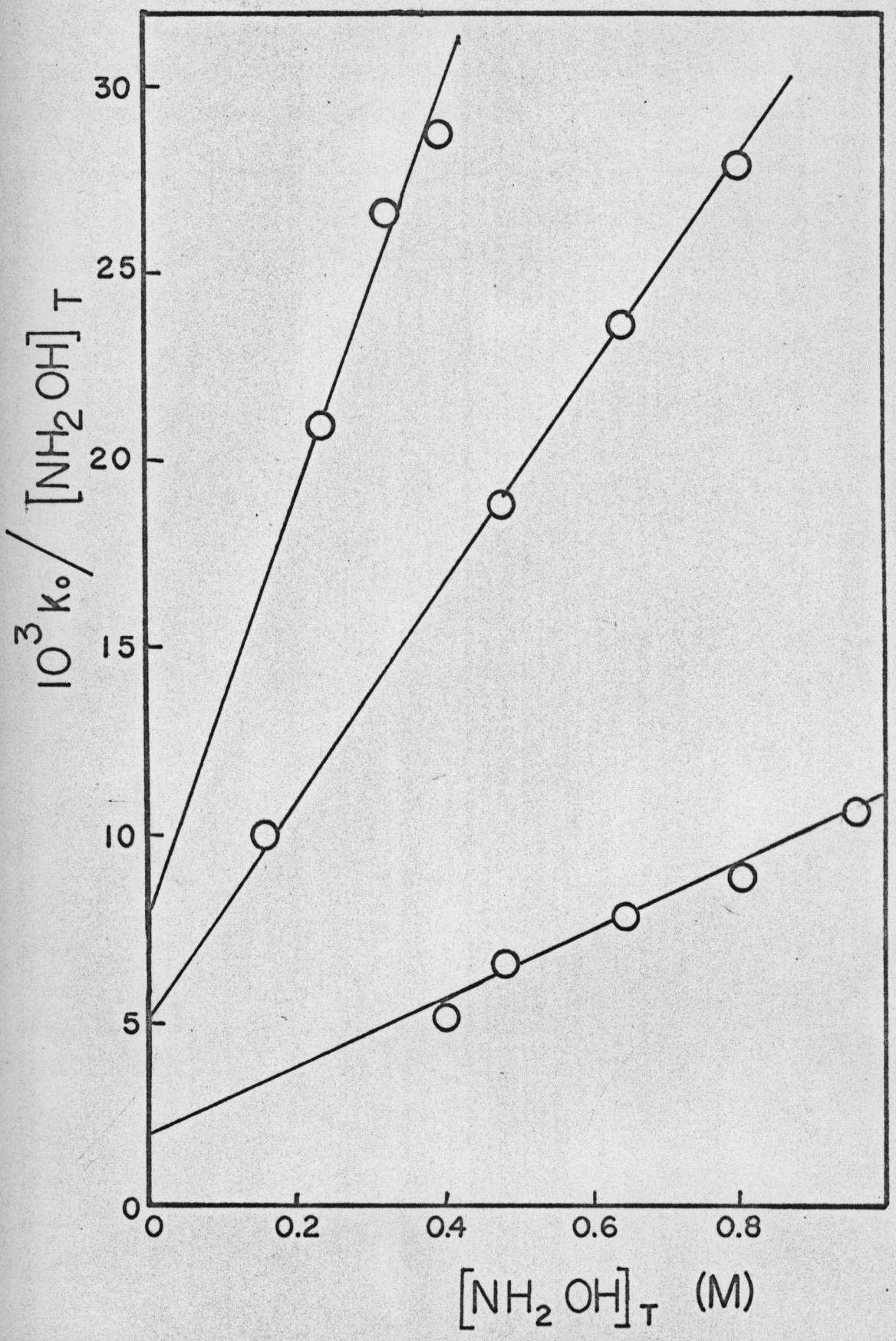
30
25
20
15
10
5
0
0
0.2
0.4
0.6
0.8
$10^3 K_o / [NH_2OH]_T$
$[NH_2OH]_T$ (M)

TABLE XXIII

Apparent Second-Order Rate Constants for Phenol Release from the Reaction of Phenyl Acetate and Hydroxylamine[a]

	$[NH_2OH]_T$	$\frac{10^2 k_{obs}}{[NH_2OH]_T}$
A. pH 5.50	0.40	0.51
	0.48	0.66
	0.64	0.79
	0.80	0.88
	0.96	1.05
B. pH 6.00		
	0.16	1.00
	0.48	1.87
	0.64	2.35
	0.80	2.78
C. pH 6.50		
	0.24	2.08
	0.32	2.66
	0.40	2.88
	0.56	3.85

[a] 25.0°; μ = 1.0

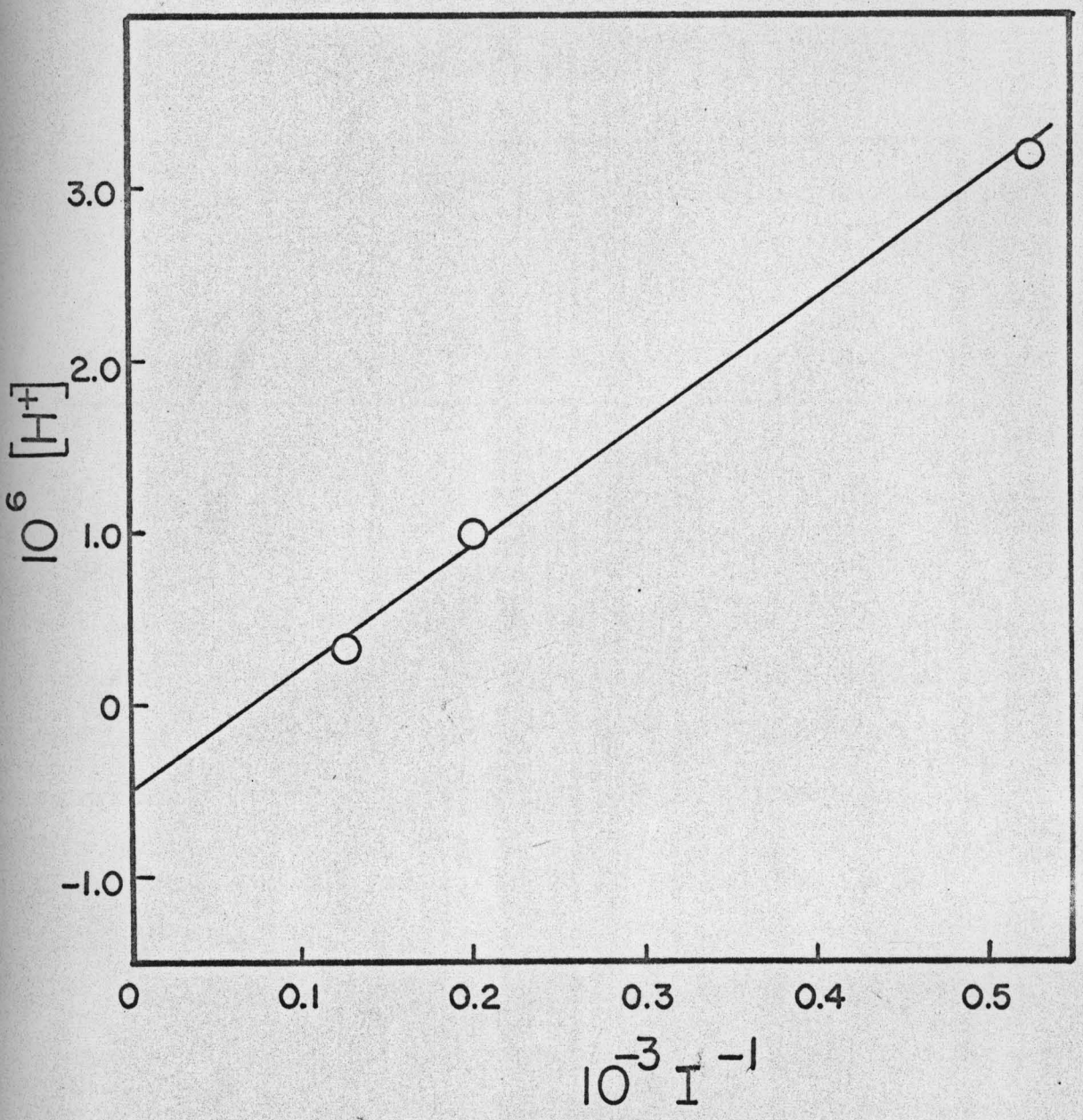

Figure 34. Plot of $[H^+]$ against reciprocal of the intercepts from plots in Figure 33. Data from Table XXIV.

TABLE XXIV

Intercepts of Plots of $k_{obs}/[NH_2OH]_T$ Against $[NH_2OH]_T$ from Figure 33

pH	10^6 $[H^+]$	10^3 Intercept (I)	10^{-3} I^{-1}
5.50	3.16	1.90	0.526
6.00	1.00	5.02	0.200
6.50	0.316	7.80	0.128

$- 5.2 \times 10^{-7}$ M; the slope is 7.2×10^{-6} sec^{-1}, giving a value for k' of 1.38×10^{-1} M^{-1} sec^{-1}. The slope of the top line in Figure 31 is 2.83×10^{-2} M^{-2} sec^{-1}, which is equal to $k'(\frac{K_a}{K_a + [H^+]})^2$. Using the experimentally determined K_a, the value for k" is calculated to be 0.226 M^{-2} sec^{-1}.

The plots of $k_{obs}/[NH_2OH]_T$ against $[NH_2OH]_T$ for various pH values in the presence of 0.04 M nickel chloride are shown in Figure 35 (Table XXV). Hydrogen ion concentration is plotted against the reciprocal of the intercepts from Figure 35 in Figure 36 (Table XXVI). The intercept, $-K_a$, is $- 2.78 \times 10^{-6}$ M and the slope $k' K_a$ is 1.19×10^{-8} sec^{-1}. The value for K_a here is an apparent dissociation constant for hydroxylammonium ion in the

Figure 35. Plots of $k_{obs}/[NH_2OH]_T$ against $[NH_2OH]_T$ for phenol release from phenyl acetate in the presence of 0.04 M nickel chloride; lines from top to bottom, pH 6.60, pH 6.00, pH 5.50. Data from Table XXV. Lines are "least squares" lines.

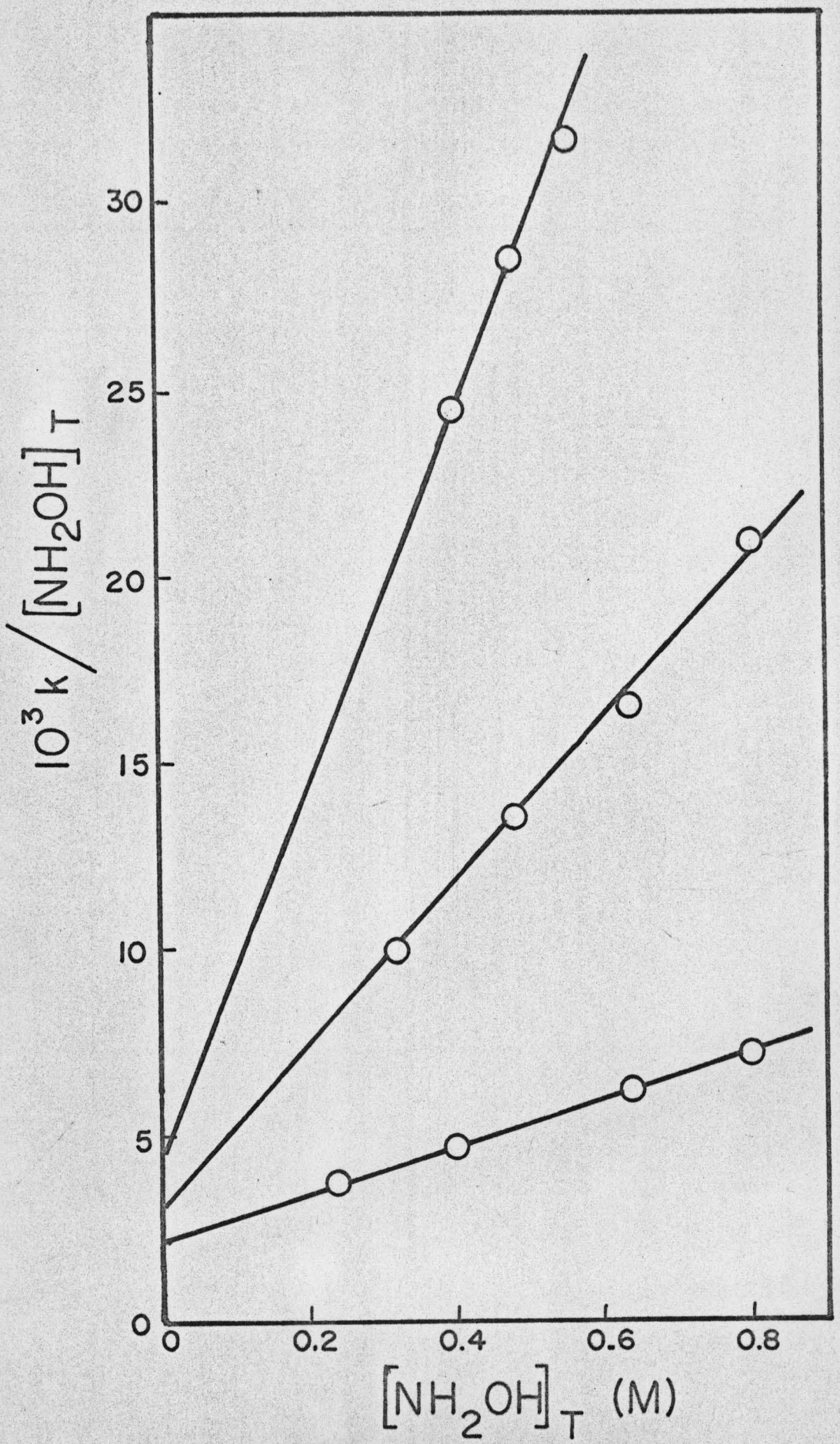
$10^3 k / [NH_2OH]_T$
30
25
20
15
10
5
0
0
0.2
0.4
0.6
0.8
$[NH_2OH]_T$ (M)

TABLE XXV

Apparent Second-Order Rate Constants for Phenol Release from Phenyl Acetate in the Presence of 0.04 M Nickel Chloride[a]

	$[NH_2OH]_T$ (M)	$10^2 k_{obs}$ / $[NH_2OH]$ (M^{-1} sec^{-1})
A. pH 5.50		
	0.24	0.35
	0.40	0.47
	0.64	0.61
	0.80	0.72
B. pH 6.00		
	0.32	0.99
	0.48	1.35
	0.64	1.64
	0.80	2.09
C. pH 6.60		
	0.40	2.45
	0.48	2.85
	0.56	3.16

[a] 25.0°; μ = 1.0

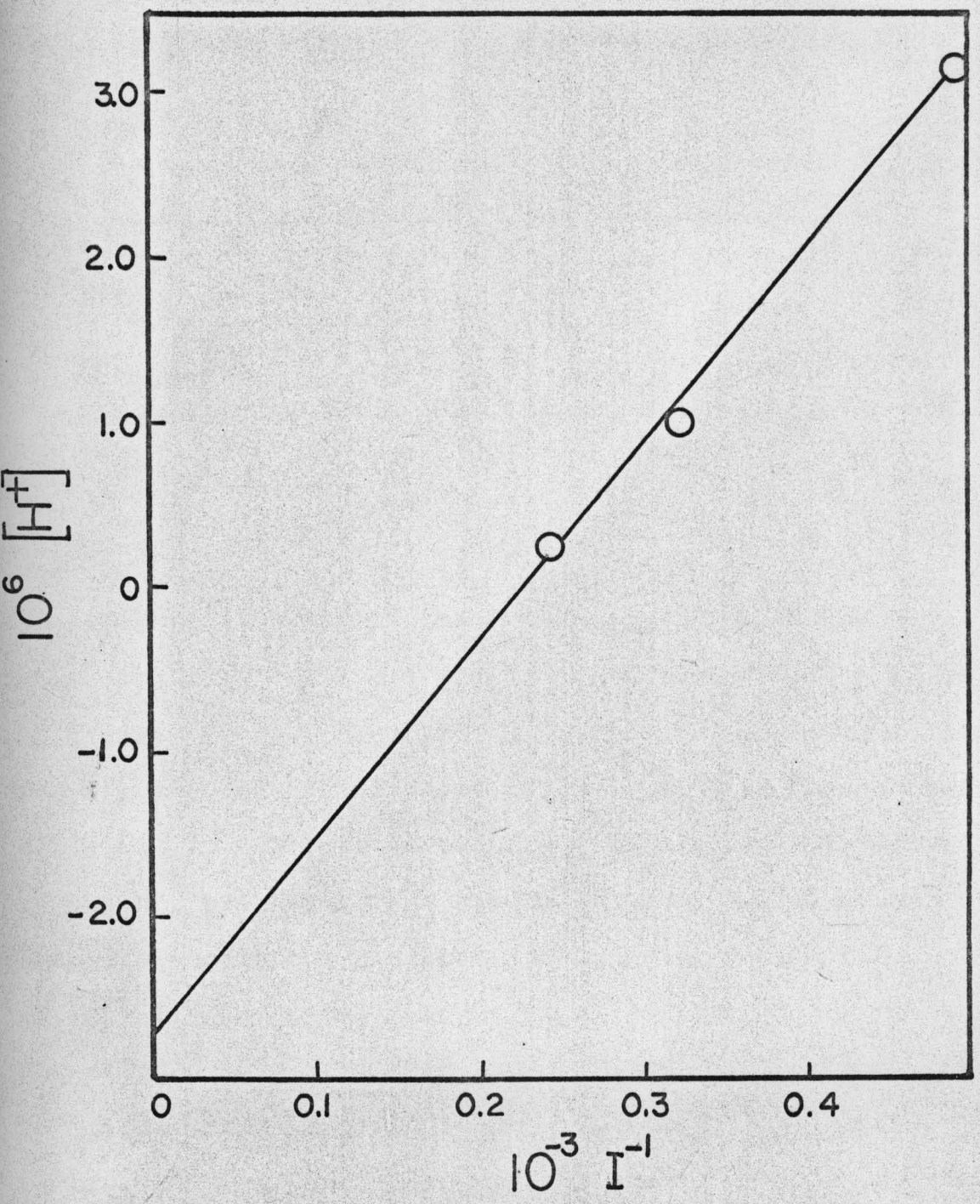

Figure 36. Plot of reciprocal of intercepts against [H^+] for phenol release from phenyl acetate in the presence of 0.04 M nickel chloride. Data from Table XXVI.

TABLE XXVI

Intercepts from Plots of $k_{obs}/[NH_2OH]_T$ Against $[NH_2OH]_T$ in Figure 35

pH	10^6 $[H^+]$ (M)	10^3 I	10^{-3} I^{-1}
5.50	3.16	2.03	0.493
6.00	1.00	3.10	0.323
6.60	0.25	4.10	0.244

presence of nickel (II) ions. The calculated value for k' is 4.3×10^{-3} $\underline{M}^{-1}$ sec^{-1}; k", calculated from the slope of Figure 32, is 3.82×10^{-2} $\underline{M}^{-2}$ sec^{-1}. Calculated values for K_a, k', and k" are shown in Table XXVII. From Table XXVII, it is apparent that the individual rate constants, k' and k", are smaller in the presence of 0.04 $\underline{M}$ nickel chloride; therefore the second mechanism, a direct nickel (II)-catalyzed N-acetylation, can be discounted. Since hydroxamic acid formation is catalyzed by nickel (II) while the phenol release is made slower by nickel (II), it is probable that there is a change in the rate determining step making the first step, O-acetylation of hydroxylamine, rate determining. Even though the rate constants for phenol release are smaller in the presence of nickel (II), the rate determining step, O-acetylation of hydroxylamine,

TABLE XXVII

Calculated Values for K_a, k' and k" for Phenol Release from Phenyl Acetate in the Presence and Absence of Nickel (II)[a]

	K_a (M)	k' (M^{-1} sec^{-1})	k" (M^{-2} sec^{-1})
no nickel	5.2×10^{-7}	1.38×10^{-2}	0.226
0.04 M $NiCl_2$	2.78×10^{-6}	4.3×10^{-3}	3.82×10^{-2}

[a]values calculated from data presented in Tables XXI, XXII, XXIV and XXVI.

is still faster than the rate determining step in the absence of nickel, conversion of O-acetylhydroxylamine to acetohydroxamic acid, hence the observed catalysis.

The rate constants, k' and k", can be calculated as a function of pH from plots of $k_{obs}/[NH_2OH]_T$ against $[NH_2OH]_T$ shown in Figures 33 and 35. These rate constants are summarized in Table XXVIII. The rate constant k' compares favorably in Tables XXVII and XXVIII and it is essentially constant over the pH range studied. The rate constant k", while comparing favorably in magnitude, appears to vary as a function of pH. However, it is quite likely that this variation is due to error accumulated in calculating k". The rate constant k" is calculated from

TABLE XXVIII

Comparison of k' and k" for Phenol Release from Phenyl Acetate in the Presence and Absence of 0.04 M Nickel Chloride[a]

	pH	k' (M^{-1} sec^{-1})	k" (M^{-2} sec^{-1})
A. No Nickel (II)			
	5.50	1.35×10^{-2}	4.5×10^{-1}
	6.00	1.46×10^{-2}	2.4×10^{-1}
	6.50	1.25×10^{-2}	1.45×10^{-1}
	AVERAGE	1.35×10^{-2}	2.78×10^{-1}
B. 0.04 M $NiCl_2$			
	5.50	4.34×10^{-3}	2.91×10^{-2}
	6.00	4.22×10^{-3}	4.01×10^{-2}
	6.60	4.46×10^{-3}	5.90×10^{-2}
	AVERAGE	4.33×10^{-3}	4.27×10^{-2}

[a]rate constants calculated from data presented in Tables XXIII, XXIV, XXV and XXVI.

the slope and the function $\left(\frac{K_a}{K_a + [H^+]}\right)^2$. Since there is some error in estimating K_a, the error is magnified in squaring the term $\left(\frac{K_a}{K_a + [H^+]}\right)$. Furthermore, error in measuring the slope would compound the error. The rate constant k' is calculated from the intercept and $\left(\frac{K_a}{K_a + [H^+]}\right)$. In this calculation, there are only two multiplications of possible error while in the calculation of k" there are three multiplications of possible error.

The effect of total nickel chloride concentration on the rates of phenol release and hydroxamic acid formation is shown in Figure 37 (Table XXIX). It is apparent from Figure 37 that an optimum nickel chloride concentration exists for catalysis. In this system, the total hydroxylamine concentration and pH are fixed. In the case of phenol release, the increasing nickel chloride concentration causes a decrease in rate. This is probably due to the complexation of hydroxylamine with nickel (II), which decreases the concentration of the effective nucleophile, NH_2OH. The rate of hydroxamic acid formation increases with nickel concentration to a maximum and then decreases. On the left-hand side of the curve, the catalytic effect of nickel overcomes the effect of complexation of the nucleophile. As the nickel (II) concentration increases, however, a maximum is reached and complexation of the nucleophile becomes the predominant factor in determining

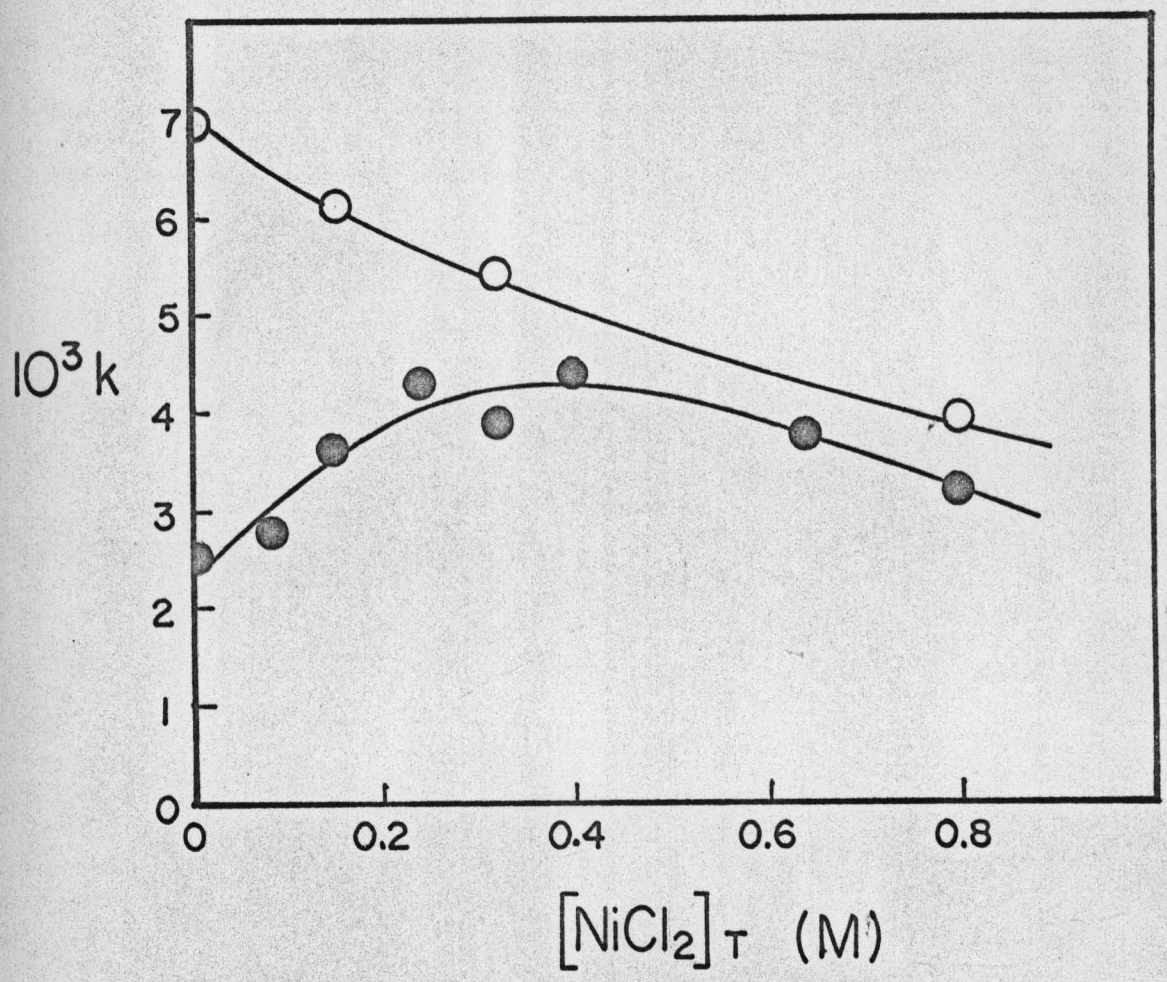

Figure 37. Plot of k_{obs} against $[NiCl_2]_T$ for phenol release and hydroxamic acid production from phenyl acetate in the presence of nickel chloride. Data from Table XXIX.

TABLE XXIX

Apparent First-Order Rate Constants for Phenol Release and Hydroxamic Acid Formation from Phenyl Acetate in the Presence of Nickel Chloride[a]

$10^3 k_{obs}$ (sec^{-1})	$[NiCl_2]_T$ (M)
A. Phenol Release	
6.93	-
6.11	0.016
5.37	0.032
3.95	0.080
B. Hydroxamic Acid Formation	
2.51	-
2.78	0.008
3.52	0.016
4.24	0.024
3.85	0.032
4.32	0.040
3.75	0.064
3.14	0.080

[a] 25.0°; μ = 1.0; 0.4 M $NH_2OH \cdot HCl$; pH 6.00

the rate, and the rate decreases with further increases in nickel chloride concentration.

F. Reactions of Ethyl Acetate with Hydroxylamine

Ethyl acetate reacts readily with hydroxylamine at alkaline pH to form acetohydroxamic acid. The reaction at neutral pH is not detectable under the concentration conditions employed in measuring the reaction at alkaline pH. Figure 38 shows a plot of absorbance against reaction time for the reaction of ethyl acetate and hydroxylamine in the presence and absence of nickel chloride; there is a significant catalysis of hydroxamic acid formation by nickel chloride. Under the conditions employed for the study of nickel catalysis of the reaction of acetic acid and hydroxylamine, ethyl acetate reacts only moderately faster than acetic acid ($k_{EtOAc} = 5.95 \times 10^{-5}$ sec^{-1}, pH 6.11 (25.0°); $k_{HOAc} = 1.98 \times 10^{-5}$ sec^{-1}, pH 6.15 (25.0°)). Since aliphatic esters can be analyzed easily by alkaline hydroxylaminolysis, the nickel catalyzed reaction, which presents no apparent advantage over the alkaline reaction, was not further investigated.

The acid-catalyzed reaction of ethyl acetate and hydroxylamine was studied using conditions similar to those used for acetic acid. Figure 39 (Table XXX) shows a partial pH-rate profile for this reaction. Rate constants were obtained from initial rate measurements. The slope

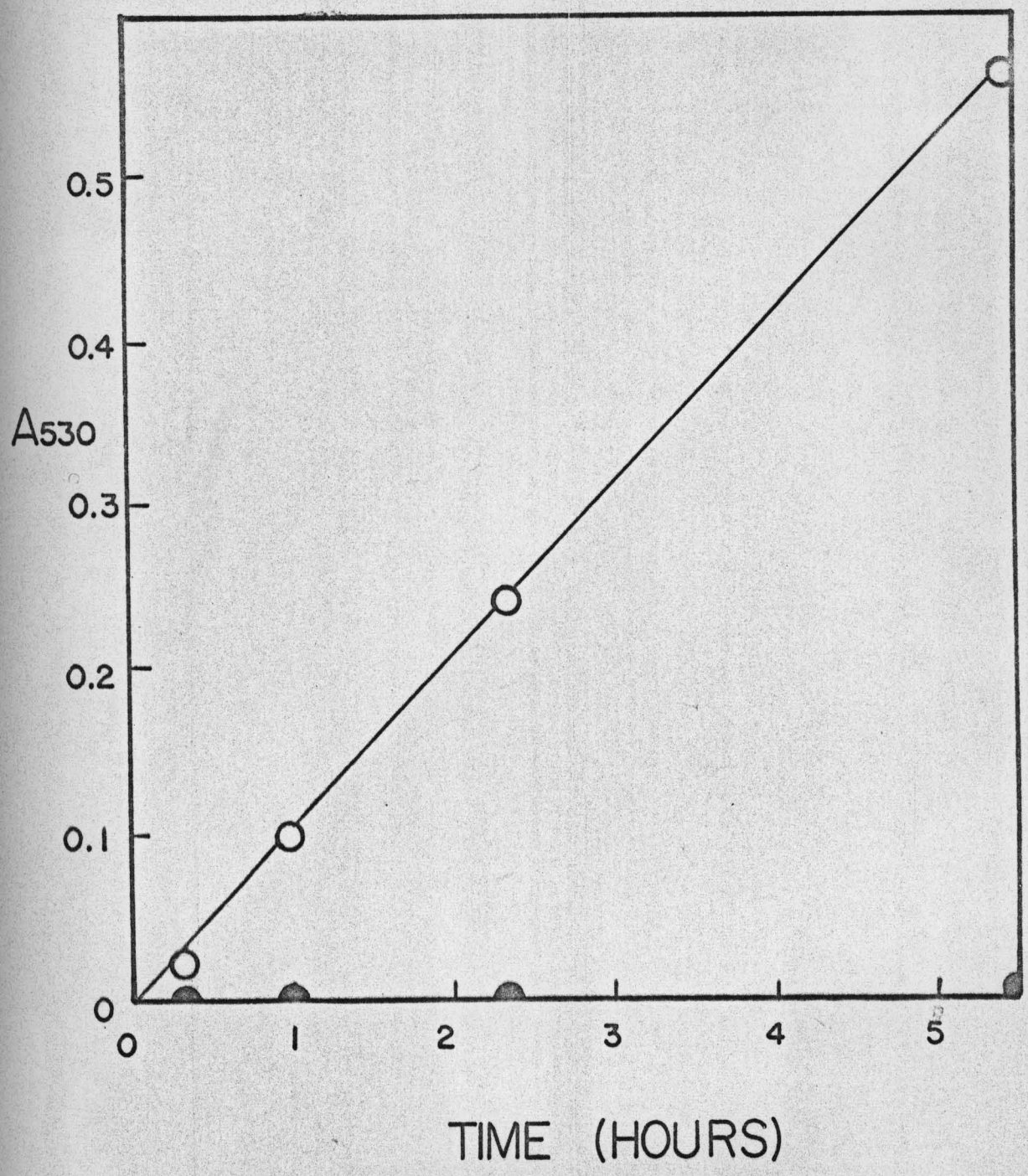

Figure 38. Plot of absorbance against time for nickel (II)-catalyzed hydroxamic acid formation from ethyl acetate; 0.50 M $NH_2OH \cdot HCl$; 0.50 M ethyl acetate; 25.0°; pH 5.11; open circles, 0.53 M $NiCl_2$; filled circles, no nickel (II).

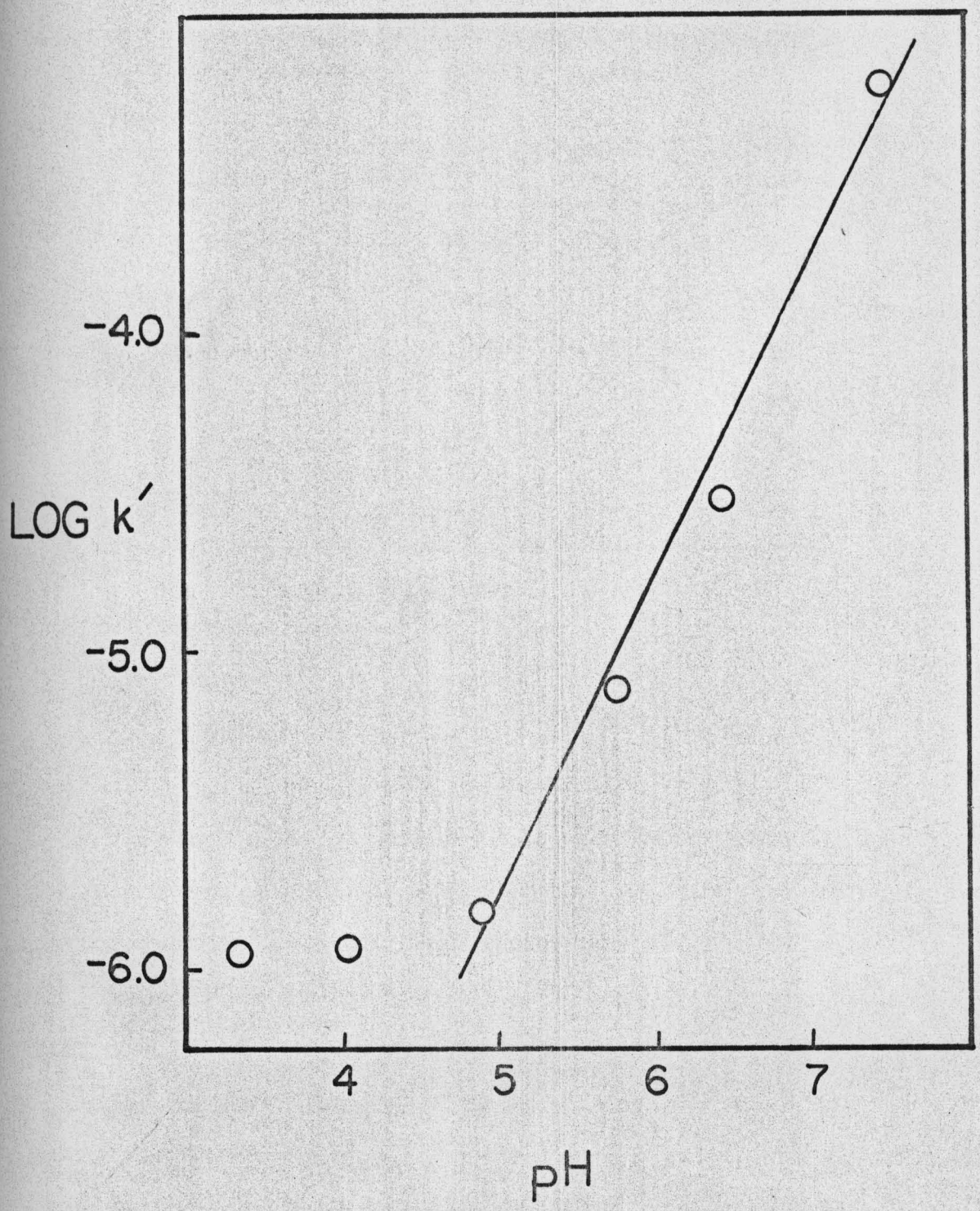

Figure 39. pH-rate profile for hydroxamic acid formation from ethyl acetate. The line has a slope of 1.0. Data from Table XXX.

TABLE XXX

Apparent Second-Order Rate Constants for Hydroxamic Acid Formation from Ethyl Acetate[a]

pH (90.5°)	10^6 k' ($\underline{M}^{-1}$ sec^{-1})	log k'
3.32	1.12	- 5.95
4.13	1.14	- 5.94
4.90	1.54	- 5.81
5.75	7.82	- 5.11
6.48	30.5	- 4.52
7.47	600.0	- 3.22

[a]90.5°; 0.80 $\underline{M}$ $NH_2OH \cdot HCl$; 0.304 $\underline{M}$ ethyl acetate; μ = 1.2.

of 1.0 is as expected for a base-catalyzed reaction of ethyl acetate. An interesting point is that the rate constants for the ethyl acetate reaction between pH 3 and 5.5 are smaller than the corresponding rate constants for acetic acid.

The rates of reaction of ethyl acetate with hydroxylamine for low pH values (less than 2) are faster than at pH 3-5, but side reactions prevent accurate measurement of rate constants. Figure 40 shows a typical plot of absorbance against reaction time for hydroxamic

Figure 40. Plot of absorbance against time for hydroxamic acid formation from ethyl acetate; 90.5°; pH 1.64; 0.80 M $NH_2OH \cdot HCl$; 0.304 M ethyl acetate; μ = 1.2.

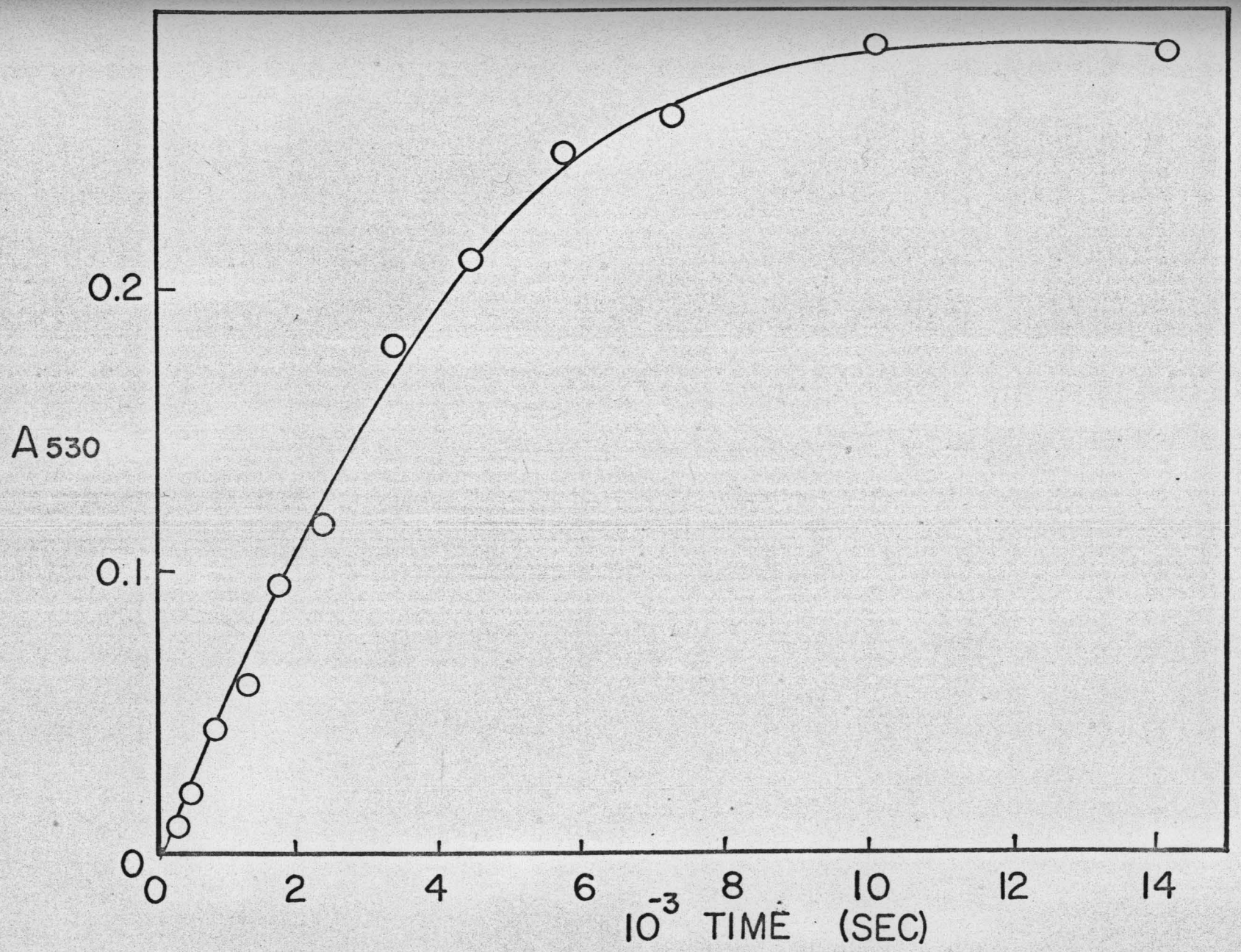
0.2
0.1
0
A 530
0
2
4
6
8
10
12
14
10^-3 TIME (SEC)

acid formation from ethyl acetate. The first-order plot for these data is shown in Figure 41. The distinct curvature indicates that the reaction is not clearly first-order and that side reactions may be taking place.

At low pH, significant concurrent hydrolysis of acetohydroxamic acid occurs during its formation from ethyl acetate. A reaction scheme is presented in Equations (55) and (56).

$$CH_3COO\text{-}C_2H_5 + NH_2OH \rightleftharpoons CH_3CONHOH + C_2H_5\text{-}OH \qquad (55)$$

$$CH_3CONHOH + H_2O \rightleftharpoons CH_3COOH + NH_2OH \qquad (56)$$

Previous experiments on the formation of hydroxamic acid from acetic acid and on the hydrolysis of acetohydroxamic have shown that these two reactions are quite important at low pH. Hence it is not readily possible to measure the rate constant for the formation of acetohydroxamic acid from ethyl acetate without knowing the concentration of acetic acid at any given time, and the system was not investigated at lower pH values.

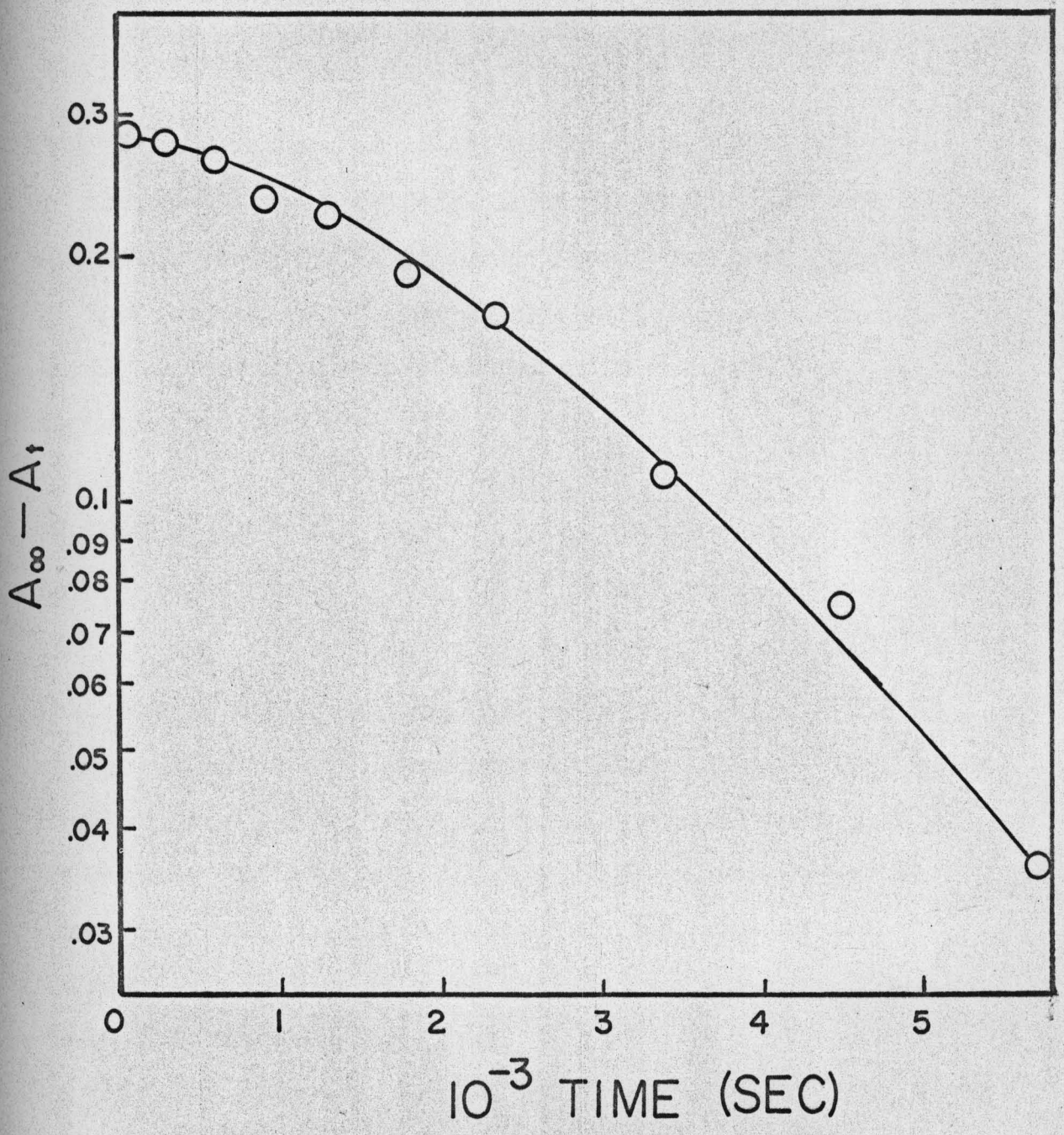

Figure 41. First-order plot for data presented in Figure 40.

G. Nickel (II)-Catalyzed Reaction of Hydroxylamine with Acid Hydrazides

In the course of studying the nickel (II) catalysis of the reaction of hydroxylamine and phenyl acetate, it was found that nickel probably exerts its catalytic effect in the conversion of O-acetylhydroxylamine to hydroxamic acid. A possible mechanism for this catalysis is suggested in Equation (57).

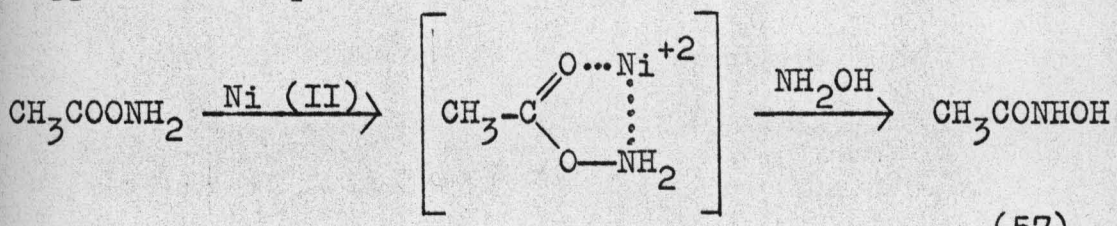

(57)

The complex of O-acetylhydroxylamine and nickel (II) is suggested to be a five-membered chelate ring. Within this complex, the carbonyl-oxygen double bond is polarized, decreasing the electron density at the carbonyl carbon. Also, complexation through the nitrogen atom of the hydroxylamine tends to make that moiety a weaker base and hence a better leaving group.

If the nickel is indeed acting as a catalyst in this manner, then carboxylic acid derivatives of the structure shown below (VIII), should also undergo nickel (II) catalyzed hydroxylaminolysis if Y is capable of coordination to nickel (II).

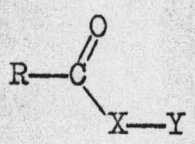

VIII

Such a class of compounds are the acid hydrazides. Possible nickel (II)-catalyzed hydroxamic acid formation from acid hydrazides was therefore investigated to test this prediction.

A plot of absorbance against reaction time for the reaction of benzhydrazide and hydroxylamine in the presence and absence of nickel (II) is shown in Figure 42. A similar plot for the alkaline reaction of hydroxylamine and benzhydrazide is also presented in Figure 42. Note that the reaction in the presence of nickel (II) is considerably faster than in the absence of nickel (II) which is in agreement with the above hypothesis. The decrease in absorbance that is seen in the top line in Figure 42 is apparently due to the nickel (II)-catalyzed hydrolysis of the benzhydroxamic acid. A first order plot for these data is shown in Figure 43. In this case, the maximum absorbance (time = 4500 sec, see Figure 42), was used as the "infinity" value. A partial pH rate profile for the nickel (II)-catalyzed reaction of hydroxylamine and benzhydrazide is shown in Figure 44 (Table XXXI). The solid line drawn has a slope of 0.60. The rate appears to continue to increase with pH, but above pH 7.0

Figure 42. Plots of absorbance against time for the reaction of benzhydrazide and hydroxylamine; 0.80 M $NH_2OH.HCl$; 0.005 M benzhydrazide; 1% (v/v) methanol; μ = 1.0; 90.5°; open circles, 0.04 M $NiCl_2$, pH 6.75; filled circles, no nickel (II), pH 11.52; half-filled circles, no nickel (II), pH 6.75.

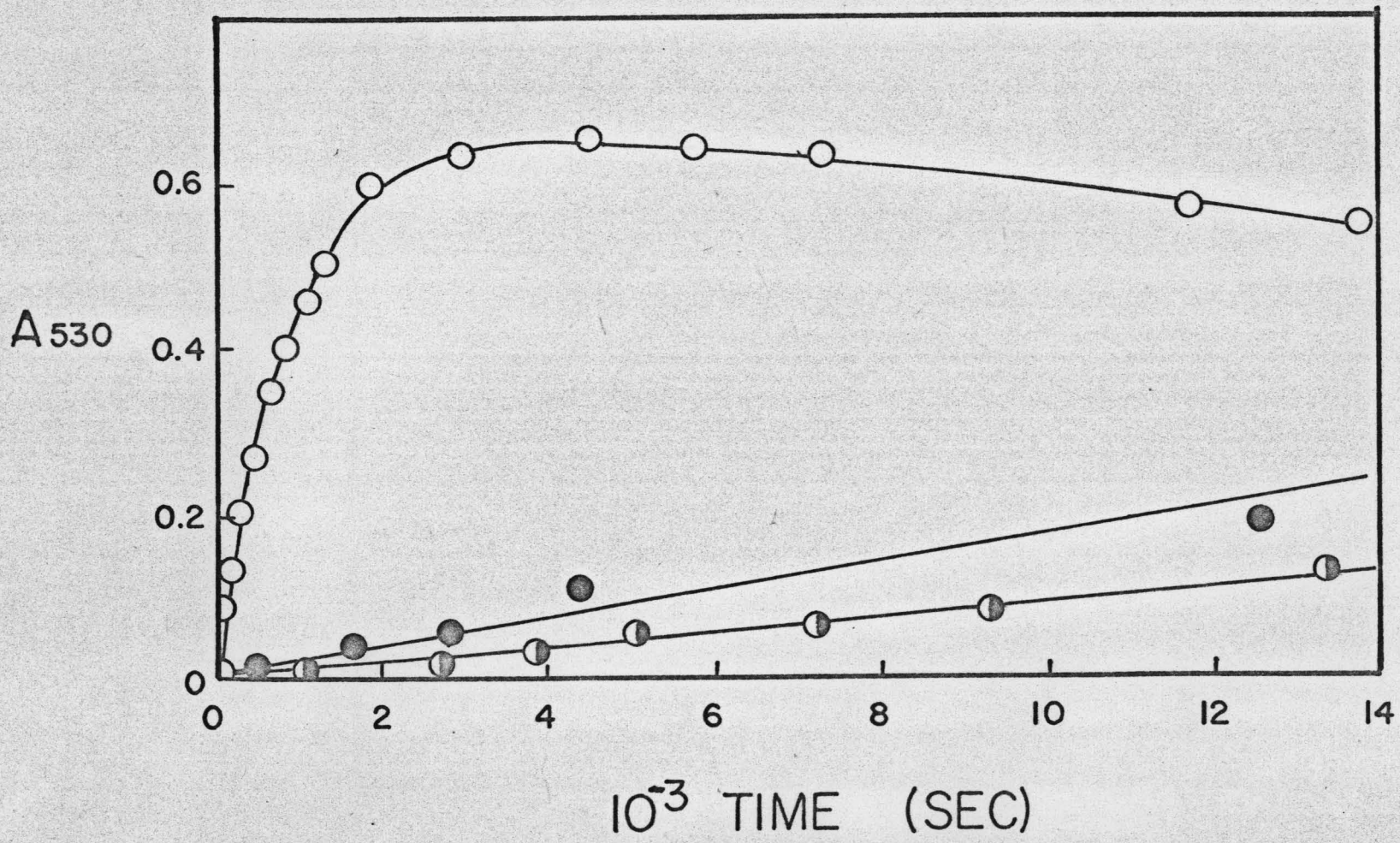
A530
0.6
0.4
0.2
0
0
2
4
6
8
10
12
14
10^-3 TIME (SEC)

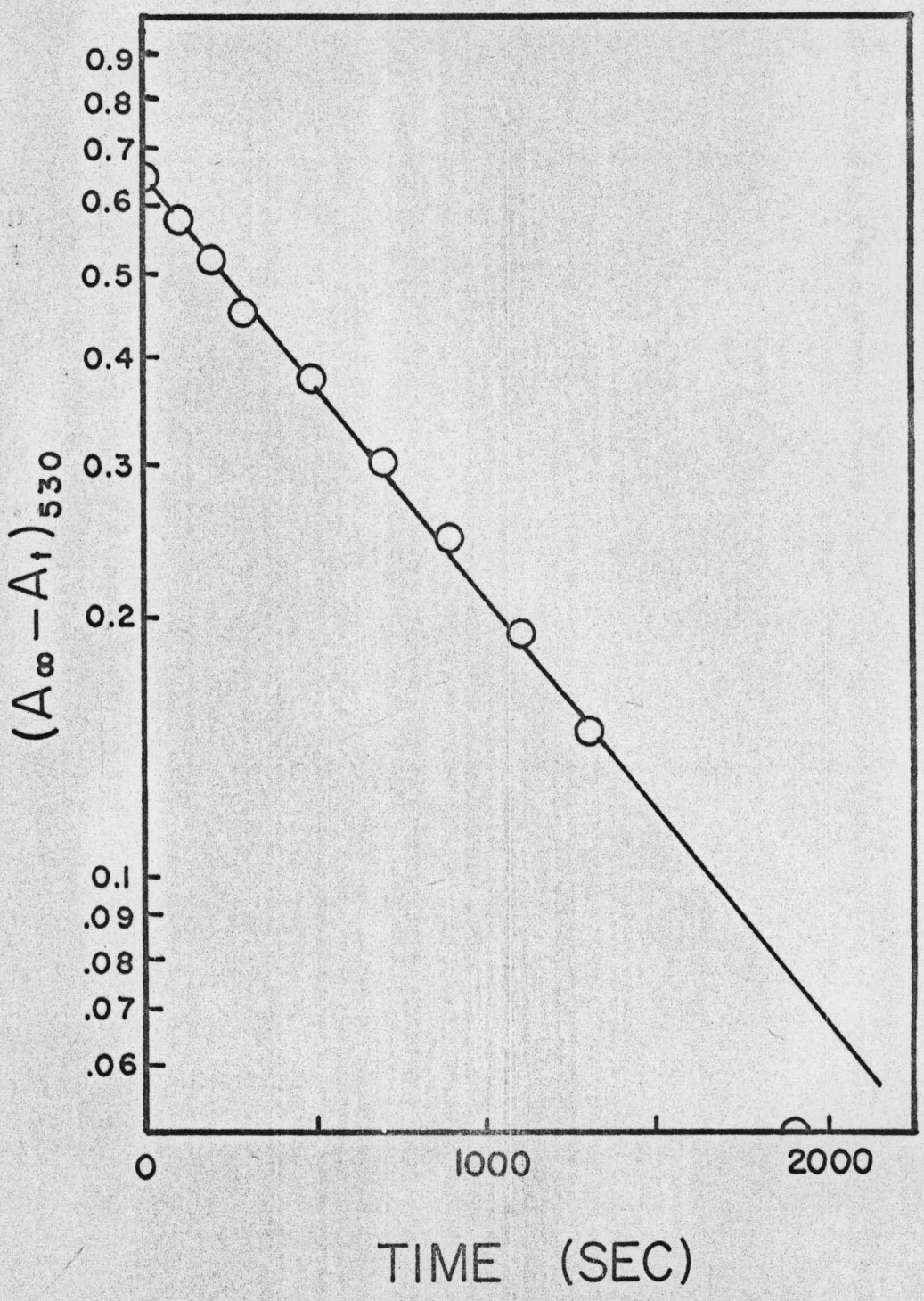

Figure 43. First-order plot for reaction of benzhydrazide and hydroxylamine; 90.5°; 0.80 M $NH_2OH \cdot HCl$; 0.04 M $NiCl_2$; 0.005 M benzhydrazide; pH 6.75 (measured at 25.0°); μ = 1.0; 1% (v/v) methanol.

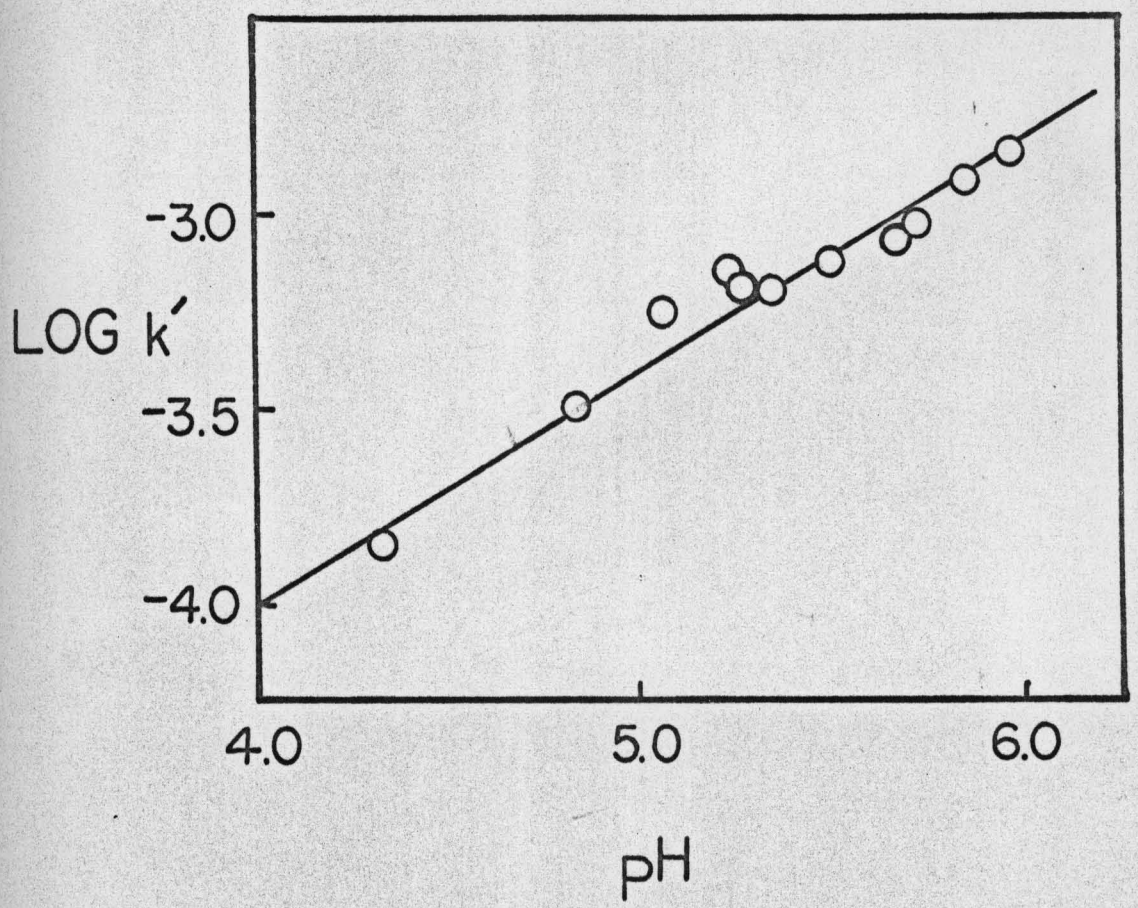

Figure 44. pH-rate profile for hydroxamic acid formation from benzhydrazide in the presence of nickel chloride. Data from Table XXXI.

TABLE XXXI

Apparent Second-Order Rate Constants for Hydroxamic Acid Formation from Benzhydrazide in the Presence of Nickel Chloride[a]

pH (90.5°)	10^4 k' ($\underline{M}^{-1}$ sec^{-1})	log k'
4.33	1.43	- 3.85
4.83	3.21	- 3.49
5.07	5.56	- 3.26
5.24	7.16	- 3.15
5.26	6.40	- 3.19
5.35	6.59	- 3.18
5.50	7.63	- 3.12
5.50	7.85	- 3.11
5.67	8.50	- 3.07
5.71	9.15	- 3.04
5.85	12.2	- 2.91
5.96	14.2	- 2.85

[a]90.5°; 0.80 $\underline{M}$ $NH_2OH \cdot HCl$; 0.04 $\underline{M}$ $NiCl_2$; 0.005 $\underline{M}$ benzhydrazide; 1% (v/v) methanol; μ = 1.0.

precipitation of nickel hydroxide occurs and rate constants cannot be accurately measured.

The results presented in Figure 42 give support to the hypothesis that acid hydrazides (and, by analogy, O-acylhydroxylamines) undergo nickel (II)-catalyzed hydroxylaminolysis by chelate formation. Furthermore, this reaction represents a possible extension of the ferric-hydroxamate method of analysis, since acid hydrazides do not react rapidly under the usual alkaline conditions. Figure 45 (Table XXXII) shows a plot of the maximum absorbance as a function of pH. These absorbances were determined in the course of measuring the reaction rates for the pH-rate profile. Note that the highest absorbances are attained at higher pH. Thus it is advisable to run the analytical reaction at pH values as high as possible, the upper limit being determined by the precipitation of nickel hydroxides. A standard calibration curve was prepared for hydroxamic acid formation from benzhydrazide (Figure 46 and Table XXXIII). The absorbance readings were made from samples that had reacted for 5000 seconds (see Figure 42). The measured absorbance for the highest concentration, 0.00378 M, represents a yield of 82 percent with respect to initial hydrazide concentration.

Figure 47 shows a plot of absorbance against time for nickel (II)-catalyzed hydroxamic acid formation from isonicotinic acid hydrazide (Isoniazid). The reaction is faster than the reaction of benzhydrazide and the hydrolysis

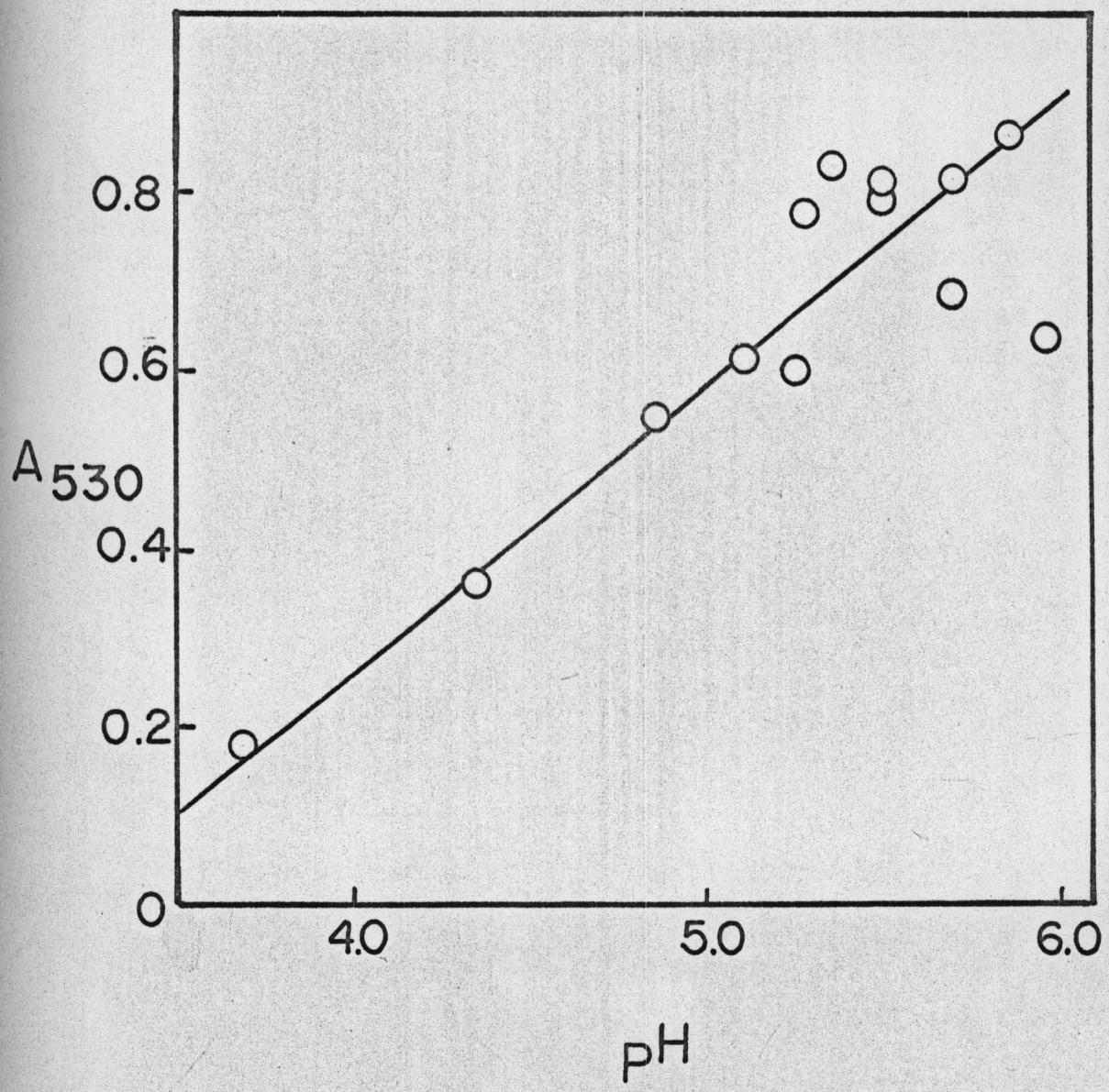

Figure 45. Plot of maximum absorbance against pH for nickel (II)-catalyzed hydroxamic acid formation from benzhydrazide. Data from Table XXXII.

TABLE XXXII

Maximum Absorbance Values from Nickel (II)-Catalyzed Hydroxamic Acid Formation from Benzhydrazide[a]

pH	$A_{530\ (max)}$[b]
3.68	0.188
4.33	0.360
4.83	0.546
5.07	0.608
5.24	0.592
5.26	0.778
5.35	0.831
5.50	0.814
5.50	0.790
5.67	0.814
5.71	0.685
5.85	0.867
5.96	0.632

[a] 90.5°; 0.80 M $NH_2OH \cdot HCl$; 0.04 M $NiCl_2$; 0.005 M benzhydrazide; 1% (v/v) methanol; μ = 1.0.

[b] obtained from plots of A_{530} against reaction time.

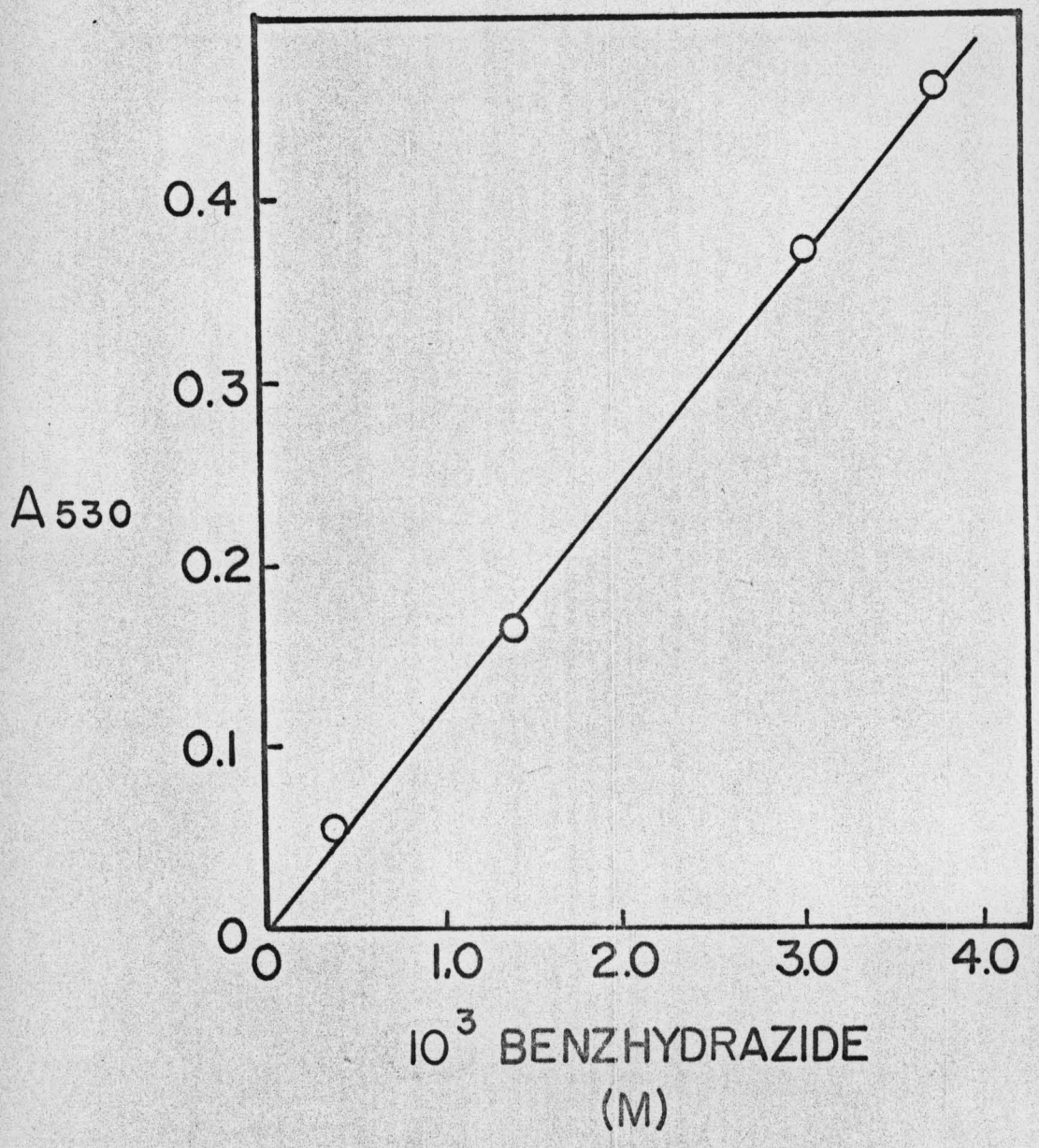

Figure 46. Calibration curve for nickel (II)-catalyzed hydroxamic acid formation from benzhydrazide. Data from Table XXXIII.

TABLE XXXIII

Calibration Curve for Nickel (II)-Catalyzed Hydroxamic Acid Formation from Benzhydrazide[a,b]

$A_{5000\ sec}$ (530 nm)[c]	10^3 Benzhydrazide (M)
0.056	0.378
0.165	1.41
0.372	3.02
0.462	3.78

[a] 90.5°; 0.80 M $NH_2OH \cdot HCl$; 0.04 M $NiCl_2$; pH 6.75 (25.0°); μ = 1.0; 10% (v/v) methanol.

[b] 1.0 ml of reaction mixture was diluted with 20.0 ml 0.15 M $Fe(ClO_4)_3$ to make the spectral solution.

[c] 2 cm cells.

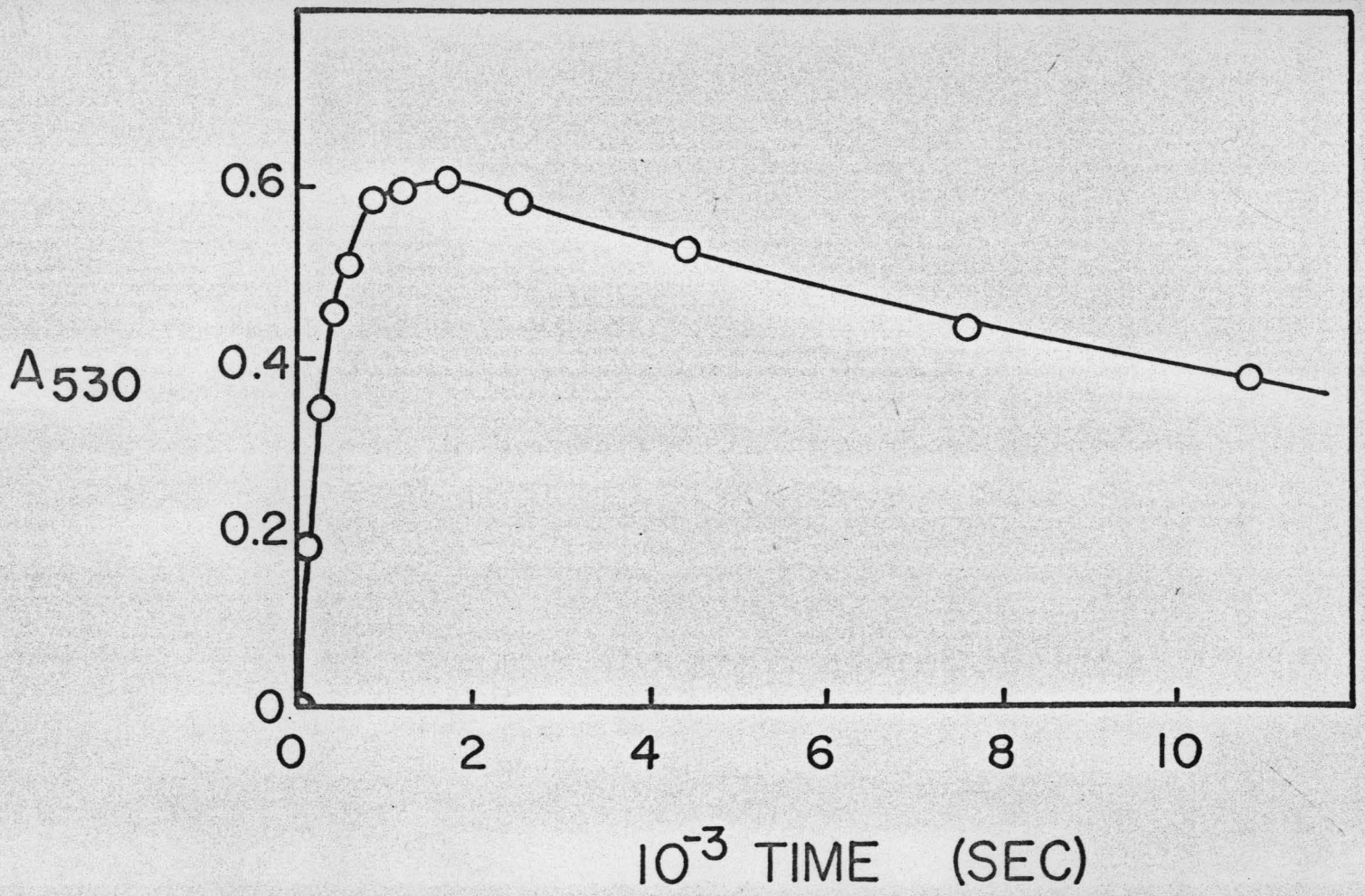

Figure 47. Plot of absorbance as a function of time for the reaction of isonicotinic acid hydrazide and hydroxylamine in the presence of nickel chloride; 90.5°; pH 6.50 (measured at 25.0°); 0.80 M $NH_2OH \cdot HCl$; 0.04 M $NiCl_2$; 0.00533 M isonicotinic acid hydrazide; μ = 1.0.

of the product hydroxamic acid also appears to be faster than the hydrolysis of benzohydroxamic acid. A calibration curve for isonicotinic acid hydrazide (Table XXXIV and Figure 48) was prepared from samples that had reacted for 1500 seconds, this time being selected by reference to Figure 48. Isonicotinic acid, the hydrolysis product of isonicotinic acid hydrazide, was shown not to react under these conditions.

Acethydrazide, IX, and p-nitrobenzhydrazide, X, reached absorbance maxima at 2500 seconds and 2700 seconds, respectively, under these reaction conditions.

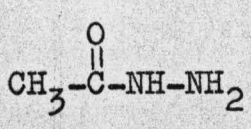

IX

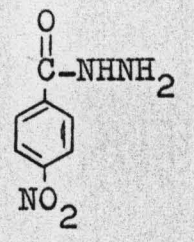

X

Acetphenylhydrazide, XI, and semicarbazide, XII, did not react under these conditions.

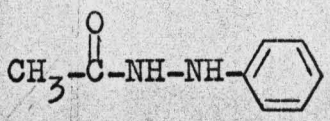

XI

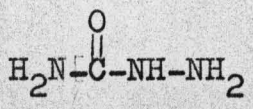

XII

TABLE XXXIV

Calibration Curve for Nickel (II)-Catalyzed Hydroxamic Acid from Isonicotinic Acid Hydrazide[a,b]

10^3 Isonicotinic Acid Hydrazide	A_{530}[c,d]
0	0.000
0.533	0.081
0.107	0.157
3.20	0.479
5.33	0.778

[a] 90.5°; pH 6.50 (25.0°); 0.80 M $NH_2OH \cdot HCl$; 0.04 M $NiCl_2$; μ = 1.0.

[b] 1.0 ml of sample diluted with 20.0 ml of 0.15 M $Fe(ClO_4)_3$ to make spectral solution.

[c] 2 cm cells.

[d] samples had reacted for 1500 seconds; see Figure 47.

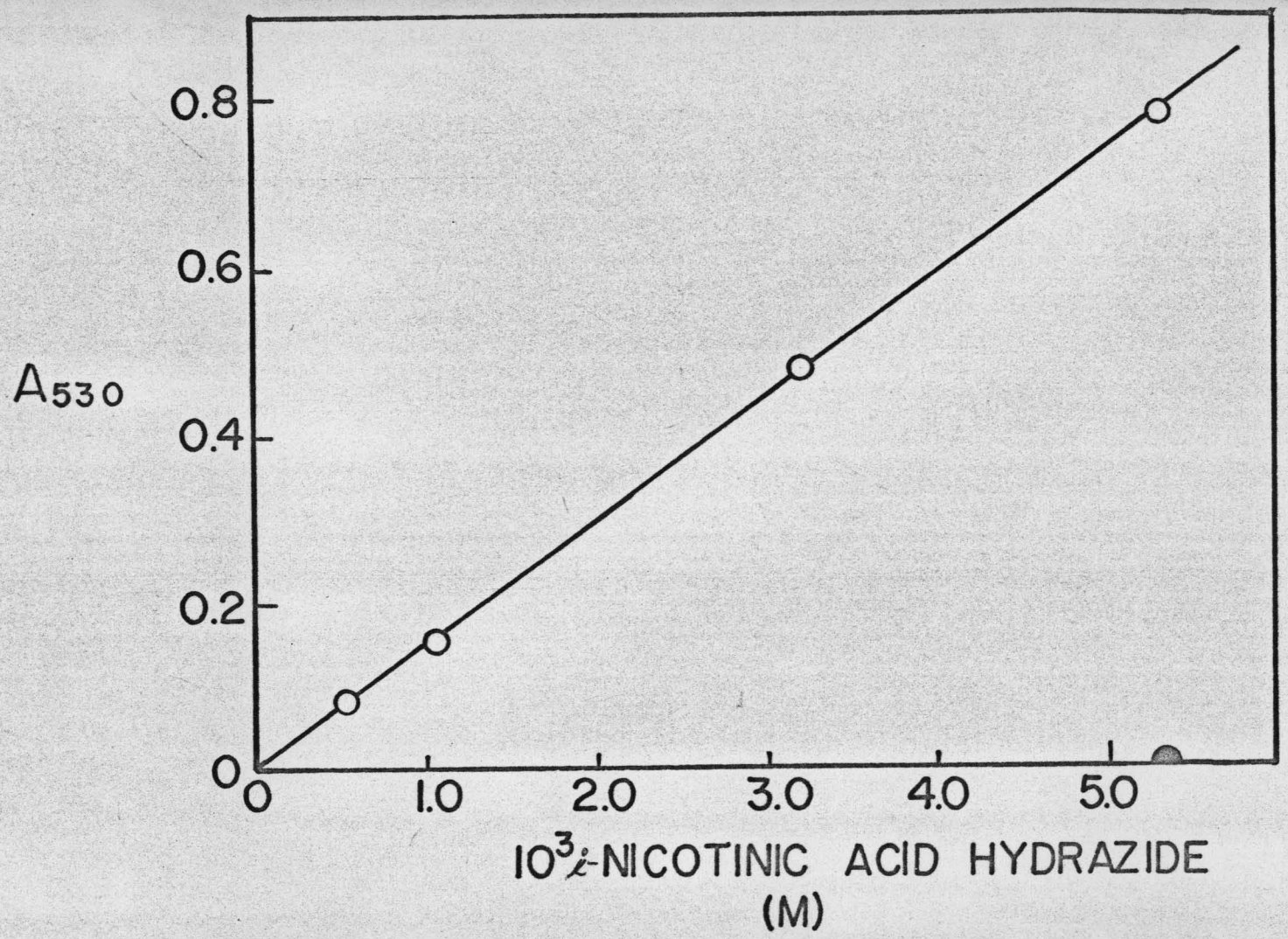

Figure 48. Calibration curve for the analysis of isonicotinic acid hydrazide by the nickel (II)-catalyzed ferric-hydroxamate method. Data from Table XXXIV. Filled semi-circle represents 0.0053 M isonicotinic acid.

A detailed description of a suggested analytical procedure for acid hydrazides will be presented later. The sensitivity limits of this analysis will also be discussed.

IV. DISCUSSION

A. Mechanisms of Nickel (II) Catalysis and Acid Catalysis

1. Nickel (II) Catalysis of Hydroxylaminolysis of Carboxylic Acids

Metal ions can function as catalysts for nucleophilic attack in several ways. They may shield negative charges on the substrate which would otherwise tend to repel the attack of the electron pair of a nucleophile, especially an anionic nucleophile. Metal ions might also increase the reactivity of the atom being attacked. For example, coordination of a carbonyl oxygen to a metal ion will decrease the electron density of the carbonyl carbon, as in XIII, thus making it more susceptible to nucleophilic attack.

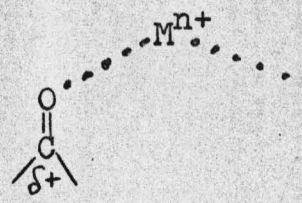

XIII

This phenomenon is manifested in the copper (II)-catalyzed hydrolysis of α-amino acid esters (82) (Eq. 58).

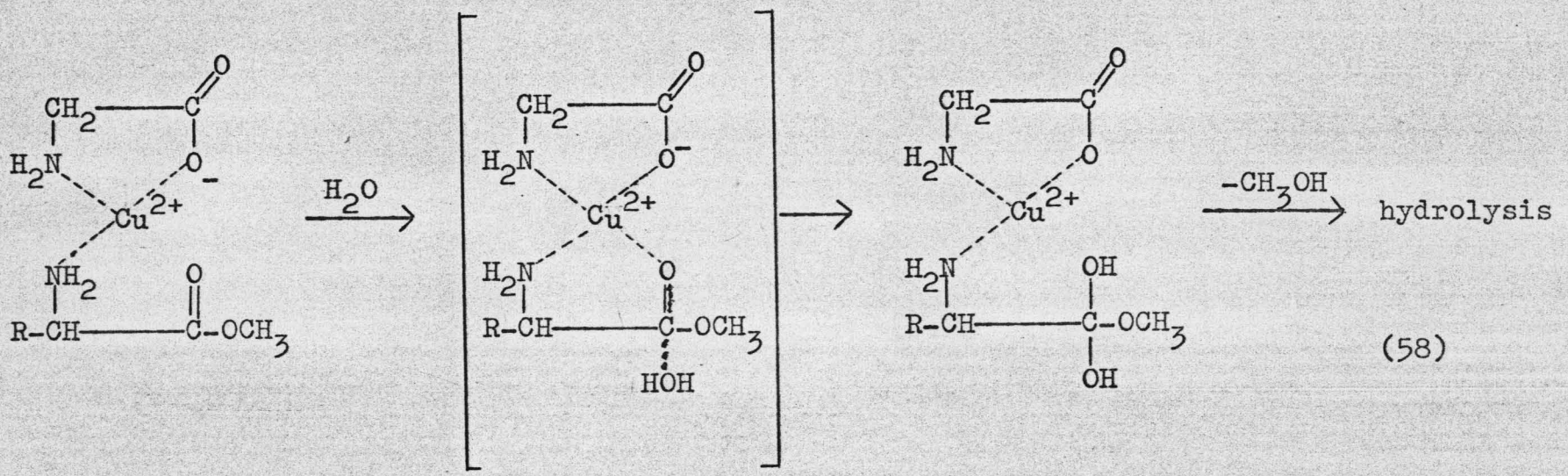

(58)

Metal ions can also act to increase the leaving tendency of the leaving group as shown in XIV.

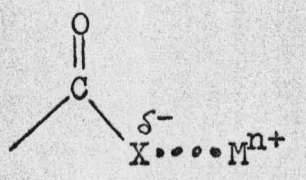

XIV

Coordination of the metal ion to the leaving group sometimes decreases the electron density of the nucleophilic atom on the leaving group. This tends to reduce its basicity and nucleophilicity, hence making it a better leaving group. Metal ions may also act as bridging groups between nucleophile and substrate. This "bridging" may lead to greater reactivity because of a proximity effect. This process is seen in a nonenzymatic acyl-transfer reaction involving the reaction of the zinc complex of pyridine-2-aldoxime and acetoxyquinoline (83). In this reaction the substrates form a mixed complex (XV), which facilitates electron transfer (Eq. 59).

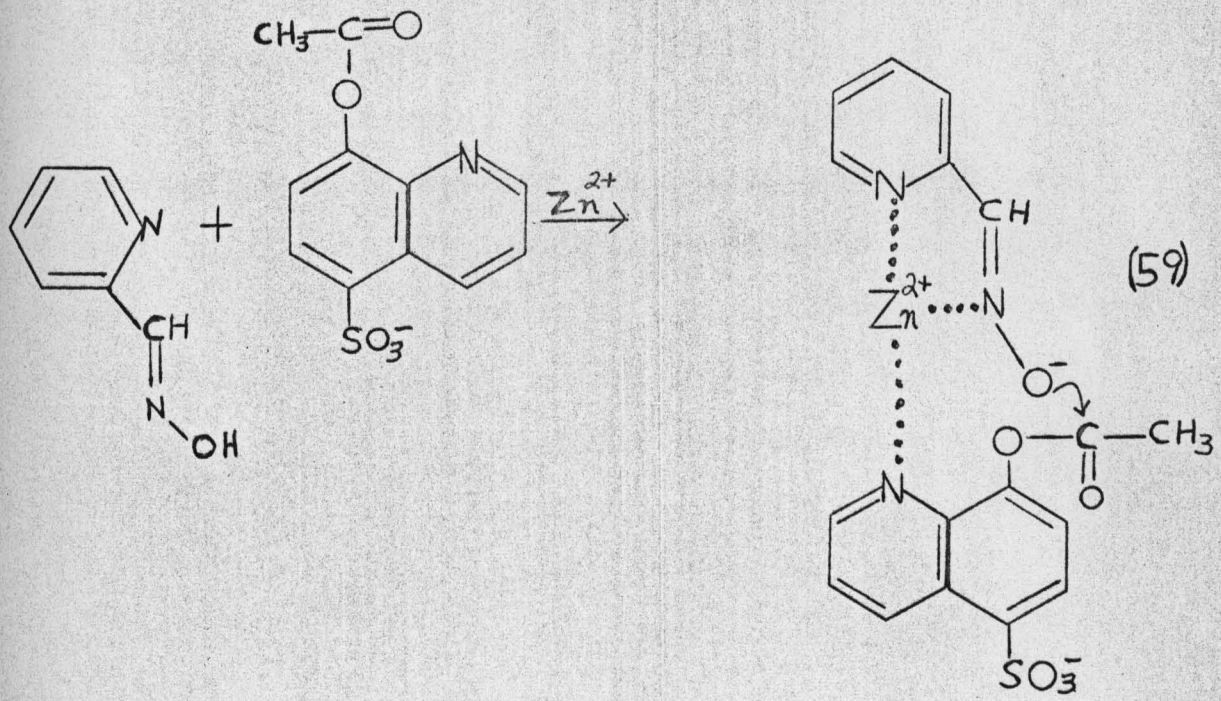

(59)

The metal ion can also act to stabilize the product, and by inference the transition state, of a reaction. In the metal ion catalyzed decarboxylation of dimethyloxaloacetate, the metal ions, Cu (II) or Al (III), can chelate with the carboxylate groups (Eq. 60), providing an electron sink for the decarboxylation process and thus stabilizing the product enolate ion (84).

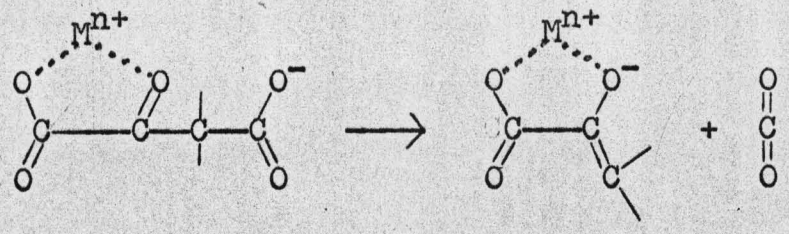

(60)

The experimental rate equation for the nickel (II)-catalyzed hydroxylaminolysis of acetic acid (Eq. 20) indicates that the nickel (II) ion catalyzes the attack of hydroxylamine on acetate ion. Complexation of the nickel ion with hydroxylamine would decrease the electron density of the nitrogen atom of hydroxylamine, making it a poorer nucleophile. A catalytically favorable complex might be formed with the acetate ion, shown as a chelate in XVI.

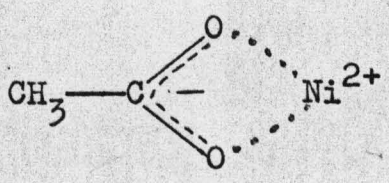

XVI

Such a complex would tend to polarize the carbon-oxygen bonds, thus decreasing the electron density at the carbonyl carbon and making it more susceptible to nucleophilic attack. Thus the catalytic effect of nickel on hydroxylaminolysis of acetic acid may be due to polarization of the carbon-oxygen bond of the acetate ion by complexation of acetate ion with nickel (II) ion.

The differences between the rate equation obtained by Lawlor (Eq. 27) and the rate equation obtained in this study (Eq. 20) can be rationalized in terms of the nickel-hydroxylamine complexes present in the reaction

mixture. In the case where hydroxylamine is in great excess (20-fold) of nickel (II), three nickel (II)-hydroxylamine complexes can be formed with the Ni (II):NH_2OH stoichiometries, 1:2, 1:4, and 1:6. These complexes have visible absorption maxima at 390 and 660 nm for the 1:2 complex, 370 and 610 nm for the 1:4 complex, and 350 and 550 nm for the 1:6 complex (85). The nickel (II) ion has absorption maxima at 400 and 690 nm. The spectra for the complexes formed when hydroxylamine is in 20-fold excess of nickel (II) (conditions in the present study) are shown in Figure 9. Note that, as the pH is increased, there is spectral evidence for all three complexes, 1:2 at lower pH and 1:4 and 1:6 at the higher pH values. The spectra of the complexes formed when nickel (II) and hydroxylamine have essentially the same concentration (Lawlor's conditions) are shown in Figure 10. Note that the maxima, which correspond to the 1:2 complex, do not shift as pH is increased. Thus it appears that only the 1:2 complex is in appreciable concentration in Lawlor's system. The presumed formula for such a complex is $[Ni(NH_2OH)_2\ (H_2O)_4]^{+2}$. This complex has the dipositive charge of the nickel (II) ion since the ligands are neutral molecules. The charge is neutralized in solution by the counter-ions present, chloride and acetate. However, if one of the ligands is replaced by a hydroxide ion, a complex with a lesser charge results,

$[Ni(NH_2OH)_2\ (H_2O)_3\ (OH^-)]^+$. Replacement of two of the ligands by hydroxide would give a neutral complex and replacement of a third ligand would produce a negatively charged complex. If the nickel (II) ion is catalyzing the attack of hydroxylamine on acetate by complexing with the acetate to decrease the electron density at the carbonyl carbon, any phenomenon that would reduce this complexing tendency would reduce the catalytic effect. Thus, the inclusion of hydroxide in the complex would decrease the catalytic activity. As a result of this consideration, the bell-shaped pH-rate profile can be explained in the following qualitative terms. The left-hand side of the curve, rate increasing with pH, is attributed to nickel (II) catalysis of hydroxylamine attack on acetate ion. The right-hand side, rate decreasing with pH, can be attributed to the same reaction except that the concentration of catalytically active nickel is being decreased by the introduction of hydroxide into the complex as pH is increased. Steinberger and Westheimer (84) found that complexing agents which do not destroy the charge of the metal do not have any effect on the copper (II)-catalyzed decarboxylation of dimethyl-oxaloacetic acid. However, complexing agents which lessened the charge, diminished the catalytic activity.

In light of these considerations, the form of the rate equation for the pH-rate profile obtained by Lawlor can be given two interpretations: a) nickel (II) acts as

a general acid in promoting the reaction of acetic acid and hydroxylamine, according to $V = k[CH_3COOH][NH_2OH][Ni^{2+}]$, or b) nickel (II) forms a complex with acetate ion to promote the reaction with hydroxylamine, $V = k[CH_3COO^-][NH_2OH][Ni^{+2}]$, *the second interpretation* giving a bell-shaped pH-rate profile only when the catalytic activity of the nickel (II) ions is diminished at higher pH.

In the case where hydroxylamine is in large excess over the nickel, the inclusion of hydroxide in the complex may be decreased by the presence of hydroxylamine in the complex. For a hydroxide ion to be included in the 1:6 complex, it must displace a hydroxylamine molecule instead of a water molecule as was the case with the 1:2 complex. The stability constants for the formation of nickel-hydroxylamine complexes are quite large (85), $K_{1:2} = 5.25 \times 10^9$, $K_{1:4} = 3.4 \times 10^{12}$, $K_{1:6} = 3.6 \times 10^{18}$ (25°), while that for the formation of nickel hydroxide is smaller (86), thus $K = 4 \times 10^4$ (30°) for the reaction

$$Ni^{+2} + OH^- \rightleftharpoons NiOH^+$$

Thus, it is expected that hydroxide complexes are not in appreciable concentrations when hydroxylamine is in large excess of nickel (II). Therefore, under the conditions employed in this study, the catalytic form of nickel (II) (the dipositive ion) can exist at higher pH values than

possible under Lawlor's conditions.

Oxygen-containing solvents have been found to increase the rate of decarboxylation of oxaloacetic acid catalyzed by copper (II) (87). This increase was attributed to an increase in the effective charge of the metal caused by the replacement of water molecules in the inner coordination sphere by the organic solvent molecules. Table VIII shows that the addition of oxygen-containing solvents to the nickel (II)-catalyzed reaction of acetic acid and hydroxylamine caused a slight increase in the rate, with dioxane being the most effective on a concentration basis. Pyridine, which does not contain oxygen, gave no appreciable increase in the rate of the reaction. While no theoretical interpretation is attached to these results, they were used in designing the analytical procedure for acetic acid.

While the fact that aromatic acids reacted very slowly in the nickel (II)-catalyzed hydroxylaminolysis reaction was disappointing in regard to the generality of the reaction, it does provide some selectivity for the analysis of aliphatic acids in the presence of aromatic acids. Currently aromatic acids can be determined in the presence of aliphatic acids by physical methods such as ultraviolet spectroscopy, the absorption of the aromatic moiety being measured. The aliphatic acids are then determined by titrimetric methods, the contribution of the aromatic acid being subtrated from the total acid found by

titrimetry. However, the presence of non-acidic compounds that absorb ultraviolet light would lead to spurious results using this method. Utilizing the nickel (II)-catalyzed hydroxylaminolysis reaction, aliphatic acids can be determined directly in the presence of aromatic acids with an error of about 2 percent, using an initial rate technique.

2. Acid Catalysis of Hydroxylaminolysis of Carboxylic Acids

The direct aminolysis of a carboxylic acid in aqueous solution does not occur readily. Morawetz and Otaki (88) measured the rates of amide formation from some simple monocarboxylic acid and simple monofunctional amines. The reactions, being very slow, required high temperatures (75 to 95°), high substrate concentrations (1.33 M acid and 6.66 M amine), and prolonged reaction times. For example, the second-order rate constant for amide formation from ammonia and propionic acid at 75.8° is 3.6×10^{-9} M^{-1} sec^{-1}. (This corresponds to a reaction half-life of 6.1 years for a solution 1 M in amine.) It was found by these investigators that amide formation from propionic acid and methylamine was first order in both propionate and unionized methylamine. All reactions were run at high pH so that the acid was essentially entirely in the ionized form and the base was completely unionized.

Under these conditions the following formulation can be utilized (Eq. 61).

$$R_1COO^- + HNR_2R_3 \underset{k_r}{\overset{k_f}{\rightleftharpoons}} R_1CONR_2R_3 + OH^- \qquad (61)$$

Thus, the rate equation for amide formation was given as $V = k[R_1COO^-][HNR_2R_3]$. The possible existence of a rate term of the form $V = k[R_1COOH][HNR_2R_3]$ was not considered. Formate was shown to be 140 times more reactive than acetate with methylamine, while the differences between the reactivities of acetate, propionate, butyrate, and isobutyrate were less pronounced. The reactivity of succinate was very similar to that of propionate, indicating that the neighboring carboxylate does not participate in the mechanism of amide formation. Equilibrium constants were calculated from the ratio of the rate constants of the forward reaction (formation) and the reverse reaction (hydrolysis) (Eq. 62).

$$K = \frac{k_f}{k_r} \qquad (62)$$

The equilibrium constants were very small with ammonia as the amine, e.g., with propionic acid, $K = 3.3 \times 10^{-6}$, and somewhat larger with methylamine, e.g., with propionic acid, $K = 3.10 \times 10^{-4}$.

Jencks, et al. (15) have examined the special kind of amide formation, hydroxamic acid formation, from acetic, hexanoic, and octanoic acids in acidic solutions. These reactions were found to be catalyzed by hydrogen ions, with the reaction rates being considerably faster than those found by Morawetz and Otaki. The half-life for acetohydroxamic acid formation in 1.0 M hydrochloric acid was found to be 350 minutes. The equilibrium constants for formation of acetohydroxamic acid were small. Based on total substrate concentrations, and water activity as unity, the equilibrium constant for the formation of acetohydroxamic acid was 1.46 at pH 7.0 and 25°. The following formulation was used in this calculation (Eq. 63).

$$K = \frac{[\text{amide}]_T\,[H_2O]}{[\text{acid}]_T\,[\text{amide}]_T} \qquad (63)$$

This convention is useful in comparing equilibrium constants at various pH values and was used in calculating the equilibrium constants shown in Figure 23 (Table XVIII).

Higuchi and coworkers (80,81) studied reversible amide formation from dicarboxylic acids. By using an aromatic amine, aniline (pK_a = 4.68), the reactions could be carried out in neutral or slightly acidic solutions where there were appreciable concentrations of unprotonated amine and free acid. It was reported that the rate of reaction of succinic acid was 2 to 3 orders of magnitude greater than

that of acetic acid with the same amine. Also, the pH-rate profile for the reaction of succinic acid and aniline indicates that the free acid, H_2A, is the reactive species. To account for the greater reactivity of succinic acid, a cyclic anhydride intermediate was proposed (Eq. 64).

$$\text{free acid} \underset{k_{-1}}{\overset{k_1}{\rightleftharpoons}} \text{acid anhydride} \underset{k_{-2}\text{-aniline}}{\overset{k_2\text{ aniline}}{\rightleftharpoons}} \text{amide} \qquad (64)$$

Although the formation of succinic anhydride in water seems unlikely, the authors were able to estimate the concentration of succinic anhydride in an aqueous solution of succinic acid from data on the rates of formation and hydrolysis of succinic anhydride reported by Koskikallio (89). These calculations show that approximately 2 parts per 10^7 at 25° and 3 parts per 10^5 at 95° of free succinic acid exist in the form of succinic anhydride. Even though these concentrations are quite small, they were said to be sufficient to account for rates of amide formation from succinic acid.

The experimental rate equation obtained in this study for the reaction of acetic acid and hydroxylamine gives three terms, two of which can be easily explained. One term, $k_3^H [CH_3COOH][NH_2OH]$, corresponds to the uncatalyzed

reaction of hydroxylamine and acetic acid (or, equivalently, the acid-catalyzed reaction with acetate ion), while the second term, k_2^H $[CH_3COOH][H^+][NH_2OH]$, corresponds to the attack of hydroxylamine on protonated acetic acid, $CH_3COOH_2^+$, or its kinetic equivalent.

The significance of the other term, k_1^H $[CH_3COOH][NH_2OH][H^+]^2$, is not readily apparent. Diprotonation of the acetic acid, as shown in XVII, is highly unlikely since the pK for the first protonation is - 6.1 (19).

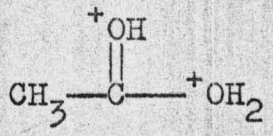

XVII

Furthermore, its kinetic equivalent, the reaction of a protonated acetic acid molecule, XVIII, with a protonated hydroxylamine molecule, XIX, seems also to be unlikely.

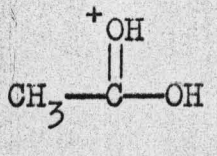

XVIII

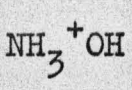

XIX

An explanation of the second-order dependence on hydrogen-ion concentration may be in postulating a tetrahedral intermediate with the decomposition of this intermediate

being the rate determining step. The following kinetic scheme is a consistent representation of the reaction of acetic acid and hydroxylamine (Eq. 65).

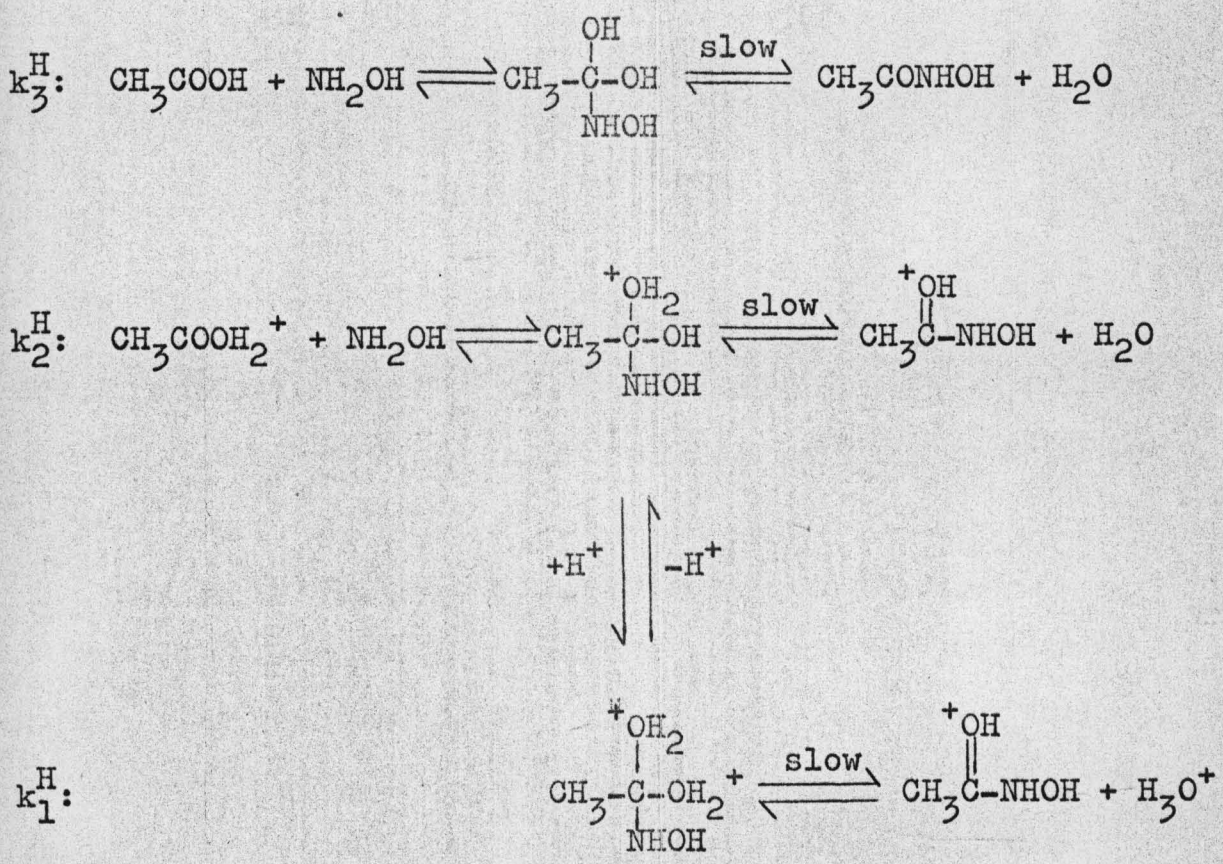

(65)

The rate equation for the hydrolysis of acetohydroxamic acid at low pH was found to be $V = k_a[CH_3CONHOH][H_3O^+]$. This rate term corresponds to the hydrogen ion catalyzed reaction of acetohydroxamic acid and water, which is the reverse of the second term in the rate equation for the formation of acetohydroxamic acid from acetic acid. The

absence of a hydrolysis term that is second order in hydrogen ion is reasonable because it would require attack of water on a diprotonated acetohydroxamic acid molecule, XX.

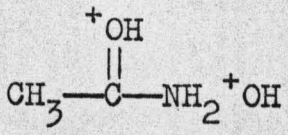

XX

The diprotonated form of acetohydroxamic acid is not likely to exist in appreciable concentrations at these conditions of pH.

The pH-rate profiles for acetohydroxamic acid formation from acetic acid in the presence and absence of nickel (II) are presented in Figure 49 (data from Tables VI and XV). It appears that below pH 2, nickel (II) does not catalyze the reaction of acetic acid and hydroxylamine, since the rate constants are the same as in the absence of nickel. This presents additional evidence that nickel (II) is not catalyzing the reaction by complexation with an unionized acetic acid molecule.

The hydrolysis of acetohydroxamic acid was found to be first order in hydrogen ion concentration as is the case with benzohydroxamic acid (90). The calculated hydrolysis rate constants, plotted in Figure 22 (data in Table XVII), are in good agreement with the experimentally

Figure 49. pH-rate profile for acetohydroxamic acid formation from acetic acid; open circles, no nickel; filled circles, 0.04 M nickel chloride. Data from Tables VI and XV.

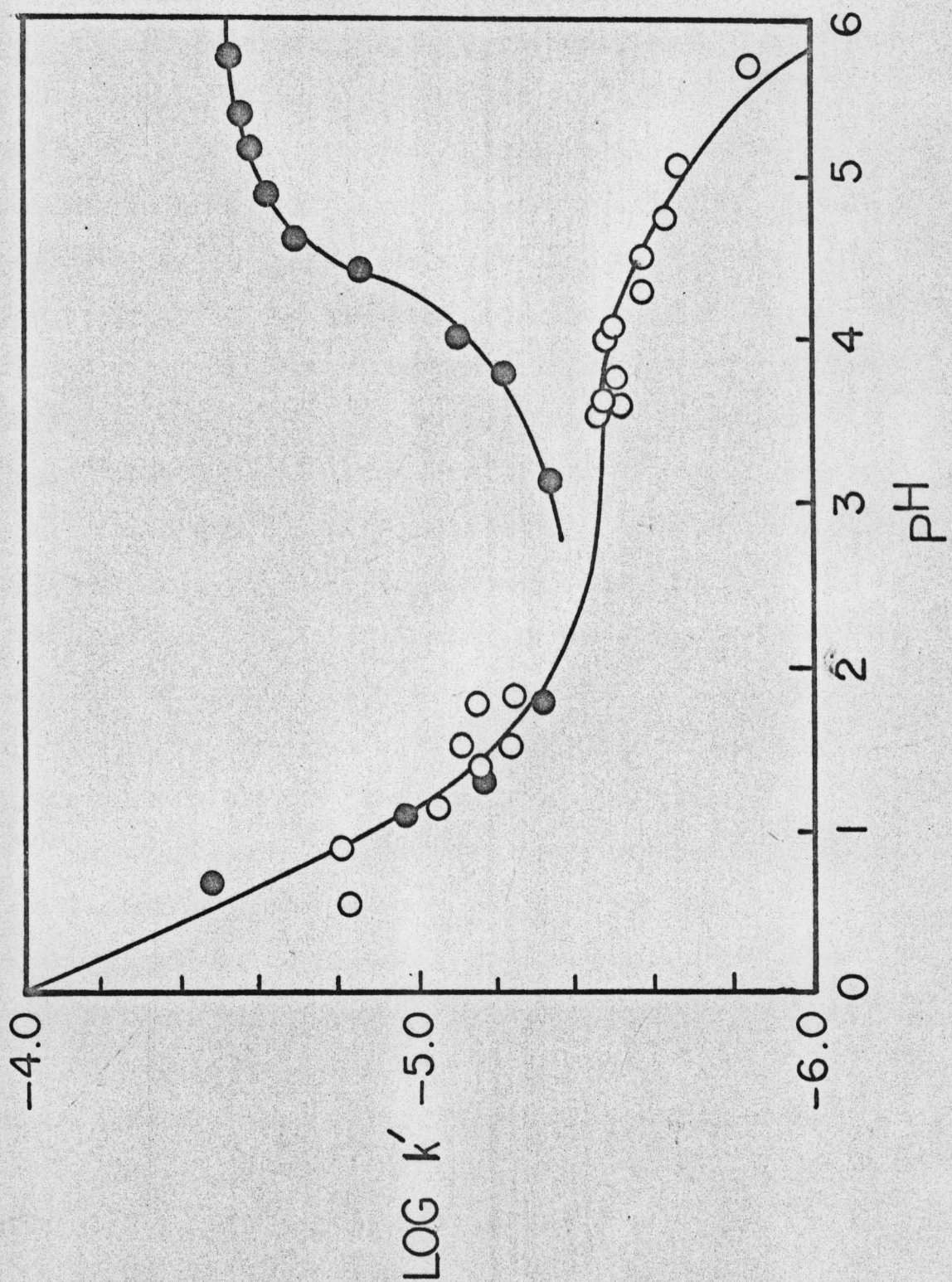

determined hydrolysis rate constants. This agreement gives assurance of the reliability of the rate constants calculated from the formation reaction.

The pH-rate profile for hydroxamic acid formation from succinic acid (Figure 26 and Table XIX) shows that the rate constants are not significantly larger than those for acetic acid. In light of these similarities it is not necessary to postulate a cyclic anhydride intermediate for the reaction of succinic acid and hydroxylamine. Furthermore, anhydride formation from acetic acid is definitely ruled out by the first-order dependence on acetic acid concentration of the rate for the reaction of acetic acid and hydroxylamine (Figure 16 and Table XIII). Anhydride formation as a necessary condition for this reaction would require a second-order dependency on acetic acid concentration. The reaction of succinic acid with hydroxylamine probably proceeds by direct attack of hydroxylamine on the free succinic acid, H_2A,

That anhydride formation is not necessary may be a manifestation of the unusually large reactivity of hydroxylamine. An estimate of the second-order rate constants for the reaction of acetic acid and hydroxylamine can be made from data presented by Fersht and Jencks (91). These authors constructed a Brønsted plot for attack of nucleophiles, such as pyridines, imidazoles, phenoxide ions, alkoxides, and acetate ion on acetic acid at 25°, as

estimated from equilibrium constants and rates of the reverse reactions. From this plot the second-order rate constant for a nucleophile with $pK_a = 6.0$ (e.g., hydroxylamine) would be approximately 10^{-17} $\underline{M}^{-1}$ sec^{-1}. Assuming that the rate increases two-fold for every 10 degrees in temperature rise, the rate constant at 90° would be approximately 10^{-15} $\underline{M}^{-1}$ sec^{-1}. This is at least 8 orders of magnitude smaller than any rate constants obtained in the present study for the reaction of acetic acid and hydroxylamine. The unusually large difference in rate constants obtained in this study is too large to be a manifestation solely of the so-called "alpha effect."* For instance, the rate of reaction of hydrazine with phenyl acetate is about 2 orders of magnitude larger than expected from a Brønsted plot for the reaction of a series of amines with phenyl acetate (92). This extraordinary reactivity of hydroxylamine is at present unaccounted for.

---

*Certain nucleophiles, including hydroxylamine, hydrazine, hydroxamic acids, N-hydroxyphthalimide, the anions of peroxides and hydrogen peroxide, hypochlorite ion and oxime anions, exhibit higher reactivities than would be expected from their basicities. This phenomenon is called the "alpha effect" since all of these nucleophiles have an unshared pair of electrons on the atom adjacent or "alpha" to the nucleophilic atom. While the mechanism is not understood, it is thought to involve transition state stabilization by the pair of "alpha" electrons (114).

3. Nickel (II) Catalysis of Hydroxylaminolysis of Phenyl and Ethyl Acetates

The nickel (II) catalysis of the hydroxylaminolysis of phenyl acetate is probably exerted in the conversion of O-acetylhydroxylamine to N-acetylhydroxylamine or acetohydroxamic acid (Eq. 66).

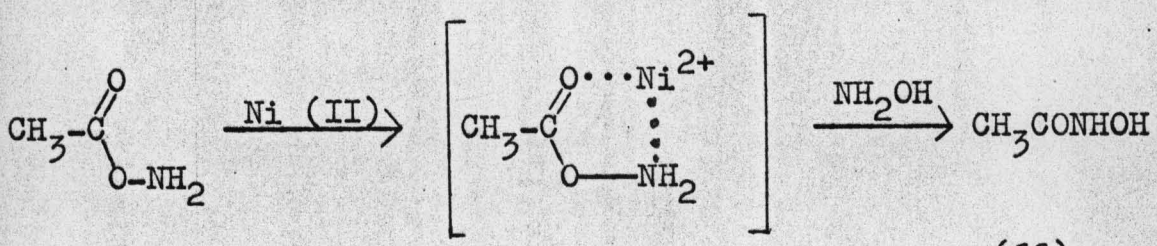

(66)

Since this catalysis is small, it does not suggest any advantages for the nickel (II)-catalyzed hydroxylaminolysis reaction for the analysis of labile phenyl esters of carboxylic acids. This proposed mechanism is important in that it suggested that compounds such as acid hydrazides will undergo nickel (II) hydroxylaminolysis, as described earlier.

The means by which nickel (II) catalyzes the reaction of ethyl acetate and hydroxylamine is probably a form of general acid catalysis, which serves to polarize the carbonyl carbon-oxygen bond. Catalysis of the conversion of O-acetylhydroxylamine to acetohydroxamic acid is ruled out since this conversion is much faster in the absence of nickel (II) than is the overall reaction for the nickel (II)-catalyzed hydroxamic acid formation from ethyl acetate.

4. Nickel (II)-Catalyzed Hydroxylaminolysis of Acid Hydrazides

One of the important findings of this study is the prediction, from the study of nickel (II)-catalyzed hydroxylaminolysis of phenyl acetate, that acid hydrazides will undergo nickel (II)-catalyzed hydroxylaminolysis. The data presented in Figure 42 clearly show that the nickel (II)-catalyzed hydroxylaminolysis reaction is much faster than either the neutral reaction or the alkaline reaction. This information was used to devise a ferric hydroxamate method for the analysis of carboxylic acid hydrazides. This method represents an extension of the ferric hydroxamate method for the analysis of carboxylic acid derivatives.

B. Analytical Applications

1. Nickel (II)-Catalyzed Ferric Hydroxamate Method for the Analysis of Carboxylic Acids

Carboxylic acids in dilute aqueous solution may be determined by potentiometric titration with base if the acid is sufficiently strong, i.e., pK_a of about 7 or less. When the acid is too weak to be titrated in water, it may be determined in a nonaqueous solution by visual or potentiometric titration. In either case, the lower limit of concentration which can be readily determined is about 0.01 M. More dilute solutions can be measured using

semimicro techniques as suggested by Belcher (93).

A variety of non-titrimetric methods for the analysis of carboxylic acids have been proposed. A few of these methods will be discussed below. More extensive discussions on the analysis of carboxylic acids can be found in references (110), (111), and (112). One of the most popular methods consists of esterifying the acid and then determining the ester by gas chromatography. Among the esterification methods used are the reactions of the acids with diazomethane, methanol-HCl, or methanol-boron trifluoride. Vorbeck, et al. (94), used all three reactions in the analysis of some fatty acids. Zaura and Metcoff (95) utilized this method for determining a series of biologically important acids. They were able to measure lactate, fumarate, pyruvate, citrate, and other acids with sensitivities of 0.8 to 2.5 micromoles per milliliter. Lactic acid and succinic acid in meat and egg samples have been determined by extraction into ether, esterification with boron trifluorido-n-propyl alcohol, and then separation and quantification by gas chromatography (96,97). Variations of this method are seen in the different methods of measuring the amount of ester formed. Mitchell, et al. (98) reacted the acids with boron trifluoride in methanol and then used the Karl Fischer titration to measure the amount of water produced (Eq. 67).

$$RCOOH + CH_3OH \longrightarrow CH_3COOCH_3 + H_2O \qquad (67)$$

Of course, this method required completely nonaqueous solutions. Other investigators have measured the ester concentration by the ferric hydroxamate method (40,41). Egashira (99) has utilized the color formed by complexes of acids and cis-dichloro-bis(ethylenediamine) chromium (III) chloride. Unfortunately, unsubstituted monobasic acids and salicylic acid gave no color.

Lauric acid has been determined by extraction into bromobenzene with the ionic dyes methylene blue and pinacyanol, and subsequent colorimetric measurement of the dye (100). Acetic acid in the presence of acetic anhydride has been determined by its reaction with rhodamine reagent (101). Other acids have been measured by reactions characteristic of that acid and not general for other acids. A discussion of these methods will not be presented here. Amino acids are conveniently measured by reactions of the -amino-group. These reactions, though important analytically, are not pertinent to the present discussion.

The nickel (II)-catalyzed ferric hydroxamate method for carboxylic acids that was suggested by this study presents several advantages as a method for carboxylic acids. It appears to be the only colorimetric method for the analysis of carboxylic acids

in aqueous solutions. The lower limits of sensitivity are about 10^{-4} M, which makes this method slightly less sensitive than the gas chromatographic methods but more sensitive than conventional titration methods. It has the advantage over the gas chromatographic methods of not requiring extensive sample preparation for aqueous samples. Furthermore, the ionic state of the acid is unimportant since the reaction mixture is adjusted to a pH where the acid is primarily in the anion form. On the other hand, any compound that forms hydroxamic acids, especially carboxylic acid derivatives, will probably interfere. As mentioned earlier, aromatic acids react much slower than aliphatic acids. Nevertheless, this method is the only reported direct ferric hydroxamate method for carboxylic acids. The following suggested analytical procedure, which is written for the analysis of 10^{-2} M solution of acetic acid, may require modification of the reaction times for other concentrations and other carboxylic acids, since this is a kinetic assay.

The reproducibility of the kinetic method depends largely on solution preparation, consistency of time of reaction (and of temperature), and the usual spectrophotometric limitations. The result is that reproducibilities typical of most spectrophotometric methods may be expected. Under the conditions of 1.0 M hydroxylamine hydrochloride, 0.1 M nickel chloride, 25% (v/v) dioxane,

0.022 M acetic acid, 90.5°, the average absorbance was 0.598 (4 trials) with the range being ±0.006 and the standard deviation being 0.004. In this connection the relative rate data of Table IX will be helpful. The suggested procedure follows:

Ferric Perchlorate Reagent. Dissolve 69.35 g of ferric perchlorate hexahydrate in 21 ml of 60% perchloric acid and 80 ml of water. Dilute this solution to 1 liter with methanol. This solution is 0.15 M in ferric perchlorate.

Nickel-Hydroxylamine Reagent. Dissolve 6.95 g of hydroxylamine hydrochloride and 2.38 g of nickel chloride hexahydrate in 25 ml of water. Add 12.5 ml of dioxane and adjust the pH to 6.3 with saturated sodium hydroxide. Bring the volume to 50.0 ml with water. Adjust the final solution to pH 6.2. This solution is 2 M in hydroxylamine hydrochloride, 0.2 M in nickel chloride and 25% (v/v) in dioxane; it should be used within three hours of preparation.

Reaction Mixture. Adjust the pH of the sample carboxylic acid solution to 6.2. Place 5.0 ml of the nickel-hydroxylamine reagent and 5.0 ml of the sample solution in a 20 ml ampule and seal the ampule. Repeat the procedure with a standard solution of the same carboxylic acid having approximately the same concentration as the sample solution. Place both ampules, standard and

sample, in a boiling water bath. Remove both samples at 30 minutes and immediately place them in an ice-water bath to quench the reaction. Bring the ampules to 25.0° and pipet 1.0 ml of the contents of each into 20.0 ml of the ferric perchlorate reagent contained in separate foil-wrapped flasks. After one hour, measure the absorbance at 530 nm against a common blank. Calculate the concentration of the sample solution using the equation,

$$C_u = C_s\left(\frac{A_u}{A_s}\right)$$

where C_u and A_u are the concentration and absorbance of the unknown sample solution and C_s and A_s are the concentration and absorbance of the standard solution. Both concentrations are of the solutions that were sealed in the ampules, so a correction may be necessary to account for the dilution of the original sample in achieving the desired pH.

2. Nickel (II)-Catalyzed Ferric Hydroxamate Spot Test for Carboxylic Acids

Spot tests for carboxylic acids are well known (21,24), but they usually require a nonaqueous sample. The proposed spot test is satisfactory for aqueous solutions. Furthermore, the ionic state of the acid is not important in this proposed test. The results shown in Table XII show that

aliphatic acids generally give positive tests while aromatic acids and amino acids do not. Esters and amides also give positive tests with this method. However, esters and amides also give positive tests with the alkaline ferric-hydroxamate method while carboxylic acids do not. The minimum amount of acetic acid giving a positive test in 15 minutes reaction time was 30 micrograms. See Table XII for the results and scope of the nickel (II)-catalyzed ferric hydroxamate spot test. A detailed description of the procedure follows:

1% Ferric Chloride Reagent. Prepare a 1% solution of ferric chloride hexahydrate in water (1 g of $FeCl_3 \cdot 6H_2O$ per 100 ml of solution). Add one milliliter of concentrated hydrochloric acid to 100 ml of this reagent.

Nickel-Hydroxylamine Reagent. Dissolve 5.56 g of hydroxylamine hydrochloride and 0.95 g of nickel chloride hexahydrate in water to make 100 ml. This solution is 0.8 M in hydroxylamine hydrochloride and 0.04 M in nickel chloride and is stable indefinitely.

Test Procedure. Add one ml of approximately 0.1 M aqueous solution of the sample acid to 5 ml of nickel hydroxylamine reagent. Adjust the solution to pH 6 with saturated sodium hydroxide solution or concentrated hydrochloric acid, using Hydrion^R papers as a pH indicator.

This solution is blue at pH 6 because of a nickel (II)-hydroxylamine complex. Place the reaction mixture in a boiling water bath and remove 3-drop samples at 30 minute intervals for testing. Transfer the 3-drop sample to a spot plate depression. Add 2 drops of concentrated hydrochloric acid followed by 2 drops of 1% ferric chloride reagent. A positive test is indicated by the immediate appearance of a reddish-brown or reddish-violet color.

3. Nickel (II)-Catalyzed Ferric Hydroxamate Method for the Analysis of Acid Hydrazides

Acid hydrazides, in particular isonicotinic acid hydrazide (Isoniazid), have been analyzed by a variety of methods usually involving the hydrazine moiety of the molecule. A review of analytical methods can be found in reference (113). A brief description of some methods will be given here. Hydrazides can be titrated potentiometrically as bases in nonaqueous solutions (102). However, this kind of titration is subject to a large number of interferences, especially hydrazine, which is also titrated. Acid hydrazides can also be determined gasometrically (Eq. 68), the volume of nitrogen produced during oxidation being measured (103-105).

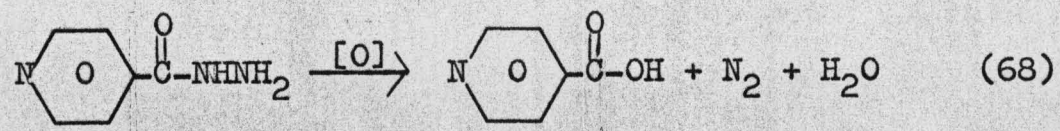

(68)

Bromine, ferricyanide, and iodate are used as oxidizing agents. A serious drawback to this method is that most hydrazine derivatives also react under these conditions. Isoniazid has been determined colorimetrically by reaction with β-naphthoquinone-4-sulfonate, the absorbance of the product at 480 nm being measured (106). Hydrazines, semicarbazide, aniline, urea, and hydroxylamine interfere in this method. Isoniazid has been reacted with flavones (107), molybdic acid (108), and 1-chloro-2,4-dinitrobenzene (109), the colors being measured to determine the isoniazid concentration.

The nickel (II)-catalyzed ferric hydroxamate method suggested here for acid hydrazides represents an extension of the ferric hydroxamate method for carboxylic acid derivatives, since acid hydrazides do not react readily under the usual alkaline conditions. Using the nickel (II)-catalyzed method, isoniazid and benzhydrazide can be measured at 10^{-4} M concentrations. This is more sensitive than titrimetric and gasometric methods, which are macro-scale methods. Hydrazine, phenylhydrazides, and semicarbazide do not react under these conditions. The reaction is sufficiently fast to allow analysis of aliphatic and aromatic hydrazides under the same conditions. The results plotted in the calibration curve (Figure 48) give a standard deviation of 0.0025 from the calculated "least squares" line. The procedure follows:

Hydroxylamine Reagent. Dissolve 27.8 g of hydroxylamine hydrochloride in 100 ml of water. This solution is 4.0 M in hydroxylamine hydrochloride.

Nickel Chloride Reagent. Dissolve 9.508 g of nickel chloride ($NiCl_2 \cdot 6H_2O$) in 100 ml of water. This solution is 0.4 M in nickel chloride.

Determination of Reaction Time. Mix 20.0 ml of hydroxylamine reagent with 10.0 ml of nickel chloride reagent and 50 ml of water. Adjust the pH to 6.5 with saturated sodium hydroxide solution. Add 1.0 ml of a 0.5 M solution of the hydrazide to be tested. Bring the volume to 100.0 ml with water. Adjust the pH of the final solution to 6.50. Seal 3-ml portions of this mixture in 5-ml ampules. Place the ampules in a boiling water bath and remove samples at 5 minute intervals. Upon removal, immediately place the ampules in an ice-water bath to quench the reaction. Store ampules in the refrigerator freezer until all samples have been withdrawn. Bring ampules to 25° and transfer 1.0 ml of the contents of each ampule to 20.0 ml of 0.15 M ferric perchlorate in separate foil-wrapped flasks. (See the procedure for aliphatic acids for directions for preparing the ferric perchlorate reagent.) After one hour, read the absorbances at 530 nm. The optimum reaction time for the determination of the sample of unknown concentration

corresponds to the time of maximum absorbance obtained in this experiment.

Analytical Procedure. Add 2.0 ml of hydroxylamine reagent and 1.0 ml of nickel chloride reagent to 5.0 ml of the sample hydrazide solution (10^{-4} to 10^{-3} M). Adjust the pH to 6.50 with saturated sodium hydroxide solution. Bring the volume to 10.0 ml with water. Seal 5 ml of this solution in a 10-ml ampule. Repeat this procedure with a known standard solution of approximately the same concentration as the sample. Place both ampules in a boiling-water bath. At the time of maximum absorption (as determined in the previous section) remove both ampules and place them in an ice-water bath. Bring samples to 25° and pipet 1.0 ml of the contents of each ampule into 20.0 ml of ferric perchlorate reagent in a foil-wrapped flask. After one hour read the absorbances at 530 nm against a common blank. Calculate the concentration of the unknown using the following formula,

$$C_u = \left(\frac{A_u}{A_s}\right) C_s$$

where C_u and A_u are the concentration and absorbance of the sample solution and C_s and A_s are the concentration and absorbance of the standard solution. Alternatively, a working curve may be prepared by subjecting graded concentrations of standard solutions to this procedure,

concomitantly treating the sample solution in the same way, and then reading the sample concentration from the working curve of absorbance *vs* concentration for the standard solutions.

V. SUMMARY

In a recent study Lawlor (16) demonstrated a nickel (II)-catalyzed reaction of hydroxylamine and acetic acid to give acetohydroxamic acid. Since carboxylic acids do not undergo conventional alkaline hydroxylaminolysis, this reaction has now been investigated kinetically to explore its mechanism and possible analytical applications. Hydrogen ion-catalyzed hydroxamic acid formation from carboxylic acids was also investigated. In addition, nickel (II)-catalyzed hydroxamic acid formation from some carboxylic acid derivatives has been studied.

Nickel (II) was found to catalyze the reaction of hydroxylamine and acetic acid at 90.5°. This catalysis is thought to occur through a complex of the nickel (II) ion and the anion of acetic acid; this complexing polarizes the carbon-oxygen bonds and renders the acetate ion more susceptible to nucleophilic attack. The ratio of hydroxylamine to nickel (II) was 20:1 in this study, while Lawlor used a ratio of 1:1. This difference leads to different pH-rate behavior, which is ascribed to different distributions of nickel-hydroxylamine complexes.

Acetic acid and hydroxylamine form acetohydroxamic acid at 90.5° in a reaction whose rate equation contains terms of the form $k[CH_3COOH][NH_2OH][H^+]^n$, where n can be 0, 1, and 2. A tetrahedral intermediate, with the

decomposition of this intermediate being rate determining, was proposed to account for the presence of the three rate terms.

Phenyl acetate reacts with hydroxylamine at 25.0° in a two-step reaction, as shown by Jencks (7,8). Nickel (II) catalysis of acetohydroxamic acid formation was observed in the present study and this catalysis was found to occur during the conversion of O-acetylhydroxylamine (formed in the first step of the reaction) to acetohydroxamic acid.

The catalysis of the second step of the reaction of phenyl acetate and hydroxylamine suggested that carboxylic acid hydrazides would also undergo nickel (II)-catalyzed hydroxamic acid formation. This prediction led to the demonstration of nickel (II)-catalyzed hydroxamic acid formation from benzhydrazide and isonicotinic acid hydrazide (Isoniazid).

A nickel (II)-catalyzed ferric hydroxamate kinetic method of analysis for aliphatic carboxylic acids has been developed and found to be useful in measuring aqueous solutions 10^{-4} to 10^{-2} M in carboxylic acid. Aromatic acids and amino acids do not interfere significantly. A spot test for carboxylic acids utilizing nickel (II)-catalyzed hydroxamic acid formation was shown to differentiate between aliphatic and aromatic acids.

A nickel (II)-catalyzed ferric hydroxamate method for the analysis of carboxylic acid hydrazides is also proposed. Calibration curves for benzhydrazide and

isonicotinic acid hydrazide were linear in the range of 10^{-4} to 10^{-2} M.

The analytical methods proposed in this thesis appear to be the first in which (a) hydroxamic acids are formed directly from carboxylic acids; and (b) acid hydrazides are converted to hydroxamic acids for analysis.

VI. BIBLIOGRAPHY

1. Lossen, H., Ann., 150, 314 (1869); Yale, H. L., Chem. Rev., 33, 209 (1943).
2. Neilands, J. B., Science, 156, 1443 (1967).
3. Shendrikar, A. D., Talanta, 16, 51 (1969).
4. Ryan, D. E., Analyst, 85, 569 (1960).
5. Tandon, S. G. and Bhattacharaya, S. C., Anal. Chem., 33, 1267 (1961).
6. Aksnes, G., Acta Chem. Scand., 11, 710 (1957).
7. Jencks, W. P., J. Amer. Chem. Soc., 80, 4581 (1958).
8. Jencks, W. P., ibid., 80, 4585 (1958).
9. Jencks, W. P., "Catalysis in Chemistry and Enzymology," McGraw-Hill Book Co., 1969, New York, pp. 105-106.
10. Jencks, W. P. and Carriuolo, J., J. Amer. Chem. Soc., 82, 1778 (1960).
11. Jencks, W. P. and Carriuolo, J., ibid., 82, 675 (1960).
12. Notari, R. E., J. Pharm. Sci., 58, 1069 (1969).
13. Bruice, T. C. and Bruno, J. J., J. Amer. Chem. Soc., 83, 3494 (1961).
14. Notari, R. E., J. Pharm. Sci., 58, 1064 (1969).
15. Jencks, W. P., Caplow, M., Gilchrist, M. and Kallen, R. G., Biochemistry, 2, 1313 (1963).
16. Lawlor, J. M., Chem. Commun., 1967, 404.
17. Hoare, D. G., Olson, A. and Koshland, D. E., Jr., J. Amer. Chem. Soc., 90, 1638 (1968).
18. Jencks, W. P. and Gilchrist, M., ibid., 86, 5616 (1964).
19. Arnett, E. M., Prog. Phys. Org. Chem., 1, 223 (1963).
20. Chou, T. C. and Lipmann, F., J. Biol. Chem., 196, 89 (1952).
21. Feigl, F., "Spot Tests in Organic Analysis," 6th ed., Elsevier Publishing Company, Amsterdam, 1960, pp. 249-254.

22. Soloway, S. and Lipschitz, A., Anal. Chem., 24, 898 (1952).

23. Buckles, R. E. and Thelen, C. J., ibid., 22, 676 (1950).

24. Knight, D. W. and Cleland, G. H., J. Chem. Educ., 47, 781 (1970).

25. Cheronis, N. D., in Proceedings, 1961, "International Symposium on Microchemical Techniques," ed. by N. D. Cheronis, Interscience, New York, 1962, pp. 128-130.

26. Goldenberg, V. and Spoerri, P. E., Anal. Chem., 30, 1327 (1958).

27. Hestrin, S., J. Biol. Chem., 180, 249 (1949).

28. Goddu, R. F., Le Blank, N. F. and Wright, C. M., Anal. Chem., 27, 1251 (1955).

29. Goldenberg, V. and Spoerri, P. E., ibid., 31, 1735 (1959).

30. Hill, U. T., Ind. Eng. Chem., Anal. Ed., 18, 317 (1946).

31. Hill, U. T., Anal. Chem., 19, 932 (1947).

32. Pilz, W., Z. Anal. Chem., 193, 338 (1963).

33. Katz, J., Lieberman, J. and Barker, H. A., J. Biol. Chem., 200, 417 (1953).

34. Meister, A., Levintow, L., Greenfield, R. E. and Abendschein, P. A., ibid., 215, 441 (1955).

35. Lipman, F. and Tuttle, L. C., ibid., 159, 21 (1945).

36. Polya, J. B. and Tardew, P. L., Anal. Chem., 23, 1036 (1951).

37. Bergman, F., ibid., 24, 1367 (1952).

38. Diggle, W. M. and Gage, J. C., Analyst, 78, 473 (1953).

39. Lehman, G. and Wilhelm, G., Z. Anal. Chem., 238, 415 (1968).

40. Duron, O. S. and Nowotony, A., ibid., 35, 370 (1963).

41. Tolbert, C. E. and Kenner, C. T., J. Pharm. Sci., 60, 597 (1971).

42. Gutnikov, G. and Schenk, G. H., Anal. Chem., 34, 1316 (1962).

43. Lien, O. G., Jr., ibid., 31, 1363 (1959).

44. McComb, E. A. and McCready, R. M., ibid., 29, 819 (1957).

45. Kaye, M. A. G. and Kent, P. W., J. Org. Chem., 1953, 79.

46. Hilf, R. and Castano, F. F., Anal. Chem., 30, 1538 (1958).

47. Brodie, A. F. and Lipman, F., J. Biol. Chem., 212, 677 (1955).

48. Cori, O. and Lipman, F., ibid., 194, 417 (1952).

49. Wollish, E. G. and Schmall, M., Anal. Chem., 22, 1033 (1950).

50. Ford, J. H., ibid., 19, 932 (1947).

51. Boxer, G. E. and Everett, R. M., ibid., 21, 670 (1949).

52. Karawya, M. S. and Ghourab, M. G., J. Pharm. Sci., 59, 1331 (1970).

53. Aihara, T., Machida, H. and Yoneda, Y., J. Pharm. Soc. Japan, 77, 1318 (1957).

54. Brochmann-Hanssen, E., Schmid, P. and Benmaman, J. B., J. Pharm. Sci., 54, 783 (1965).

55. Feldman, J. A., Frank, S. G. and Holmes, T. J., Jr., ibid., 60, 920 (1971).

56. Nery, R., Analyst, 91, 388 (1966).

57. Lowenstein, J. M. and Schatz, M. N., J. Biol. Chem., 236, 305 (1961).

58. Gibbs, I. S. and Juckerman, M. N., J. Pharm. Sci., 59, 395 (1970).

59. Kundiger, D. G. and Richardson, E. E., J. Amer. Chem. Soc., 77, 2897 (1955).

60. Wise, W. M. and Brandt, W. W., ibid., 77, 1058 (1955).

61. Fishbein, W. N., Daly, J. and Streeter, C. L., Anal. Biochem., 28, 13 (1969).

62. Jones, L. W. and Hurd, C. D., J. Amer. Chem. Soc., 43, 2422 (1921).

63. Adams, R. and Thal, A. F., "Organic Syntheses," Collective Volume I, John Wiley and Sons, New York, 1941, pp. 436-437.

64. Kanno, S., J. Pharm. Soc. Japan, 72, 1193 (1952).

65. Marvel, C. S., Hager, F. D. and Candle, E. C., "Organic Syntheses," Collective Volume I, John Wiley and Sons, New York, 1941, p. 224.

66. Brewster, R. Q. and Williams, B., "Organic Syntheses," Collective Volume III, John Wiley and Sons, New York, 1955, p. 337.

67. Jessup, R. S. and Green, C. B., J. Res. Nat. Bur. Stand., 13, 469 (1934).

68. Clarke, H. T. and Taylor, E. R., "Organic Syntheses," Collective Volume I, John Wiley and Sons, New York, 1941, p. 298.

69. Gatterman, L. and Wieland, H., "Laboratory Methods of Organic Chemistry," The Macmillan Company, New York, 1937.

70. Curtius, T., Ber., 23, 3023 (1890).

71. Curtius, T. and Hofman, T. S., J. Prakt. Chem., [2], 53, 524 (1896).

72. Thiele, J. and Stange, O., Ann., 283, 20 (1895).

73. Leighton, V. L., Am. Chem. J., 20, 677 (1898).

74. Hashmi, M. H., Adil, A. S., Malik, F. R. and Ajmal, A. J., Mikrochim. Acta, 1969, 772.

75. Curtius, T. and Trachman, O., J. Prakt. Chem., 159, 165 (1895).

76. Bates, R. G., J. Res. Nat. Bur. Stand., 66A, 179 (1962).

77. Notari, R. E. and Munson, J. W., J. Pharm. Sci., 58, 1060 (1969).

78. Guggenheim, E. A., Phil. Mag., 2, 538 (1926).

79. Harned, H. S. and Hamer, W. J., J. Amer. Chem. Soc., 55, 2194 (1933).

80. Higuchi, T. and Miki, T., ibid., 83, 3899 (1961).

81. Higuchi, T., Miki, T., Shah, A. C. and Herd, A. K., ibid., 85, 3655 (1963).

82. Bender, M. L. and Turnquest, B. W., ibid., 79, 1889 (1957).

83. Breslow, R. and Chipman, D., ibid., 85, 4195 (1965).

84. Steinberger, R. and Westheimer, F. H., ibid., 73, 429 (1951).

85. Falqui, M. T., Ponticelli, G. and Sotgui, F., Ann. Chim. (Rome), 56, 464 (1966).

86. Chaberek, S., Jr., Courtney, R. C. and Martell, A. E., J. Amer. Chem. Soc., 74, 5057 (1952).

87. Bonchev, P. B., Yordanov, N. D. and Michaylova, V., Z. Phys. Chem., 242, 408 (1969).

88. Morawetz, H. and Otaki, P. S., J. Amer. Chem. Soc., 85, 463 (1963).

89. Koskikallio, J., Ann. Acad. Sci. Fenn., Series A-II, 57, 4 (1954).

90. Berndt, D. C. and Fuller, R. L., J. Org. Chem., 31, 3312 (1966).

91. Fersht, A. R. and Jencks, W. P., J. Amer. Chem. Soc., 92, 5442 (1970).

92. Bruice, T. C. and Benkovic, S., "Bioorganic Mechanisms," Volume 1, W. A. Benjamin, Inc., New York, 1966, p. 80.

93. Belcher, Ronald, "Submicro Methods of Organic Analysis," Elsevier Publishing Co., Amsterdam, 1966.

94. Vorbeck, M. L., Mattick, L. R., Lee, F. A. and Pederson, C. S., Anal. Chem., 33, 1512 (1961).

95. Zaura, D. Z. and Metcoff, J., ibid., 41, 1781 (1969).

96. Salwin, H. and Bond, J. F., J. Assoc. Offic. Anal. Chem., 52, 41 (1969).

97. Staruskiewicz, W. F., ibid., 52, 471 (1969).

98. Mitchell, J., Jr., Smith, D. M. and Bryant, W. M. D., J. Amer. Chem. Soc., 62, 4 (1940).

99. Egashira, S., Anal. Chem., 33, 1928 (1961).

100. Mukerjee, P., ibid., 28, 870 (1956).

101. Mitra, B. C., Ghosh, P. and Paht, S., ibid., 36, 673 (1964).

102. Alicino, J. F., J. Pharm. Sci., 41, 401 (1952).

103. Krivis, A. F., Gazda, E. S., Supp, G. R. and Kippur, P., Anal. Chem., 35, 1955 (1963).

104. McKennis, H., Jr., Weatherby, J. H. and Dellis, E. P., ibid., 30, 499 (1958).

105. Harting, H., J. Pharm. Sci., 42, 323 (1953).

106. Pratt, E. L., Anal. Chem., 25, 814 (1953).

107. Hawker, C. D., Margraf, H. W. and Weichlebaum, T., ibid., 32, 122 (1960).

108. Colarusso, J., Schmall, M., Wollish, E. G. and Shafer, E. G. E., ibid., 30, 62 (1958).

109. Ballard, C. W. and Scott, P. G. W., Chem. Industry, 1952, 715.

110. Tiwari, R. D. and Sharma, J. P., "The Determination of Carboxylic Functional Groups," Pergamon Press, New York, 1970, pp. 4-66.

111. Ma, T. S. in "The Chemistry of Carboxylic Acids and Esters," edited by S. Patai, Interscience, New York, 1969, pp. 871-921.

112. Weiss, F. T., "Determination of Organic Compounds, Methods and Procedures," Wiley-Interscience, Series in Chemical Analysis, Vol. 32, New York, 1970, pp. 63-83.

113. Cheronis, N. D. and Ma, T. S., "Organic Functional Group Analysis by Micro and Semimicro Methods," Interscience, New York, 1964, pp. 289-296.

114. Edwards, J. O. and Pearson, R. G., J. Amer. Chem. Soc., 84, 16 (1962).

VII. APPENDIX

SIMPLE MONTE CARLO CALCULATION OF CONCENTRATION-TIME CURVES FOR PHARMACOKINETIC MODELS

by James W. Munson and Kenneth A. Connors